UNIVERSITY OF CALIFORNIA, SAN DIEGO

Polymerization and partitioning: a novel mechanism for regulating metabolic enzyme activity in *Saccharomyces cerevisiae*

A dissertation submitted in partial satisfaction of the requirements for the degree

Doctor of Philosophy

in

Biology

by

Chalongrat Noree

Committee in charge:

Professor James Wilhelm, Chair
Professor Arshad Desai
Professor Douglass Forbes
Professor Randolph Hampton
Professor Maho Niwa

2013

The Dissertation of Chalongrat Noree is approved, and it is acceptable in quality and form for publication on microfilm and electronically:

_____

_____

_____

_____

_____
Chair

University of California, San Diego

2013

DEDICATION

This work is dedicated to

my family,

teachers,

colleagues,

and friends

who have made me strong in both science and social life.

TABLE OF CONTENTS

LIST OF FIGURES

LIST OF TABLES

ACKNOWLEDGEMENTS

I would like to acknowledge Professor James Wilhelm for his supervision of my thesis. It is not that easy to find a PI who is smart, nice, and helpful all-in-one, but Jim has all those characteristics so I was very lucky to have him as my PI. All his advice and guidance helped me not to get lost throughout the run toward my Ph.D. Also, I really appreciate his generosity for taking care of my financial support from September 2012 to the present and also my future post-doctoral support.

I would like to acknowledge Professor Arshad Desai, Professor Douglass Forbes, Professor Randolph Hampton, and Professor Maho Niwa as the members of my committee. Having amazing scientists on my committee made me feel thankful. Tons of questions, ideas, comments from them let me know that they truly wanted me to develop and become a good scientist and that helped me a lot to keep my thesis work still being on the right track.

In addition, I would like to thank Professor Suresh Subramani, Professor Yang Xu, and Professor Raffi Aroian for giving me the opportunity to do the rotations in their labs. I learned a lot from them and found their passion for scientific research inspirational. During the rotations, I was mentored by Dr. Saurabh Joshi, Dr. Sharon Lim, and Dr. Yan Hu. It was my pleasure to have them as my mentors. In particular I would like to thank Ferdinand Los who was a graduate student in the Aroian Lab. He taught me how to use the deconvolution microscope. I really appreciated his great help on that so I could have very beautiful images of fluorescent yeast for my thesis and publications.

I would like to thank everyone, both present and past members, in the Wilhelm Lab: Risa Maruyama Broyer, Elena Monfort-Prieto, Brian Sato, Andy Shiau, Dane

Samilo, Kyle Begovich, Phillip Kyriakakis, Phillip Jiang, Juliana Chang, Amir Motamedi, Anna Pang, Theresa Wong, and Stephanie Choi. They were not only my colleagues, but were also my American family. They made the Wilhelm Lab into my second home. I was very happy making and sharing lots of good memories about science and non-science stuff with them. Risa was very helpful and at the same time she was the best entertainer and event-organizer ever. She always made big surprises like the welcome party for me as a new member of the Wilhelm Lab, the party after my first committee meeting, and all my birthday parties. Elena was our lab mother as she is a good listener and caretaker. She knew if you had something on your mind and she was the one who really wanted to help you out. Brian was very helpful and generous. He always kept asking me to send him the drafts of my reports for annual committee meetings, so he could help correct and revise my writings. Andy is the expert on protein structures. He helped look at molecular 3D structure of CTP synthase in order to find mutation sites for ATP binding. Dane and Kyle were my lifesavers as they helped prepare several materials and collect some of the data present in Chapter 4 of my thesis. Besides, they were both good comedians and entertainers, making the lab full of smiles and laughs. Phil was very entertaining and generous. I was surprised at how he was so addicted to Korean culture and cuisine. It was great to see an American who really appreciated and was willing to learn Eastern things, especially everything related to Korea. It was so much fun to hang out with all of them, what I called ‘the Wilhelm babies’.

I would like to acknowledge the Ministry of Science and Technology, Royal Thai Government for the financial support of my Ph.D. from August 2007 to August 2012.

Also, if I did not get help from the faculty at the Institute of Molecular Biology and Genetics (or currently named as the Institute of Molecular Biosciences), Mahidol University, I could not be able to have a chance to study in the USA. Unforgettably amongst those are Professor Emeritus Sakol Panyim, Professor Chartchai Krittanai, and Professor Chalermporn Ongvarrasopone.

Thanks to all my Thai friends at UCSD for their infinite help and support, especially, Thanathom (Earl) Chailangkarn, Poochit (Mike) Nonejuie, Nongluk (P'Knoy) Plongthongkum, Pongsakorn (A) Teeraparpwong, Patipan (Au) Uttayarat, and the staff at the Hi Thai restaurant on UCSD campus. We have treated each other like we were real brothers and sisters in the same family. Earl was my best buddy at UCSD. Mike was a good cook. Earl and Mike were not just my roommates, but also were true friends. P'Knoy was so generous, helping us to move off campus and lending her car for our emergency time. 'A' was a guru of computer and electronics devices. Au was very kind to help me survive in the beginning of my life in the USA. The 'Hi Thai' people generously gave me free food very often. As well, I would like to thank Supansa (P'Photo) Yodmuang and Yannawan (Dream) Wongchai, graduate students at Columbia University, for their calls to check if I was still alive. I thank Pimonrat (Som-O) Tiensawat, a graduate student at University of Illinois at Urbana-Champaign, who helped me pick an easy-to-say name 'Charlie' (Chalongrat Noree) for my life in the USA.

Most importantly, without unconditional love and support from my family, I don't know how I could keep going and moving on. I would like to thank Dad, Mom, and my sister for always being by my side, although they were thousands of miles away. Dad drove a hundred miles back home across several mountains on the curvy road every

weekend just to spend time with his family. Mom was the strongest person I've ever known, working so hard; 2 or 3 days in a row without sleep. My parents never said 'No' if I asked for something related to my education. My sister is such a good medical doctor with a really big heart, caring about poor and old people. They are all my idols and are the reason why I've been working hard and trying to be a better son and brother.

And last, I would like to thank 'Science'. It is very challenging to understand and discover the mysterious facts behind you. And many thanks to let me know that my patience working on you is not wasteful.

Chapter 2 is a reprint of Noree, Chalongrat; Sato, Brian K.; Broyer, Risa M.; Wilhelm, James E. "Identification of novel filament-forming proteins in *Saccharomyces cerevisiae* and *Drosophila melanogaster*" *Journal of Cell Biology*. 2010. 190(4): 541-551. I was the primary experimenter. B. Sato performed the experiments appeared in Figures 2.3 (C-H), 2.4 and Table 2.2. The experiments appeared in Figure 2.7 were performed by R. Broyer. J. Wilhelm wrote the manuscript and performed experiments in Figure 2.6.

Chapter 3 is the manuscript which has been submitted for publication. It may appear in Proceedings of the National Academy of Sciences of the United States of America 2013. Noree, Chalongrat; Monfort-Prieto, Elena; Shiau, Andrew K.; Wilhelm, James E. "Common regulatory control of CTP synthase enzyme activity and filament formation". I was the primary investigator and author of this paper. E. Monfort-Prieto created the yeast strains expressing c-terminally GFP-tagged CTP synthase with the

following mutations; G148A, C404G, R381M, R381P, G382A, E161K-C404G and performed Western blot analysis. J. Wilhelm and A. Shiau wrote the manuscript.

Chapter 4 is a manuscript in preparation and will be submitted for publication. D. Samilo and K. Begovich helped collect the data, create yeast strains expressing double fluorescently-tagged proteins, and perform epistasis and Western blot analysis. Imaging, data analysis, and writing the manuscript was my responsibility. J. Wilhelm helped edit/revise the manuscript for publication.

VITA

2004	Bachelor of Science, Chiang Mai University, Thailand
2007	Master of Science, Mahidol University, Thailand
2013	Doctor of Philosophy, University of California, San Diego

PUBLICATIONS

Noree, C., Sato, B.K., Broyer, R.M., and Wilhelm, J.E. "Identification of novel filament-forming proteins in Saccharomyces cerevisiae and Drosophila melanogaster" *Journal of Cell Biology*. 2010. 190(4):541-51.

Noree, C., Prieto, E.M., Shiau, A., and Wilhelm, J.E. "Common regulatory control of CTP synthase enzyme activity and filament formation". Manuscript submitted for publication (Proceedings of the National Academy of Sciences of the United States of America).

Noree, C., Samilo, D., Begovich, K., and Wilhelm, J.E. "Regulation of metabolic pathways via assembly into high-order complexes". Manuscript in preparation.

ABSTRACT OF THE DISSERTATION

Polymerization and partitioning: a novel mechanism for regulating metabolic enzyme activity in *Saccharomyces cerevisiae*

by

Chalongrat Noree

Doctor of Philosophy in Biology

University of California, San Diego, 2013

Professor James Wilhelm, Chair

Only four intracellular filaments are known: actin, tubulin, intermediate filaments, and septin. However, these were identified based on the fact that they are highly abundant in particular tissues and/or have unusual locations, i.e. in the spindle, bud neck, etc. We hypothesized that there might be additional proteins capable of forming filaments that might have been missed due to the fact that they are less abundant. Thus, we manually

conducted a visual screen of the yeast GFP collection (about 40% of entire collection) and we could identify 4 novel filaments formed by CTP synthase, glutamate synthase, GDP-mannose pyrophosphorylase, and eIF2/2B translation initiation proteins complex. In addition to these filaments, we also reported 29 proteins which were able to form visible foci inside the cells. We also found that the ability of at least one of these proteins to form filaments, CTP synthase, is conserved in yeast, *Drosophila*, and mammals. The fact that 3 of 4 novel filaments we found are metabolic enzymes raised the question of whether polymerization is used to regulate enzyme activity. Next, we focused on CTP synthase assembly in order to elucidate the mechanism of its assembly. Media shift experiments and mutational studies of CTP synthase *in vivo* demonstrated that CTP synthase assembled into filaments once the enzyme was inactivated. This indicated that the assembly of CTP synthase was coupled to enzyme activity under different growth and environmental changes. We next examined the entire pathway of purine biosynthesis and found that enzymes at the nodes of the pathway were the only ones forming visible intracellular structures. The appearance and disappearance of these structures depended on the availability of their substrates and products, suggesting that structure formation by the enzymes at the nodes of the pathway was connected to the regulation of metabolic flux. These findings have led further to the future directions in exploring if the enzymes at the nodes of other biochemical pathways possess a similar characteristic in switching on/off the enzymatic activity, therefore controlling the flux through their pathways.

Chapter 1

Introduction

Chemistry + Organization = Life

Cell Biology is the transition point where Chemistry becomes Biology. While there are many features that distinguish a living cell from a bag of enzymes, the most important of these is the high degree of biochemical organization that is present within the cell. This organization prevents different biochemical reactions from interfering with each other and also permits a high degree of regulatory control that allows the cell to adapt to changes in the environment. This high degree of biochemical organization is reflected in the large number of membrane-bound organelles that serve as miniature reaction vessels for subsets of biochemical reactions. In contrast, the cytoplasm has long been considered to be a homogenous mixture of proteins and other macromolecules that support the "more interesting" specialized chemistry occurring within the membrane-bound compartments. However, if organization is the central concept delineating the boundary between lifeless chemistry and bountiful biology, one might expect that there might be additional organizational principles at work in the cytoplasm that might have been missed due to the limits of traditional microscopy.

The focus of my thesis was to test this hypothesis by conducting genetic screens to identify novel structures within the cytoplasm and assess their role in regulating critical biochemical pathways within the cell. Chapter 2 of my thesis describes a pilot screen to identify such structures and the characterization of a set of novel intracellular filaments comprised of metabolic enzymes. We have been able to identify four novel filament systems formed by, glutamate synthase, GDP-mannose pyrophosphorylase, and CTP synthase, and subunits of translation initiation factor (eIF2/2B). Several treatment

conditions have been tested on the formation of each of these filaments, including carbon starvation, energy depletion, translational repression, and phosphorylation inhibition. This data reveals that the formation of these four filaments is regulated differently from one another and the filament formation is not just a uniform global response to certain environmental conditions. Rather, their assembly could serve additional functions which might be more beneficial than having the enzyme diffuse or scattered throughout the cells.

Among the novel filament-forming proteins identified from our screen, CTP synthase is the most interesting as it is the key enzyme for making precursors for several biomolecules including RNA, DNA, and phospholipids (Carman and Zeimetz, 1996). Moreover, CTP synthase catalyzes the last and rate-limiting step of pyrimidine ribonucleotide biosynthesis; therefore it controls the balance of nucleotide pools. Abnormality in CTP levels can be seen in several types of cancers and tumors (Williams et al., 1978). This is caused by misregulation of or mutations in CTP synthase (Aronow and Ullman, 1986). This made CTP synthase a focus of past research with the result that biochemistry and enzymology of this enzyme have been extensively characterized. It has been intriguing in the present work to see how the polymerization of CTP synthase is related to its molecular structure and biochemical function.

CTP synthase as a model to study self-assembly of metabolic enzymes

CTP synthase is the final enzyme in pyrimidine ribonucleotide biosynthesis, catalyzing the conversion of UTP to CTP (Figure 1.1). To make CTP, the oxygen-4 position of the uracil base of UTP is first replaced with phosphate, donated from ATP.

The phosphorylated UTP is then aminated by ammonia, either derived from glutamine hydrolysis (glutamine-dependent reaction) or obtained exogenously (glutamine-independent reaction), generating CTP as a final product (Long and Pardee, 1967). CTP synthase is composed of two structural domains; an amidoligase (or synthase) domain is located at the N-terminus, and a glutamine amidotransferase (or glutaminase) domain is located at the C-terminus of the enzyme. Glutamine hydrolysis takes place in the glutamine amidotransferase domain, resulting in glutamate and ammonia. Ammonia is then transferred to the amidoligase domain where UTP is phosphorylated by ATP. After the nucleophilic attack of phosphorylated UTP by ammonia, CTP is eventually generated.

CTP synthase is an allosteric enzyme that requires oligomerization to activate its enzyme activity (Pappas et al., 1998). In the absence of its substrates ATP and UTP, CTP synthase exists predominantly as inactive dimeric form. Once ATP and UTP are present, tetramerization of CTP synthase is promoted between two pairs of dimers. Based on crystallographic studies, binding of ATP and UTP to the enzyme causes a conformational change of CTP synthase subunits that leads to the formation of ATP and UTP binding sites among three subunits of the two dimers (Endrizzi et al., 2004). CTP has its own binding site, predicted to be very close to UTP binding site. However, the triphosphate moieties of UTP and CTP seem to occupy the same pocket. This might explain why CTP at low concentration mimics UTP so that it can promote tetramerization of CTP synthase *in vitro*, while CTP at higher concentrations, on the other hand, brings about negative feedback inhibition.

GTP, although it is neither the substrate nor product of CTP synthase, does help stimulate the glutamine hydrolysis reaction occurring in the glutamine amidotransferase

domain by stabilizing the transition state intermediate of the reaction (Kizaki et al., 1982). Upon GTP binding, GTP triggers the local conformational change that accommodates the glutamine hydrolysis, prevents the leakage of ammonia, and also promotes the tunnel formation for transporting ammonia from the glutamine amidotransferase domain to the amidoligase domain. Therefore, all four ribonucleotides are essential for the regulation of CTP synthase activity: ATP and UTP as substrates, GTP as the positive allosteric activator, and CTP as the product and also negative feedback inhibitor. In addition, CTP synthase activity has been shown to be stimulated by phosphorylation. In yeast, phosphorylation of CTP synthase by the protein kinases A and C, as well as the presence of ribonucleotides, is required for tetramerization and activation of CTP synthase (Choi et al., 2003; Park et al., 2003; Park et al., 1999; Yang et al., 1996; Yang and Carman, 1996). In sum, CTP synthase activity is under the regulation of the following processes; (1) binding of ribonucleotides, (2) phosphorylation, and (3) substrate-induced tetramerization.

As mentioned above, we have chosen CTP synthase as a model enzyme to study the assembly of metabolic enzymes into cytoplasmic structures as CTP synthase has been well studied for its biochemical and molecular aspects. In Chapter 3, we have introduced molecular structure and function-guided mutations from previous studies (Choi et al., 2003; Endrizzi et al., 2004; Park et al., 2003; Willemoes et al., 2005) to investigate the effect of these mutations on polymerization of CTP synthase into cytoplasmic structures *in vivo*. We hypothesized that biopolymer formation of CTP synthase could be directed either by the activity of the enzyme or alternatively by the regulators which have the effect on the molecular structure and function of the enzyme. By substituting amino acid

residues at the catalytic/active sites, this would allow us to test whether the activity of the enzyme normally directs the assembly of CTP synthase into cytoplasmic structures. On the other hand, if the supramolecular assembly of the enzyme relies instead on the regulators of enzyme structure (folding/tetramerization) and function (catalysis), disruption of the regulatory sites (either the binding sites of ribonucleotides, phosphorylation sites, or tetramerization interface) would show an effect on CTP synthase assembly. Thus, this study should help elucidate the relationship between molecular structure, biochemical function, and biopolymer formation of CTP synthase.

Organizational principles for the cytoplasm: the cytoskeleton and processing bodies

Imagine that before the victory of the first living cell to emerge and live on earth, enormous attempts to organize cell composition by nature were randomized until one was able to find the right recipe. The earliest components would be simple, solid, and non-mobile. Thus, we could imagine that all the proteins at the beginning might be made having only a function in structural support, needed to maintain cell shape and to resist mechanical stress from any external forces. Through evolution, some of these proteins could then have evolved from primitive to advanced states where they could have multiple tasks, involving more than being just structural support proteins. They might start adopting dynamic or catalytic properties. During these advancements, some might still retain their ability to assemble into large structures, whereas some might lose their self-assembling property. This could explain why--at present--a relatively small number of proteins have been identified as filament-forming proteins.

The best understood cytoplasmic feature within the cell is the classic cytoskeleton. There are four general classes of cytoskeletal filaments: (1) actin/actin-like, (2) tubulin-based microtubules/tubulin-like (3) intermediate filaments, and (4) septins. Three of these cytoskeletal elements are found both in prokaryotes, which largely lack membrane-bound organelles, as well as in eukaryotes. The major filament forming proteins in prokaryotes and eukaryotes are summarized in Tables 1.1 and 1.2, respectively.

Actin was first identified by the extraction of muscular tissues (Halliburton, 1887). The extracts containing actin and myosin (the motor protein), became less viscous when ATP was added. Later, G-actin (globular) and F-actin (filament) were studied and characterized using X-ray crystallography (Holmes et al., 1990; Kabsch et al., 1990) and electron microscopy (Narita et al., 2006). The key structural motif of actin was revealed, which is the ATPase fold. This motif is responsible for ATP hydrolysis, providing energy for polarized polymerization of ATP-bound actin monomers at the plus end, whereas depolymerization of ADP-bound actin occurs at the minus end (Korn et al., 1987). ATP hydrolysis by the ATPase fold is the driving factor for the dynamics feature of actin, therefore it can be utilized in certain biological processes such as cytokinesis.

Tubulin was discovered by taking advantage of colchicine, a chemical used for studying mitosis (Wells, 2005). Colchicine-binding activity allowed scientists to isolate microtubule-containing structures, i.e., spindle fibers, cilia, and sperm tails, and later tubulin was found to be the building block of these intracellular structures. Unlike actin, tubulin has different types of subunits. Formation of protofilaments occurs through addition of heterodimers consisting of alpha- and beta-tubulins. Polymerization of tubulin into protofilaments requires that the tubulin be in a GTP-bound state (Carlier et al.,

1987). The lateral attachment of multiple protofilaments then creates hollow tubulin-based microtubules. The assembly of GTP-bound tubulin dimers takes place at the plus ends, whereas hydrolyzed tubulin dimers disassemble from the minus ends.

Intermediate filaments are much different from actin and tubulin in term of dynamic nature of polymerization and depolymerization of intermediate filament does not involve the hydrolysis of nucleotides. The organization of intermediate filament is therefore non-polarized. Recently, a bacterial intermediate filament has been discovered, named Crescentin (Ausmees et al., 2003). This protein has been tested to function in maintenance of the curved shape of the bacteria *Caulobacter crecentus* due to the helical structure formed by crescentin along one side of the bacterial plasma membrane.

Prokaryotic counterparts of actin and tubulin had long been thought to be non-existent. Interestingly, recent findings have revealed that bacteria indeed have actin- and tubulin-like structures, which cannot be recognized by simple alignment of the primary sequences between the two kingdoms. Their amino acid sequences show very low similarity. A better way to identify these bacterial actin- and tubulin-like proteins is to compare their folded structures with those of eukaryotic actin and tubulin (Erickson, 2007; Moller-Jensen and Lowe, 2005; Wickstead and Gull, 2011). Consequently, sequence comparison might not be an ideal methodology to identify novel members of a protein family.

Advancement in biological instrumentation and technology led to identification of other novel intracellular structures. The processing body or P-body, which is a structure for mRNA storage and processing, is one of those novel structures identified through protein labeling and advanced microscopic techniques (Bashkirov et al., 1997; Eystathioy

et al., 2002; Ingelfinger et al., 2002; van Dijk et al., 2002). Compared to previous biochemical and molecular techniques, visual microscopic screens would be more direct for identifying novel intracellular structures formed inside cells. Thus, we decided to analyze the yeast GFP collection, where the location and distribution pattern of individual proteins can be visualized as they have been tagged with green fluorescent protein (Chapter 2 and 4), and rescreen it for the existence of hitherto unexpected structures. Indeed, using fluorescent labeling techniques a previous study showed that all six enzymes involved in *de novo* purine biosynthesis co-assemble into visible granular structures in HeLa cells when purine levels are dropped (An et al., 2008). Their assembly was reversible when purine was added back to the culture media. The authors have suggested that the transient assembly of these purine enzymes into a structure, dubbed the purinosome, is required to maintain intracellular purine levels. Their hypothesis is that, upon clustering, enzymes are much more productive due to the formation of substrate channeling. In Chapter 4, we surveyed the entire pathway of *de novo* purine biosynthesis (Figure 1.2), including the neighboring steps; PRPP, GMP and AMP biosynthesis in budding yeast to determine which enzymes might form cytoplasmic structures. Several do and their location in the pathway is revealing. We have also characterized the conditions triggering assembly and disassembly of these enzymes. In addition, we have provided data to initially predict the status of activity of enzymes within the structures, using gene epistasis and genetic mutation approaches. Based on our current data, we have demonstrated that a global purinosome, containing all the purine biosynthetic enzymes, does not exist in yeast. Rather, only those enzymes at the nodes of the *de novo* purine biosynthetic pathway are able to form cytoplasmic structures. These structures are

independent from one another. According to the results of epistasis and mutation analysis, the cytoplasmic assembly of these enzymes might well be used to regulate their enzymatic activities, controlling metabolic flux and the balance between intermediate pools.

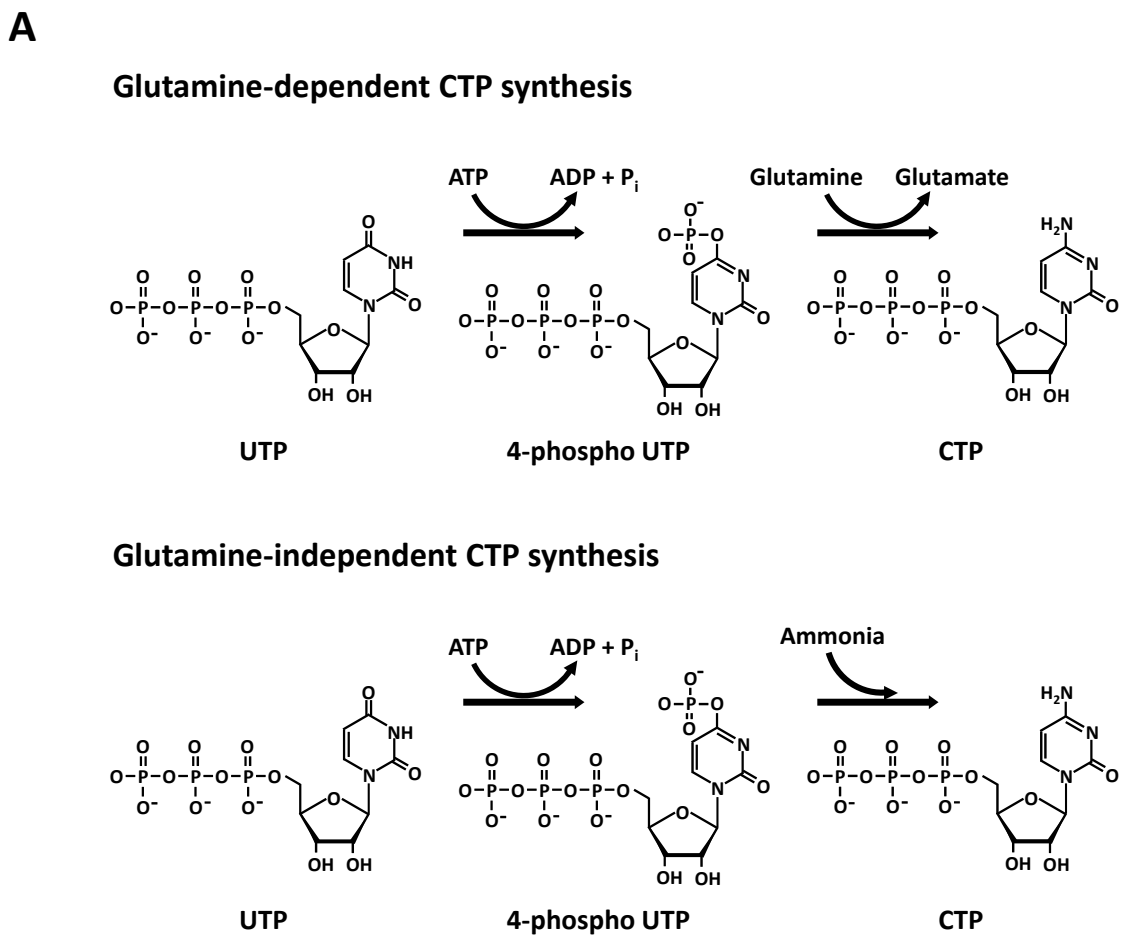

Figure 1.1 CTP biosynthetic reactions and oligomerization of CTP synthase

CTP can be synthesized via either a glutamine-dependent reaction (A) or a glutamine-independent reaction (B). Tetramerization is required for activation of CTP synthase activity, and is promoted by phosphorylation and the binding of substrates to the enzyme (B).

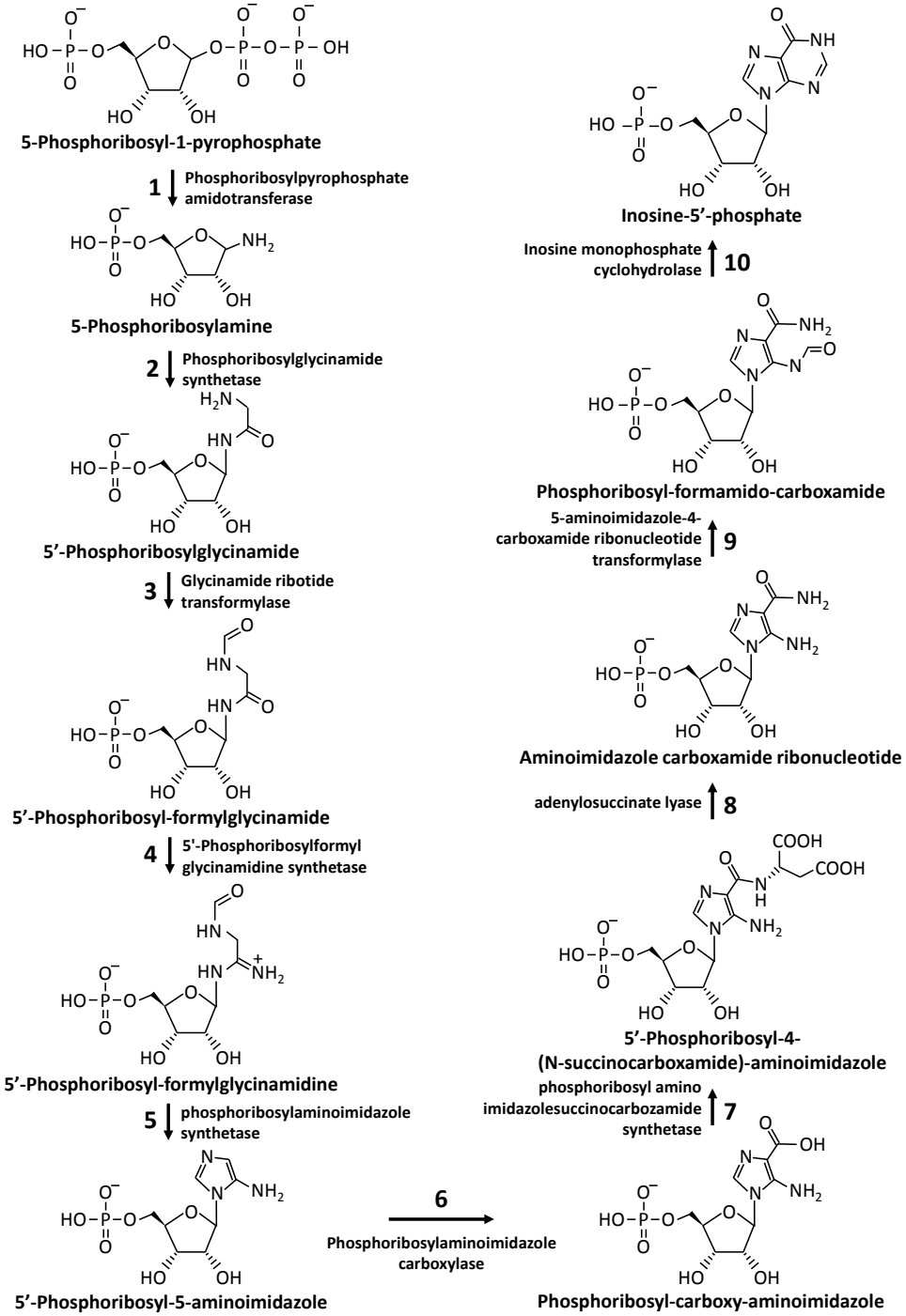

Figure 1.2 *De novo* purine biosynthesis

De novo purine biosynthesis is composed of 10 reactions, catalyzed by 6 enzymes (in mammals) or 8 enzymes (in yeasts). In mammals, the trifunctional enzyme, TrifGART, is responsible for catalyzing the reactions in steps 2, 3, and 5. Steps 6 and 7 are catalyzed by the bifunctional enzyme, PAICS. Steps 9 and 10 are catalyzed by the bifunctional enzyme, ATIC. In yeast, step 2 and 5 are catalyzed by Ade5/7p, whereas steps 9 and 10 are catalyzed by Ade16/17p.

Table 1.1 Filament-forming proteins in prokaryotes and archaeans

Protein	Type	Function	References
FtsZ	Bacterial tubulin	Cell division	(Bi and Lutkenhaus, 1991; de Boer et al., 1992a; Desai and Mitchison, 1998; RayChaudhuri and Park, 1992)
FtsA	Bacterial actin	Cell division	(Bork et al., 1992; Lara et al., 2005; van den Ent and Lowe, 2000)
MinCDE		Septum-site determination	(de Boer et al., 1992b; Lutkenhaus, 2007)
MreB	Bacterial actin	Cell shape determination/chromosome segregation/cell polarity	(Doi et al., 1988; Figge et al., 2004; Gitai et al., 2005; Jones et al., 2001; Kruse and Gerdes, 2005; Kruse et al., 2003; Soufo and Graumann, 2003; van den Ent et al., 2001)
ParM	Bacterial actin	Plasmid segregation	(Moller-Jensen et al., 2003; van den Ent et al., 2002)
Crenactin	Archaeal actin	Cell shape determination	(Ettema et al., 2011)
Crescentin	Bacterial intermediate filaments	Cell shape determination/cell motility	(Ausmees et al., 2003)
Flagellin	Bacterial flagella	Bacterial mobility	(Brown, 1945; Gatenby, 1961; Owen, 1949)
Pilin	Bacterial pili	Bacterial conjugation/cell adhesion	(Keizer et al., 2001; Telford et al., 2006)

Table 1.2 Filament-forming proteins in eukaryotes

Protein	Type	Function	Cell/tissue distribution	References
Actin	Actin-based microfilaments	Cytoskeleton/cell motility/cell division/cytokinesis/cell signaling/organelle movement/cell junction maintenance/cell shape	Muscles	(Barany et al., 2001; Halliburton, 1887; Holmes et al., 1990; Kabsch et al., 1990; Straub and Feuer, 1989)
Tubulin	Tubulin-based microtubules	Cytoskeleton/mitosis		(Cowan, 1984; Lockwood, 1978; Mohri, 1976; Sackett, 1995; Stearns and Kirschner, 1994)
Keratin (cytokeratin)	Type I and II intermediate filaments	Cytoskeleton/cell integrity/cell-cell adhesion/epithelial tissue		(Franke et al., 1979; Schweizer et al., 2006)
Desmin	Type III intermediate filaments	Cytoskeleton	Muscles	(Costa et al., 2004; Izant and Lazarides, 1977; Lazarides and Hubbard, 1976)
GFAP (glial fibrillary acidic protein)	Type III intermediate filaments	Cell-cell communication/mitosis	Astrocytes/glia/central nervous system	(Fuchs and Weber, 1994; Jacque et al., 1978; Tardy et al., 1990; Weinstein et al., 1991)
Peripherin	Type III intermediate filaments	Neurite and axonal outgrowth and regeneration/	Peripheral nervous system	(Baudoin et al., 1993; Portier et al., 1983)
Vimentin	Type III intermediate filaments	Cytoskeleton/ Maintenance of cell integrity by anchoring positions of organelles in cytoplasm	Fibroblasts/leukocytes/blood vessels/endothelial cells	(Bignami et al., 1982; Katsumoto et al., 1990; Osborn et al., 1980)
α-Internexin	Type IV intermediate filaments	Axonal outgrowth	Central nervous system	(Chien and Liem, 1994; Kaplan et al., 1990; Pachter and Liem, 1985; Shea and Beermann, 1999)
Synemin/ desmuslin	Type IV intermediate filaments	Cell integrity	Muscles	(Granger and Lazarides, 1980; Mizuno et al., 2001)
Syncoillin	Type IV intermediate filaments	Cytoskeleton	Muscles	(Newey et al., 2001; Poon et al., 2002)
Lamin	Type V intermediate filaments	Nuclear skeleton/transcriptional regulation/nucleus assembly & breakdown/positioning of nuclear pores	Nucleus	(Benavente and Krohne, 1986; Burke et al., 1983; Dagenais et al., 1984; McKeon, 1987; Shelton et al., 1981)
Nestin	Type VI intermediate filaments	Cell proliferation and migration/axonal outgrowth	Neurons	(Dahlstrand et al., 1992; Michalczyk and Ziman, 2005)
Septin		Scaffold/cytokinesis/cell polarity/trapping pathogens	Fungi, plasma	(Chant, 1996; Cid et al., 1998; Fares et al., 1996; Frazier et al., 1998; Longtine et al., 1996; Wright et al., 1992)

Chapter 2

Identification of novel filament-forming proteins in *Saccharomyces cerevisiae* and *Drosophila melanogaster*

Abstract

The discovery of large supramolecular complexes such as the purinosome suggests that subcellular organization is central to enzyme regulation. A screen of the yeast GFP strain collection to identify proteins that assemble into visible structures identified four novel filament systems comprised of glutamate synthase, guanosine diphosphate-mannose pyrophosphorylase, cytidine triphosphate (CTP) synthase, or subunits of the eIF2/2B translation factor complex. Recruitment of CTP synthase to filaments and foci can be modulated by mutations and regulatory ligands that alter enzyme activity, arguing that the assembly of these structures is related to control of CTP synthase activity. CTP synthase filaments are evolutionarily conserved and are restricted to axons in neurons. This spatial regulation suggests that these filaments have additional functions separate from the regulation of enzyme activity. The identification of four novel filaments greatly expands the number of known intracellular filament networks and has broad implications for our understanding of how cells organize biochemical activities in the cytoplasm.

Introduction

The principle of self-assembly is believed to underlie the ability of cells to build amazingly complex macromolecular structures such as the mitotic spindle. Most studies of self-assembling structures have focused on either the polymerization properties of cytoskeletal filaments such as actin or microtubules or on the formation of membrane-bound compartments (Gardner et al., 2008; Howard and Hyman, 2009; King and Marsh, 1987; Kueh and Mitchison, 2009). However, the last several years have seen an explosion in the identification of novel intracellular structures such as processing bodies, U bodies, and purinosomes (An et al., 2008; Liu and Gall, 2007; Sheth and Parker, 2006), providing a new arena for identifying the mechanisms that drive the self-assembly of these supramolecular complexes. The identification of these structures has also raised the question of whether this type of organization is an important general mechanism for compartmentalizing the various biochemical reactions that take place in the cytoplasm.

Recently, a partial screen of the yeast GFP collection identified 33 proteins that are capable of self-assembling into large punctate structures that can be isolated biochemically, arguing that this form of regulation might be quite common (Narayanaswamy et al., 2009). However, it remained unclear whether these structures are evolutionarily conserved, and the role of these structures in regulating the biochemical activity of the enzymes remained an open question. Because a large fraction of the yeast GFP collection remained unexamined, we have conducted a more extensive screen of the yeast GFP strain collection to identify proteins that are capable of assembling into previously undescribed intracellular structures. This screen identified nine proteins that assemble into four distinct cytoplasmic filaments, indicating that the self-assembly of

enzymes into large cytoplasmic structures is more common than has been previously believed and that they can form structures other than puncta within the cytoplasm.

We have built on the results of this screen to address the second major question concerning supramolecular complexes: how their assembly is regulated. Allosteric regulation has been thought to control the assembly of enzyme supramolecular complexes such as the purinosome; however, this has never been tested directly (An et al., 2008). To define the relationship between the regulatory state of the enzyme and the formation of filaments/foci, we focused our experiments on the assembly of CTP synthase structures because the regulation of CTP synthase activity has been extensively studied in *Saccharomyces cerevisiae* (Nadkarni et al., 1995; Ostrander et al., 1998; Pappas et al., 1998; Yang et al., 1994). Our experiments revealed that end product inhibition of CTP synthase is necessary for filament assembly, arguing that in CTP synthase, filaments are comprised of an inhibited form of CTP synthase. This suggests that regulation of enzyme activity is central to the assembly of many supramolecular complexes. Furthermore, the discovery of four novel filaments effectively doubles the number of known filament networks present in eukaryotic cells, opening a new area for study with implications for enzyme regulation and cellular organization.

Results and Discussion

A visual screen for novel cytoplasmic structures in *S. cerevisiae*

The yeast GFP strain collection is comprised of 4,159 strains of the budding yeast *S. cerevisiae*, which each have GFP fused to the C terminus of a single protein (Huh et al., 2003). However, the original screen of this collection failed to identify several structures, such as P bodies or eisosomes (Sheth and Parker, 2006; Walther et al., 2006). To identify novel intracellular structures, we have visually screened 1,632 GFP-tagged yeast strains comprising 40% of the collection. This screen has identified nine proteins that are capable of forming filaments and foci *in vivo* and that were reported as having only a cytoplasmic localization in the original characterization of the collection. These proteins are Glt1p (glutamate synthase), Psa1p (GDP-mannose pyrophosphorylase), Ura7p/Ura8p (CTP synthase), Gcd2p (eIF2B-δ), Gcd6p (eIF2B-ε), Gcd7p (eIF2B-β), Gcn3p (eIF2B-α), and Sui2p (eIF2-α; Figure 2.1A). In addition, we identified 29 proteins that were localized to discrete cytoplasmic foci but were not capable of forming filaments (Table 2.1). Although the subcellular localization of Glt1p, Psa1p, and Ura7p has not been previously described, various components of eIF2 and eIF2B have been reported as being present in a novel cytoplasmic body (Campbell et al., 2005). However, the filamentous nature of these eIF2/2B-containing structures was not commented on in those experiments.

One concern with our screen is that the GFP tag might alter the structure or function of the proteins, causing them to form filaments or foci. However, when the GFP tag was replaced with a HA epitope tag, all of the proteins continued to form filaments,

arguing that GFP was not responsible for causing these nine proteins to self-assemble (Figure 2.2).

As a second assay for the effects of the tag on protein function, we tested whether the GFP-tagged version of each protein exhibited altered growth or viability. Psa1p, Gcd2p (eIF2B-δ), Gcd7p (eIF2B-β), Gcd6p (eIF2B-ε), and Sui2p (eIF2-α) are all essential genes, and GFP-tagging each of these genes at the endogenous locus did not affect viability, arguing that the addition of GFP did not alter the function of these proteins. Ura7p, although nonessential, is one of two genes that encode for CTP synthases in *S. cerevisiae*, and the *ura7Δ ura8Δ* double mutant is inviable. We took advantage of this synthetic lethality to examine the effects of the GFP tag on Ura7p function. To do this, we created a *ura8Δ* deletion in a *URA7::GFP* background. The *URA7::GFP; ura8Δ* yeast strain was viable, arguing that the GFP tag did not alter the function of the Ura7p. Unlike the other seven filament-associated proteins that we identified, there is no known phenotype associated with deletion of *GLT1*. Consequently, we were unable to assess whether the GFP tag affected Glt1p function. From these experiments, we conclude that the ability to form filaments is not dependent on GFP and that the GFP tag does not affect protein function for eight of the nine filament-forming proteins that we identified.

Ura7p/Ura8p, Psa1p, Glt1p, and eIF2/2B form distinct cytoplasmic filaments

The identification of nine filament-forming proteins raised the question of whether they are all part of the same filament network or whether they represent distinct cytoplasmic structures. To address this issue, we performed pairwise colocalization

experiments between Ura7p, Ura8p, Psa1p, Glt1p, and representative subunits of the eIF2 and eIF2B complexes in which one protein was tagged with GFP while the second was tagged with mCherry. Although representative subunits of the eIF2 and eIF2B complexes were present in the same filament, Ura7p, Psa1p, and Glt1p were each present in distinct filaments (Figure 2.1B). Furthermore, Ura7p and Ura8p, which both encode for CTP synthases in *S. cerevisiae*, coassembled into a common filament, arguing that the ability to self-assemble is conserved between these two proteins (Figure 2.1B). Therefore, we have identified four distinct filaments in yeast. Interestingly, although we observed 100% colocalization between the filaments formed by different eIF2/2B subunits, we also found that eIF2/2B subunits form filaments at different frequencies (Table 2.2). This suggests that although all eIF2/2B subunits assemble into a common structure, the association of certain subunits such as GCN3 that are only observed infrequently in filaments may be regulated.

Ura7p, Psa1p, Glt1p, and eIF2/2B filaments are not affected by known regulators of prion biogenesis

All four of the filaments we have identified bear a superficial resemblance to the filaments formed by prions when they are induced *de novo* (Zhou et al., 2001). This suggested that some or all of the filaments identified in our screen could be regulated by the same factors that control prion formation or that the filaments that we have identified are novel prions. To test this hypothesis, we deleted two genes required for prion formation/maintenance, *RNQ1* and *HSP104*, from strains in which a filament-associated protein had been tagged with GFP (Chernoff et al., 1995; Sondheimer and Lindquist,

2000). The frequency of filament formation for each of the four classes of filaments was unaltered in either *rnq1Δ* or *hsp104Δ* strains (Figure 2.3A). Thus, neither Rnq1p nor Hsp104p contributes to the formation of any of the four filament networks that we have identified. Consistent with this interpretation, overexpression of Hsp104p had no effect on Ura7p or Psa1p filaments and only weak effects on Glt1p filament formation (Figure 2.3B). Thus, the ability of Ura7p, Psa1p, Glt1p, and eIF2/2B to form filaments is not regulated by *HSP104*or *RNQ1*, and they are unlikely to be novel prions.

Identification of environmental conditions that regulate filament formation

The effects of nutrient deprivation on filament formation

Nutrient deprivation is known to induce the assembly of several cytoplasmic structures such as the processing body (Teixeira and Parker, 2007). To test the role of nutrient deprivation on the assembly of Psa1p, Glt1p, Ura7p, and eIF2/2B filaments, we compared the number of filaments present in log-phase cells with cells grown to saturation (OD_{600} > 5.0). Although the number of eIF2/2B filaments declined in saturated cultures relative to log-phase cultures, the number of Glt1p filaments remained fairly constant, whereas Ura7p and Psa1p filaments were significantly increased in saturated cultures (Table 2.2). Each protein also formed foci to varying degrees, with the formation of foci typically being coordinately regulated with filament formation (*URA7*, *URA8*, *PSA1*,*GCD2*, and *GCN3*) or unchanged between log phase and saturation (*GLT1*, *SUI2*, *GCD6*, and *GCD7*; Table 2.2).

One simple explanation for the changes in frequency of filament/foci formation under different growth conditions is that the ability to form these structures merely

reflects different protein levels in log phase or saturation. To test this possibility, we measured GFP levels in each of our filament-forming strains in either growth phase through flow cytometry. In general, protein level varied little between log-phase growth and saturation despite dramatic changes in filament formation for these two growth conditions (Figure 2.4). Thus, increases in filament/foci formation are not caused by increases in protein expression.

Effects of carbon source depletion on filament formation

Because growth to saturation is a potent inducer of both Ura7p and Psa1p filament formation, we next examined whether media from saturated cultures was capable of inducing filament formation in cultures undergoing log-phase growth. Exposure to YPD (2% peptone, 1% yeast extract, and 2% dextrose) from saturated cultures caused a 4.87-fold increase in the number of cells with Ura7p filaments but had no effect on Psa1p, Glt1p, Sui2p, or Gcd2p filament formation (Figure 2.3C). This result argues that either the depletion of a critical nutrient or the accumulation of a metabolite in the media as cultures approached saturation was responsible for inducing Ura7p filament formation. Furthermore, these results also argue that the mechanism for inducing Psa1p filaments is distinct from that used to promote Ura7p filament formation, even though both filaments are strongly induced in yeast grown to saturation.

Because carbon source depletion is a characteristic feature of saturated cultures that is known to induce other structures such as the processing body (Teixeira et al., 2005), we tested the ability of YP without glucose, water, and water with glucose to induce filament formation in log-phase cultures. Although none of these treatments had a

significant effect on Psa1p, Glt1p, Sui2p, or Gcd2p filament formation, treatment with either YP without glucose or water strongly induced Ura7p filament formation (Figure 2.3C). Furthermore, treatment of log-phase cultures with water containing glucose did not induce Ura7p filament formation (Figure 2.3C). Thus, glucose depletion is a potent inducer of Ura7p filament formation and is likely responsible for Ura7p filament formation as cells reach saturation.

These results raised the question of whether filament formation could be reversed by transferring yeast grown to saturation into fresh YPD. The shift to rich media caused no change in the number of Psa1p, eIF2/2B, or Glt1p filaments within 15 min of the shift, whereas the number of Ura7p filaments was decreased 50-fold (Figure 2.3D). Furthermore, when the media shift experiment was conducted with YP lacking glucose, the number of Ura7p filaments only decreased by 1.4-fold, arguing that reversal of filament formation was also strongly dependent on the presence of glucose in the media (Figure 2.3D). Together, these results argue that the presence of glucose in the growth media is a central regulator of Ura7p filament formation and that Ura7p filaments can undergo rapid assembly and disassembly in response to changes in nutrient conditions.

Effect of sodium azide on filament formation

These results suggested that the energy status of the yeast cell rather than the presence or absence of a particular metabolic intermediate in the cell was a critical factor in regulating filament formation. To test this hypothesis, we assayed the effects of treating yeast cells with azide for 15 min to determine whether altering the energy status of the cell without altering the carbon source could also regulate filament formation.

Although Ura7p and Psa1p filaments were strongly induced by treatment with sodium azide, the number of Glt1p or eIF2/2B filaments remained unaltered (Figure 2.3E). These results argue that Ura7p and Psa1p filament formation is strongly influenced by the energy status of the cell, whereas Glt1p and eIF2/2B regulation is dependent on other factors.

Effect of protein synthesis inhibitors on filament formation

Because the ability of eIF2/2B to assemble into cytoplasmic bodies had been previously shown to be highly sensitive to treatment with cycloheximide (Campbell et al., 2005), we examined the ability of 100 μg/ml cycloheximide to affect Ura7p, Psa1p, and Glt1p filament formation. For all three of these filaments, treatment with 100 μg/ml cycloheximide for 15 min had no effect on the number of cells possessing filaments, again highlighting the differences in filament regulation (Figure 2.3F).

Effect of temperature on filament formation

Many cytoskeletal filaments such as microtubules depolymerize at low temperatures. To test the role of temperature in filament formation, we shifted both log-phase and saturated yeast cultures to low temperatures for 15 min to determine whether acute changes in temperature would change the proportion of cells possessing filaments. We tested Ura7p, Psa1p, Glt1p, and eIF2/2B filament formation at 0°C. For all of the filaments, we did not detect any change in the frequency of filament formation for either log-phase or saturated cultures at low temperature (Figure 2.3G). Thus, none of the filaments we have identified exhibit the cold-sensitive polymerization characteristic of many cytoskeletal proteins.

Effects of the kinase inhibitor staurosporine on filament formation

Because the assembly of some intermediate filaments is regulated by phosphorylation, we tested whether the kinase inhibitor staurosporine could alter the frequency of filament formation. Exposure of cells to media containing 50 μg/ml staurosporine had no effect on the frequency of Glt1p or eIF2/2B filaments in either log-phase yeast or yeast grown to saturation (Figure 2.3H). However, staurosporine caused a dramatic effect on the number of cells that had either Ura7p or Psa1p filaments, and this effect occurred in both log-phase and saturated yeast cultures (Figure 2.3H). Although further experiments will be necessary to determine whether the effect of staurosporine on Ura7p and Psa1p filaments is direct, the fact that neither Glt1p nor eIF2/2B filaments are affected by the same treatment argues that the effects are not caused by a nonspecific disruption of cellular function.

CTP synthase filament formation is evolutionarily conserved from *S. cerevisiae* to *Drosophila melanogaster*

Given the large number of filaments that we have identified and the fact that they are often regulated by different environmental conditions, we focused our subsequent experiments on one type of filament to determine whether these structures are evolutionarily conserved and to define whether enzyme activity is linked to filament formation. Ura7p filaments provided an excellent starting point for these experiments because CTP synthase is evolutionarily conserved and its enzymology has been extensively characterized. Because a previous study of mammalian CTP synthase found that it colocalized with microtubules, we first tested whether Ura7p was associated with

microtubules in yeast (Higgins et al., 2008). Immunostaining for both Ura7p and microtubules showed no colocalization between these structures, arguing that Ura7p filaments are distinct from microtubules (Figure 2.5).

We next examined whether the ability of CTP synthase to form filaments was conserved in other species. For these experiments, we took advantage of the fact that the CTP synthase in *Drosophila* had been tagged with GFP at its endogenous locus as part of a genome-wide protein trap screen (Buszczak et al., 2007). Analysis of GFP-CTP synthase in the *Drosophila* egg chamber revealed that filaments formed in all three of the cell types that make up the egg chamber: the nurse cells, the oocyte, and the somatic follicle cells. In nurse cells, two distinct types of filaments were seen: a network of small filaments near the plasma membrane as well as a single large filament that was present in each nurse cell (Figure 2.6A). To confirm the results of the GFP-CTP synthase protein trap, we generated polyclonal antibodies against *Drosophila* CTP synthase. Immunostaining using CTP synthase antibodies confirmed that endogenous CTP synthase assembles into filaments in the three cell types that comprise the egg chamber (Figure 2.6B).

Although CTP synthase is present in all of the cell types of the egg chamber, it remained an open question as to whether all cells and tissues possessed CTP synthase filaments. We approached this question by examining the distribution of CTP synthase filaments in the adult *Drosophila* gut. Our staining revealed that CTP synthase forms filaments in a subset of cells in the gut that are proximal to the gut stem cell (Figure 2.6C). Thus, CTP synthase does not form filaments in every cell within a given tissue

in *Drosophila*. Together, these results argue that CTP synthase filament formation is highly regulated in different cell types and tissues.

CTP synthase filament formation is restricted to axons in hippocampal neurons

Because the spatial regulation of cytoskeletal filaments is a common feature of highly polarized cells, we next examined the question of whether CTP synthase filaments could be restricted to particular subcellular domains. To test this possibility, we used immunofluorescence to determine the distribution of CTP synthase filaments in rat hippocampal neurons. These experiments revealed that CTP synthase filaments/foci are restricted to axons and do not occur in dendrites (Figure 2.7). Thus, the ability of CTP synthase to form filaments is spatially controlled within neurons, and these filaments represent a novel axon-specific structure.

Mutations in URA7 that prevent feedback inhibition also block filament formation

Self-assembly of enzymes into large cytoplasmic structures has been hypothesized to play several roles ranging from facilitating biosynthetic pathways to storage of inactive enzymes (An et al., 2008; Sheth and Parker, 2003; Teixeira et al., 2005). However, very little is known about how enzyme activity is coupled to the assembly or disassembly of these large cytoplasmic structures. We have taken advantage of previous enzymatic studies of Ura7p to address this issue.

URA7 encodes the major CTP synthase in *S. cerevisiae* that catalyzes the ATP-dependent transfer of the amide nitrogen from glutamine to UTP to generate CTP and glutamate (Ozier-Kalogeropoulos et al., 1994; Ozier-Kalogeropoulos et al., 1991). CTP synthase activity is regulated by all four nucleotides, and this regulation plays an

important role in maintaining the balance in the pyrimidine nucleoside triphosphate pools. Although GTP is an allosteric regulator of the glutaminase activity of the enzyme, ATP, CTP, and UTP all promote the conversion of CTP synthase to the active tetramer. Interestingly, although CTP binding promotes conversion to the active tetramer, it is unique in that it also acts as a competitive inhibitor of CTP synthase activity (Aronow and Ullman, 1987; Endrizzi et al., 2005; Long and Pardee, 1967; Pappas et al., 1998). Previous enzymatic experiments of Ura7p identified a mutation, E161K, that decreased end product inhibition by lowering the affinity of the enzyme for CTP (Ostrander et al., 1998). This prior work presented us with a unique reagent for testing whether enzyme activity was linked to the ability to form filaments. We constructed strains that expressed E161K Ura7p-GFP as the only form of *URA7* to examine filament formation when grown to saturation. E161K Ura7p formed 20-fold fewer filaments than Ura7p, implying that Ura7p filament formation is strongly associated with decreased CTP binding (Figure 2.8A). Interestingly, although the ability to form filaments was virtually eliminated by the E161K mutation, the frequency of foci formation increased 4.51-fold as compared with wild-type Ura7p. This suggests that the E161K mutation specifically blocks the ability of Ura7p foci to form filaments.

If end product inhibition promotes filament formation, one would also predict that increasing CTP levels would promote self-assembly of CTP synthase. To test this hypothesis, we treated log-phase GFP-Ura7p yeast cells with 10 mg/ml CTP for 15 min (Figure 2.8B). Log-phase yeast cells normally have few Ura7p foci; however, brief exposure to CTP triggered Ura7p self-assembly, causing a 4.4-fold increase in foci. The equivalent treatment of GFP-Glt1p yeast caused no change in the number of Glt1p

filaments and foci, indicating that the effect of CTP was specific for Ura7p self-assembly. These results together with our mutant analysis strongly argue that CTP binding is a potent regulator of CTP synthase self-assembly.

To determine whether other regulatory ligands could also drive foci assembly, we treated log-phase GFP-Ura7p yeast cells with 10 mg/ml ATP for 15 min (Figure 2.8B). Treatment with ATP caused a threefold increase in CTP synthase structures, whereas treatment with GTP caused no significant change in foci formation (Figure 2.8B). These results suggested that regulatory ligands that cause enzyme tetramerization also cause CTP synthase to assemble into foci. To test this possibility, we treated cells with AMP-PNP (adenosine 5′-[β,γ-imido]triphosphate), a nonhydrolyzable analogue of ATP which has been previously shown to inhibit Ura7p tetramerization (Pappas et al., 1998). AMP-PNP treatment caused a fivefold decrease in the formation of CTP synthase structures (Figure 2.8B) (Pappas et al., 1998). Thus, only regulatory ligands that promote tetramerization are capable of triggering foci formation. These results together with the finding that the E161K mutation blocks filament formation without affecting foci formation suggest that both foci and filament formation by CTP synthase structure are regulated: enzyme tetramerization facilitates foci assembly, whereas end product inhibition is required for filament formation. Future studies directed at the precise regulatory state of the enzyme that allows either filaments or foci to form will help determine whether these two structures are related or whether they represent distinct regulatory states of CTP synthase.

The results of our screen of the yeast GFP strain collection argue that regulated self-assembly of different enzymatic pathways is a common type of biochemical

compartmentalization in yeast. Furthermore, we have found that different supramolecular complexes assemble or disassemble in response to distinct environmental conditions. This argues that these different complexes do not form as part of a general stress response but in fact form either to promote or inhibit particular enzymatic processes in response to changing environmental conditions. Additionally, we have found that CTP synthase self-assembly is modulated by the binding of ligands that regulate enzyme activity. This suggests that self-assembly could be a fundamental mode for regulating the enzymes that comprise purinosomes, P bodies, and the additional novel structures that we have identified.

One of the central questions raised by our work in *S. cerevisiae* is whether these structures have additional roles apart from inhibiting or promoting enzyme activity. Clearly, the ability of large cytoplasmic structures to undergo assembly and disassembly in response to changes in the cytoplasmic milieu presents the cell with a unique sensor that could be used to regulate several cellular processes. Although it is currently unclear whether cells use these structures for such a purpose, the fact that CTP synthase forms filaments in axons and not in dendrites suggests that local regulation of filament formation is possible and may be tied to additional cellular functions. Future work directed at understanding how this spatial regulation is achieved will help identify what additional functions these filaments may serve in neurons as well as in other cell types.

Materials and Methods

Yeast strains and media

All yeast strains were derived from a parent strain with the genotype *MATa his3Δ1 leu2Δ0 met15Δ0 ura3Δ0* (S288C). Strains with GFP-tagged genes were from the yeast GFP collection (Howson et al., 2005). All yeast strains were grown at 30°C in YPD unless otherwise indicated. For the testing of various growth conditions, the indicated treatment was applied for 15 min at 22°C unless otherwise noted. For experiments using altered growth media, cells were pelleted, rinsed once with water, and resuspended in the indicated media. Log-phase growth was studied for cells with an OD_{600} under 1.0, and stationary-phase cultures were grown to an OD_{600} of ~5. For Hsp104p overexpression experiments, cells were grown overnight in SD-Leu$^-$ (YNB + 2% glucose + 1× Leu dropout amino acid mix) and then diluted into SGR-Leu$^-$ medium (YNB + 2% galactose + 1% raffinose + 1× Leu dropout amino acid mix) and grown for 4.5 h. These growth conditions blocked the formation of eIF2/2B filaments, preventing the assessment of the effect of Hsp104p overexpression on filament formation.

Plasmids and DNA methods

For plasmid transformation, genomic tagging of specific loci or gene disruption, the LiOAc method was used (Ito et al., 1983). Genomic tagging and gene disruption were accomplished by transforming yeast strains with a PCR product that encoded G418 resistance and 5′ and 3′ 50-bp flanks homologous to the gene of interest (Baudin et al., 1993). Cells with the G418 cassette were allowed to grow on YPD for ~24 h and then replica plated onto YPD + 400 μg/ml G418. Gene disruption or genomic tagging was

confirmed by PCR. The yeast parent strain was a gift from L. Pillus (University of California, San Diego, La Jolla, CA).

PCR for genomic tagging and gene disruption was performed as follows: KOD hot start polymerase (EMD) was used in 100-µl reactions (1× KOD buffer, 1.25 mM $MgSO_4$, 200 µM dNTP, 0.3 µM of each oligonucleotide, and 100 ng of template). The PCR reaction was performed for 95°C for 2 min, followed by 30 cycles of 95°C for 20 s, 50°C for 10 s, and elongation at 70°C for varying amounts of time. The mCherry-tagging construct (pBS34) was obtained from the University of Washington Yeast Resource Center.

URA7-GFP plasmids were constructed with standard molecular biology techniques. To create the E161K point mutant, the splicing by overlap elongation (SOEing) PCR technique was adapted from (Horton et al., 1989). The mCherry-tagging construct (pBS34) was obtained from the University of Washington Yeast Resource Center. The vector used to construct the URA7-GFP plasmids (pRS403) and the construct used for the G418 deletions (pRH728) were gifts from R. Hampton (University of California, San Diego). The Hsp104p overexpression plasmid was a gift of D. Masison (National Institutes of Health, Bethesda, MD) (Hung and Masison, 2006).

Antibody generation

The full-length coding region of CG6854-C, the *Drosophila* CTP synthase, was cloned into ProEXHis and expressed as an N-terminal 6xHis-tagged fusion protein in *Escherichia coli*. Soluble His–CG6854-C was purified using a Ni–nitrilotriacetic acid

affinity column, eluted with imidazole, and injected into rabbits (antiserum production by Covance).

Microscopy

Microscopy was performed on a microscope (Axiovert 200M; Carl Zeiss, Inc.) using the software Metavue version 6.3 (MDS Analytical Technologies). Colocalization experiments were performed with a DeltaVision restoration microscopy system (Applied Precision) and microscope (IX70; Olympus) using the software SoftWoRx (Applied Precision).

Flow cytometry

Cells were grown in liquid YPD cultures to the indicated growth phase. Approximately 1 OD of cells was then centrifuged in an Eppendorf tube, rinsed once with water, and resuspended in water. Fluorescence was measured by a Typhoon 9400, and data were analyzed using ImageQuant 5.2 software (GE Healthcare).

Immunofluorescence

For immunofluorescence, yeast cells were removed directly from a selective plate and fixed in 3.7% formaldehyde for 1 h. This was followed by a wash with SK buffer (1 M sorbitol, 45 mM K_2HPO_4, and 7 mM KH_2PO_4) and then a 20-min incubation in SK buffer with 1% β-mercaptoethanol and 10 U zymolyase. Spheroplasts were resuspended in SK buffer and added to slides coated with polylysine (each well treated with 500 µg/ml polylysine for 10 min, rinsed once with water, and air dried) for 10 min. Samples were fixed in methanol at −20°C for 6 min and then in acetone at −20°C for 2 min. Samples

were blocked with 1% BSA in PBS for 20 min, followed by incubation with α-HA antibody (12CA5; Roche) at 4°C overnight. After BSA-PBS washes, samples were incubated with anti–mouse secondary antibody for 2.5 h at room temperature, followed by further washes and mounting of the coverslip. *Drosophila* immunofluorescence was performed as previously described (Wilhelm et al., 2003). This staining used either α-CG6854 antibodies (1:2,000) to stain wild-type ovaries or α-GFP antibody (1:2,000) to stain the GFP protein trap line, CA07332 (M. Buszczak, University of Texas Southwestern Medical School, Dallas, TX), which tags endogenous CG6854 with GFP (Buszczak et al., 2007).

For neuronal staining, neurons dissected from the hippocampus of rat embryos were plated on coverslips and cultured for 14 d using standard conditions (Patrick et al., 2003). Neurons were washed twice in PBS-MC (1× PBS, 1 mM $MgCl_2$, and 0.1 mM $CaCl_2$) and then fixed in 1× PBS, 4% paraformaldehyde, and 4% sucrose for 10 min at room temperature. The coverslips were then washed twice with 1 ml PBS-MC, followed by additional fixation in 1 ml of 100% MeOH (stored at −20°C) for 2 min at −20°C. The coverslips were then washed twice with 1 ml PBS-MC, followed by blocking with 1 ml blocking/permeabilization solution (1× PBS-MC with 2% BSA and 0.2% Triton X-100) for 20 min. The blocking solution was then removed, and the coverslips were incubated overnight at 4°C in 1× PBS-MC and 2% BSA with primary antibody. The slides were then rinsed three times with PBS-MC, followed by three 5-min PBS-MC washes at room temperature while rotating. The coverslips were then treated with secondary antibody in PBS-MC and 2% BSA for 1 h at room temperature. The secondary antibody was then removed by one 5-min wash in PBS-MC at room temperature while rotating. Slides were

then incubated for 10 min in PBS-MC with 2 µg/ml DAPI, followed by one 5-min wash at room temperature with PBS-MC while rotating. Coverslips were then mounted on slides using Vectashield (Vector Laboratories) and imaged using a laser confocal microscope (TCS SP5; Leica). Primary antibodies were used at the following concentrations: 1:5,000 chicken α-map2c (G. Patrick, University of California, San Diego), 1:100 rabbit α-CG6854 (CTP synthase; bleed no. 110–5), and 1:500 mouse α-tau5 (S. Halpain, University of California, San Diego). Alexa Fluor 488– and Alexa Flour 568–conjugated α-chick, α-rabbit, and α-mouse secondary antibodies (Invitrogen) were all used at 1:200.

Screening of the yeast GFP collection

Individual strains from the yeast GFP collection were inoculated into 5 ml YPD and cultured overnight at 30°C. The overnight culture was then diluted in YPD to an OD_{600} of ~0.1–0.2 and cultured at 30°C until the OD_{600} = 0.4–0.6. Cells from the original overnight culture and the log-phase culture were pelleted and then washed once with sterile water. The cell pellet was then resuspended in 1.2 M sorbitol and 0.1 M KPO_4 and mounted for imaging with a spinning disk confocal microscope.

Acknowledgements

We would like to thank L. Pillus, R. Hampton, G. Patrick, D. Masison, and M. Buszczak for reagents and technical assistance with this project.

Chapter 2 is a reprint of Noree, C., Sato, B.K., Broyer, R.M., Wilhelm, J.E. "Identification of novel filament-forming proteins in *Saccharomyces cerevisiae* and *Drosophila melanogaster*". *Journal of Cell Biology*. 2010. 190(4): 541-551. I was the primary experimenter. B. Sato performed the experiments appeared in Figures 2.3C-H, 2.4 and Table 2.2. The results appeared in Figure 2.7 were obtained by R. Broyer. J. Wilhelm wrote the manuscript and performed experiments in Figure 2.6. The paper was edited to be in a proper format for this Chapter.

Figure 2.1 Identification of nine proteins capable of filament formation in *S. cerevisiae*

(A) Nine filament-forming proteins were identified by visual screening of the *S. cerevisiae* GFP strain collection: Glt1p (glutamate synthase), Psa1p (GDP-mannose pyrophosphorylase), Ura7p (CTP synthase), Ura8p (CTP synthase), Gcd2p (eIF2B-δ), Gcd6p (eIF2B-ε), Gcd7p (eIF2B-β), Gcn3p (eIF2B-α), and Sui2p (eIF2-α). (B) The nine proteins that are capable of forming filaments were found to reside in four distinct filaments. All images are of cells grown to saturation except for subunits of the eIF2/2B complex, which were from log-phase cultures. These conditions were chosen because they maximized filament formation for the respective subunits.

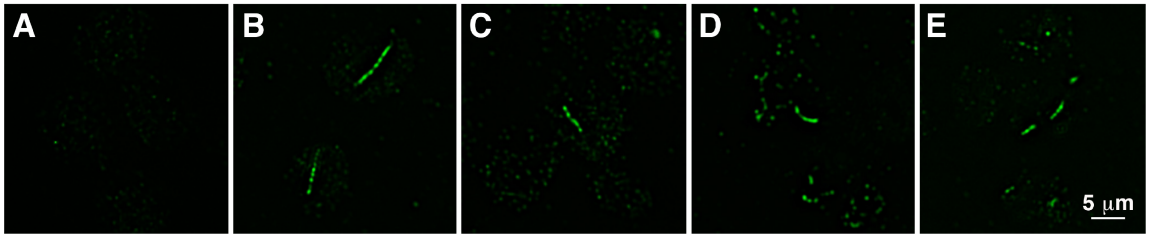

Figure 2.2 Filament formation is independent of the GFP tag

Filament formation occurs normally when a HA epitope tag is used to label filament-forming proteins. (A) Wild-type untagged strain. (B) Gcd2p-HA. (C) Glt1p-HA. (D) Psa1p-HA. (E) Ura7p-HA.

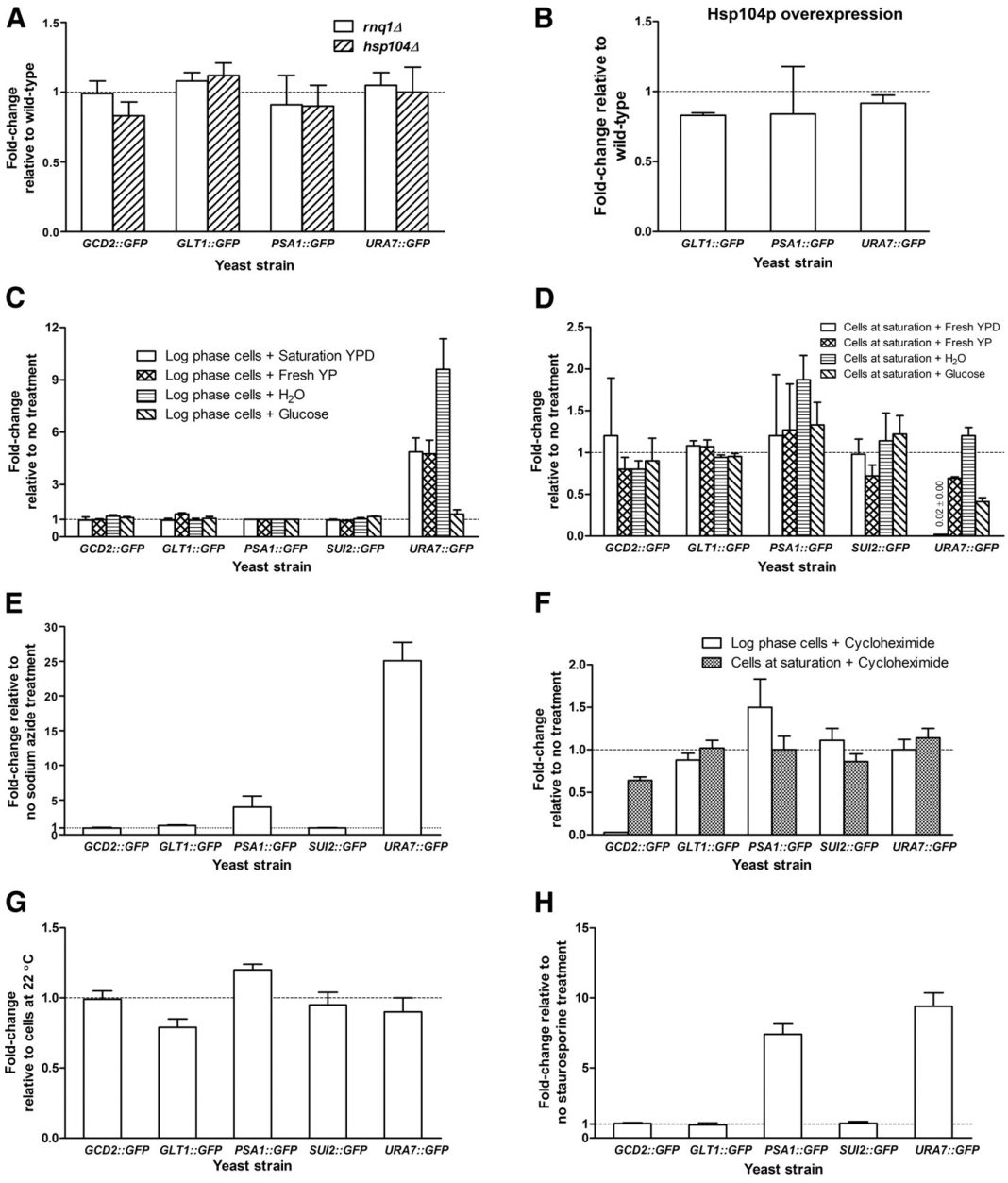

Figure 2.3 Regulation of filament formation

(A) Filament formation is not dependent on either *HSP104* or *RNQ1*. (B) Overexpression of Hsp104p does not affect the formation of Glt1p, Psa1p, or Ura7p filaments. (C) Media lacking glucose strongly induces Ura7p filaments. (D) The addition of media containing glucose triggers disassembly of Ura7p filaments. (E) Treatment with sodium azide causes an increase in Psa1p and Ura7p filaments. (F) Treatment with the translation inhibitor cycloheximide decreases the number of Gcd2p filaments. (G) Exposure of cells to 4°C has no effect on filament formation. (H) Treatment with the kinase inhibitor staurosporine increases Psa1p and Ura7p filaments. (A–H) Error bars represent standard error of the mean. Dashed lines mark the position on the graph where there is no change relative to the reference condition.

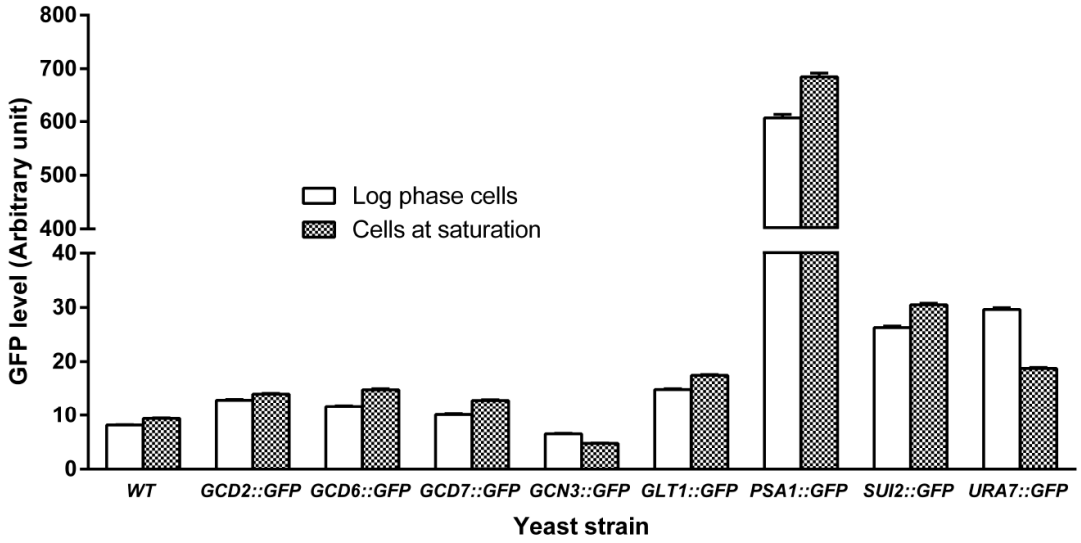

Figure 2.4 The protein expression level of filament-forming proteins does not change greatly between log-phase growth and saturation

For the majority of filament-forming proteins, there was little change in protein levels between log-phase growth and saturation. For Ura7p, protein levels declined for cells grown to saturation. Together, these results argue that filament formation is driven by large-scale changes in protein level. Error bars represent standard error of the mean.

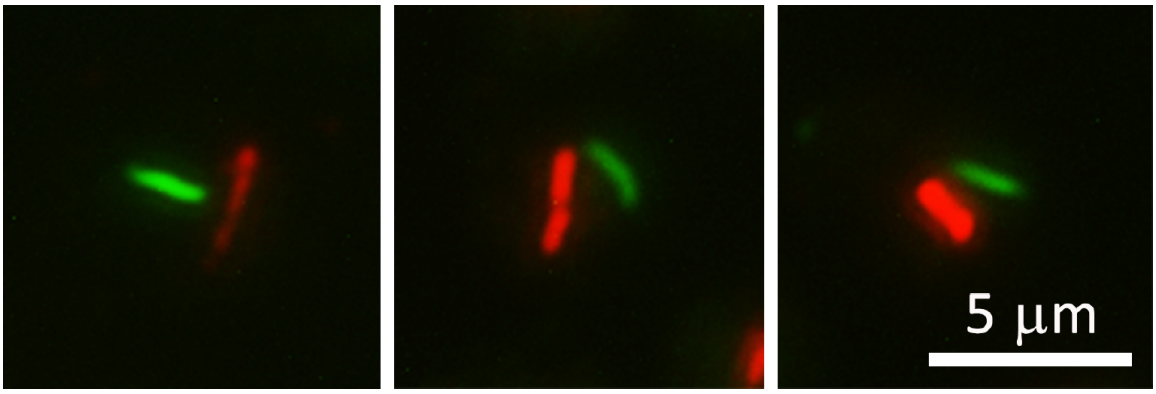

Figure 2.5 Ura7p filaments do not colocalize with microtubules

Images of three different yeast cells stained for both microtubules and Ura7p-GFP are shown. Ura7p is green, and microtubules are red.

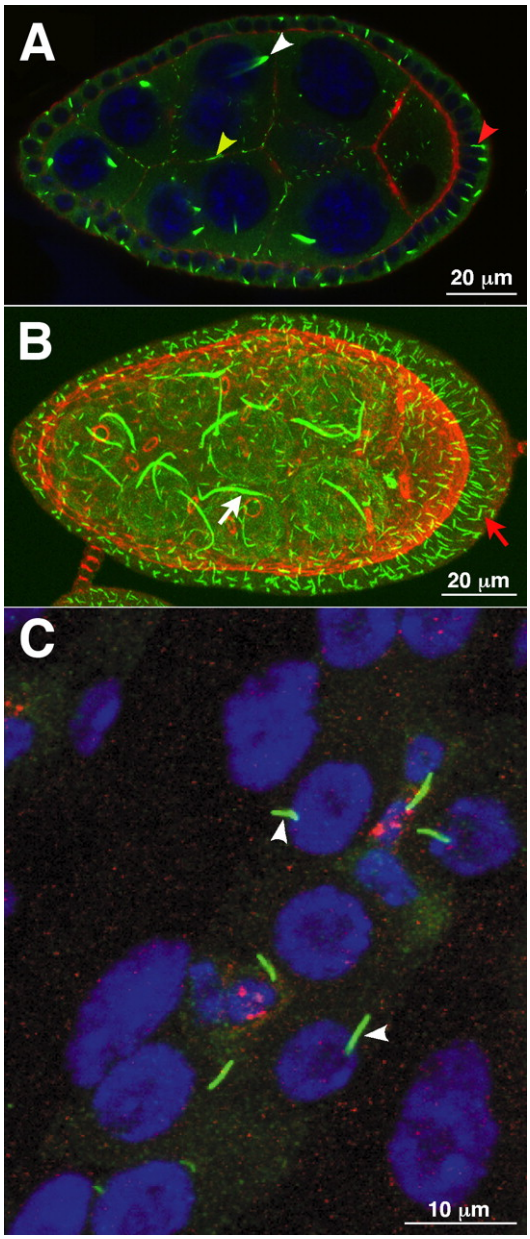

Figure 2.6 Filament formation is evolutionarily conserved

(A) A single confocal section of a *Drosophila* egg chamber. GFP–CTP synthase (green) is present in small filaments (yellow arrowhead) along the plasma membrane and in large filaments in both the somatic follicle cells (red arrowhead) and nurse cells (white arrowhead). Actin is red, and DNA is blue. (B) A projection of multiple confocal sections of an egg chamber stained with anti–CTP synthase antibody. Large filaments are present in the germline (white arrow) as well as in the somatic follicle cells (red arrow). Actin is red, and CTP synthase is green. (C) In the adult *Drosophila* gut, GFP–CTP synthase (green) labels filaments (arrowheads) in cells clustered near the presumptive gut stem cell, labeled with Delta (red). DNA is blue.

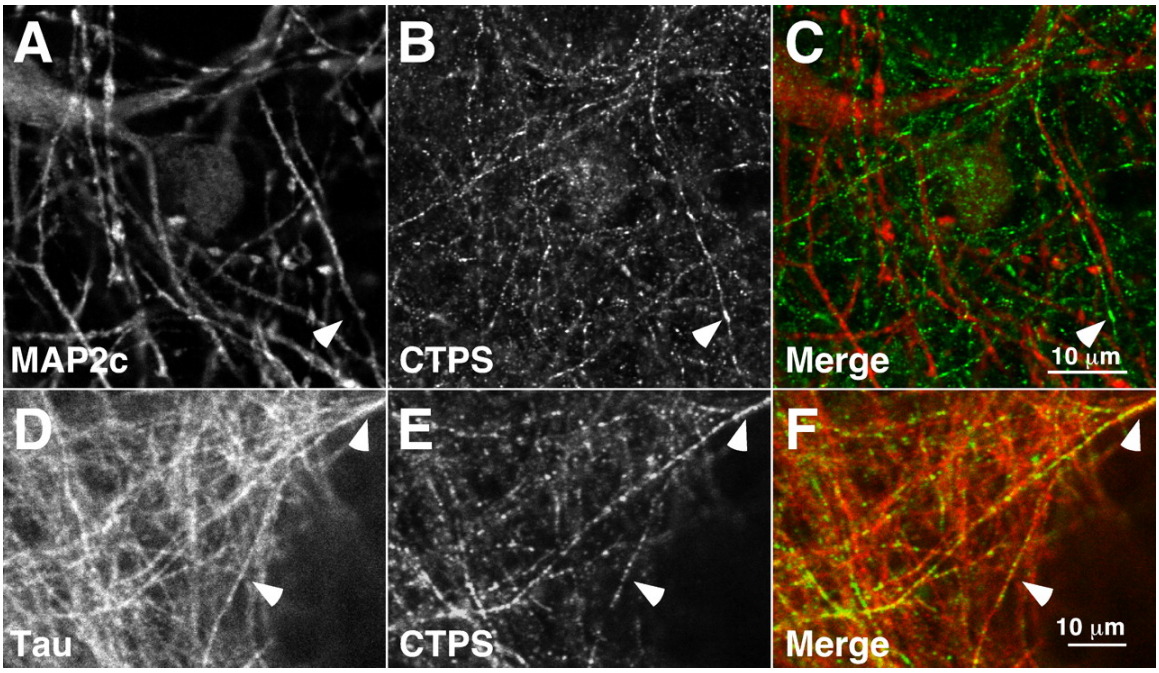

Figure 2.7 CTP synthase self-assembles in axons but not in dendrites

CTP synthase (CTPS) filaments are present in axons (arrowheads) but not dendrites. CTP synthase does not form filaments or foci in dendritic processes. (A–C) MAP2c (A), CTP synthase (B), and a merge (C) are shown. MAP2c is red, and CTP synthase is green. CTP synthase forms filaments and foci in axons (arrowheads). (D–F) Tau (D), CTP synthase (E), and a merge (F) are shown. Tau is red, and CTP synthase is green.

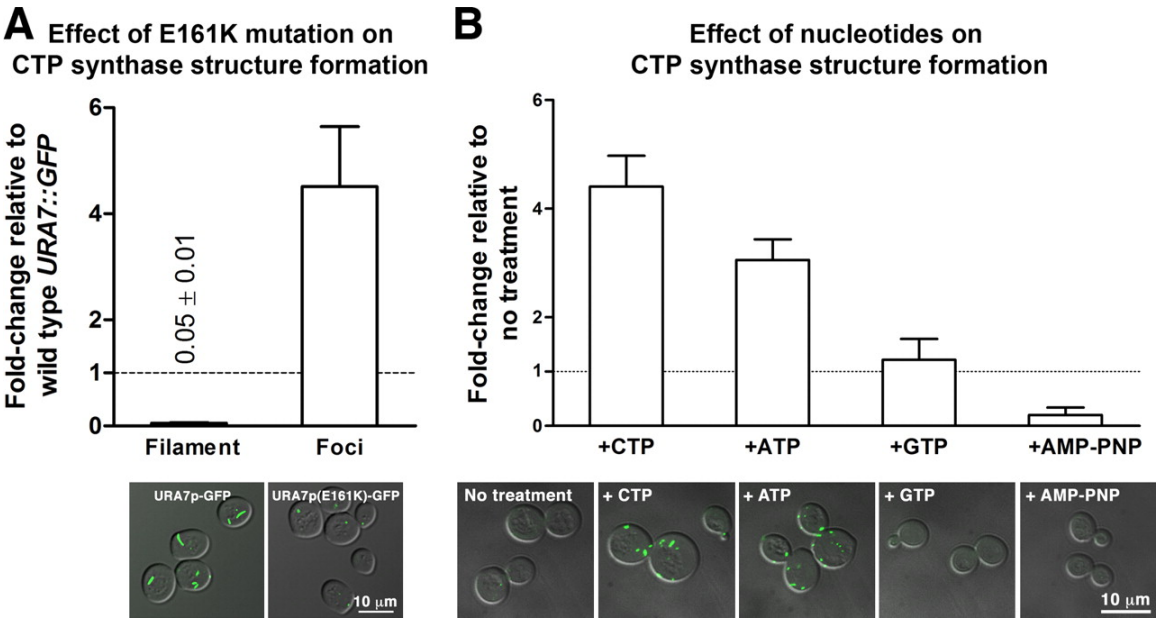

Figure 2.8 End product inhibition promotes CTP synthase filament formation

(A) The E161K mutation causes a 20-fold decrease in Ura7p filament formation. (B) Treatment with CTP and ATP increases Ura7p self-assembly into foci. (A and B) Error bars represent standard error of the mean. Dashed lines mark the position on the graph where there is no change relative to the reference condition.

Table 2.1 Proteins that assemble into intracellular structures

Foci-forming protein	Biological process
Prs4p	5-phosphoribose 1-diphosphate biosynthetic process
Acs1p	Acetate fermentation/acetyl-CoA biosynthetic process/histone acetylation
Glt1p	Ammonia assimilation cycle/glutamate biosynthetic process
Ssd1p	Cell wall organization/chronological cell aging/replicative cell aging
Ura7p	CTP synthesis
Hsp42p	Cytoskeleton organization/response to stress
Rnr4p	Deoxyribonucleotide biosynthetic process
Rnr2p	Deoxyribonucleotide biosynthetic process
Psa1p	GDP-mannose biosynthetic process/protein amino acid glycosylation
Gln1p	Glutamine biosynthetic process/nitrogen compound metabolic process
Dug2p	Glutathione catabolic process
Gly1p	Glycine biosynthetic process/threonine catabolic process
Gsy2p	Glycogen biosynthetic process
Gdb1p	Glycogen catabolic process
Gph1p	Glycogen catabolic process
Hem2p	Heme biosynthetic process
His4p	Histidine biosynthetic process
Hek2p	Intracellular mRNA localization/telomere maintenance via telomere
Rim20p	Invasive growth in response to glucose limitation/protein processing/proteolysis
Sam1p	Methionine metabolic process/S-adenosylmethionine biosynthetic process
Sam2p	Methionine metabolic process/S-adenosylmethionine biosynthetic process
Hsp104p	Protein folding
Ssa1p	Protein folding
Sse2p	Protein folding
Ssa2p	Protein folding
Sis1p	Protein folding
Rpn9p	Proteosome assembly/ubiquitin-dependent protein catabolic process
Gcd6p	Regulation of translation initiation
Sui2p	Regulation of translation initiation
Gcd2p	Regulation of translation initiation
Gcd7p	Regulation of translation initiation
Gcn3p	Regulation of translation initiation
Sgt2p	Response to heat (glutamine-rich cytoplasmic protein of unknown function)
Thr1p	Threonine metabolic process
YAR009Cp	Transposition, RNA mediated
YLR143Wp	Unknown
YMR253Cp	Unknown

Table 2.2 Frequency of filament formation in yeast during log-phase growth and at saturation

GFP strain	Percentage of cells with filaments during log phase (%)	Percentage of cells with foci during log phase (%)	Percentage of cells with filaments at saturation (%)	Percentage of cells with foci at saturation (%)
URA7	0.00 ± 0.00	3.80 ± 1.35	15.20 ± 2.35	5.60 ± 0.38
URA8	0.00 ± 0.00	0.00 ± 0.00	16.40 ± 1.80	3.60 ± 0.74
PSA1	0.00 ± 0.00	0.40 ± 0.08	7.80 ± 0.67	4.80 ± 1.17
GLT1	26.80 ± 3.69	10.40 ± 1.38	39.20 ± 2.05	6.40 ± 1.95
SUI2	66.20 ± 0.87	6.00 ± 0.63	34.60 ± 3.36	5.20 ± 1.17
GCD2	58.40 ± 2.17	9.00 ± 0.37	18.60 ± 2.88	3.60 ± 0.97
GCD6	11.00 ± 0.60	6.40 ± 1.04	18.80 ± 0.98	7.20 ± 1.36
GCD7	37.60 ± 4.52	24.00 ± 4.63	21.00 ± 1.54	19.80 ± 2.17
GCN3	2.80 ± 0.75	0.00 ± 0.00	12.20 ± 0.59	2.80 ± 0.98

Chapter 3

Common regulatory control of CTP synthase enzyme activity and filament formation

Abstract

The initially unexpected ability of enzymes to assemble into large supramolecular complexes is now appreciated to be a widespread phenomenon. Such complexes have been hypothesized to play a number of roles, such as the facilitation of substrate channeling and the storage of inactive enzymes. However, little is known about how the regulation of enzyme activity is coupled to the assembly, or disassembly, of these large cellular structures. To begin addressing this question, we have characterized the yeast enzyme CTP synthase (Ura7p) using a structure-function approach in which specific regulatory sites were disrupted by mutagenesis and the effects on filament assembly assayed. CTP synthase is an ideal model system because of its evolutionarily conserved ability to form filaments and its regulation by at least four distinct mechanisms common among enzymes, including oligomerization, feedback inhibition, allosteric activation, and phosphorylation. Our results reveal that destabilization of the active tetrameric form of the enzyme increases the frequency of filament formation, suggesting that the observed filaments are comprised of inactive CTP synthase dimers. Furthermore, the sites responsible for feedback inhibition and allosteric activation control the length of filaments formed, implying that multiple regions of the enzyme can influence filament structure. In contrast to these regulatory mutations, a catalytically inactivating mutation does not affect filament formation frequency or length. Together our results argue that the regulatory sites that control CTP synthase function, but not enzymatic activity *per se*, are critical for controlling the process of filamentation. We predict that the ability of biosynthetic enzymes to form supramolecular structures in general may be closely coupled to mechanisms that regulate their enzymatic activity.

Introduction

The last several years have seen an explosion in the identification of novel intracellular structures (An et al., 2008; Campbell et al., 2005; Ingerson-Mahar et al., 2010; Liu, 2010; Narayanaswamy et al., 2009; Noree et al., 2010; Sheth and Parker, 2003). While the macromolecular components and putative functions of these large cytoplasmic structures are diverse, they share a common theme: each class of structure is formed from enzymes that act in a specific biochemical or regulatory pathway. For example, processing bodies are visible supramolecular complexes comprised of messenger RNAs and many of the enzymes that regulate their translation and stability (Sheth and Parker, 2003). Similarly, purinosomes assemble from a subset of enzymes in the *de novo* purine biosynthesis pathway in response to purine deprivation, in order to accelerate flux through the pathway via substrate channeling (An et al., 2010a; An et al., 2008; An et al., 2010b). Strikingly, recent visual screens of the yeast GFP strain collection have revealed that multiple metabolic enzymes self-assemble into filaments, arguing that this mode of regulation could play a role in the control of many biosynthetic pathways (Narayanaswamy et al., 2009; Noree et al., 2010). However, while the pace at which novel cytoplasmic structures are being identified continues to accelerate, little is known about how specific enzyme regulatory mechanisms impact the large cytoplasmic structures they form.

In order to assess whether the regulation of enzyme activity controls the assembly of such supramolecular structures, we have focused our studies on a single class of novel intracellular filaments: those formed by the *S. cerevisiae* enzyme CTP synthase (Ura7p). *URA7* encodes the major CTP synthase in *S. cerevisiae*, which catalyzes the ATP-

dependent transfer of nitrogen from glutamine to UTP, generating CTP and glutamate (Figure 3.1A) (Ozier-Kalogeropoulos et al., 1994; Ozier-Kalogeropoulos et al., 1991). The two halves of this reaction require both the C-terminal glutamine amidotransferase (glutamine → glutamate + NH_3) and the N-terminal amidoligase (ATP + UTP + NH_3 → ADP + CTP) domains of the enzyme (Figure 3.1A).

Ura7p/CTP synthase has several features that make it an ideal model system for exploring the functional principles underlying intracellular structure formation. First, extensive studies of CTP synthase regulation in yeast and other organisms have defined multiple ligands that either stimulate (ATP, GTP, and UTP) or inhibit (CTP) enzyme activity (Aronow and Ullman, 1987; Endrizzi et al., 2005; Levitzki and Koshland, 1972a; Levitzki and Koshland, 1972b; Long and Pardee, 1967; Pappas et al., 1998). These nucleotides regulate catalysis via three distinct mechanisms that control many enzymes: allosteric activation (GTP), tetramerization (ATP, UTP, CTP), and competitive feedback inhibition (CTP) (Aronow and Ullman, 1987; Endrizzi et al., 2005; Levitzki and Koshland, 1972a; Levitzki and Koshland, 1972b; Long and Pardee, 1967; Pappas et al., 1998). In addition, several phosphorylation sites have been identified that also modulate enzyme activity (Chang et al., 2007; Choi and Carman, 2007; Choi et al., 2003; Park et al., 2003; Park et al., 1999; Yang et al., 1996; Yang and Carman, 1996). Mutations that disrupt each of these regulatory mechanisms have been previously identified and characterized (Lunn et al., 2008; Whelan et al., 1993; Willemoes et al., 2005). Finally, multiple prokaryotic and eukaryotic CTP synthases form filaments, arguing that this property is evolutionarily conserved (Figure 3.2) (Ingerson-Mahar et al., 2010; Liu, 2010; Noree et al., 2010). Thus, CTP synthase is an excellent proving ground for deciphering

how classical mechanisms of enzyme regulation are connected to the assembly of supramolecular structures.

Here we have utilized a structure-guided site-directed mutagenesis strategy to specifically target the major regulatory sites in CTP synthase (Figure 3.1B and 3.1D) and assess their role in controlling the frequency of CTP synthase filament/foci formation as well as filament/foci length. Mutations that perturb a regulatory loop adjacent to the putative allosteric GTP binding cleft and the ATP, UTP and CTP binding sites stimulate the frequency of filament/foci formation. Given that ATP, UTP and CTP all stabilize the catalytically active tetramer of CTP synthase, our results argue that the basic unit of CTP synthase filaments is the inactive dimeric form of the enzyme. Our studies of filament length demonstrate that there are two populations of wild type CTP synthase filaments: very short "foci-like" structures and long filaments. Sites of substrate binding and end-product inhibition located on the amidoligase domain as well as allosteric activation on the glutamine amidotransferase domain are key regulators of filament length. A phosphorylation site on the glutamine amidotransferase domain also plays a role. These data suggest that both domains of the protein contribute to polymer structure. In contrast, a non-regulatory mutation that compromises the glutamine amidotransferase active site has no effect on CTP synthase filament/foci formation or length. In sum, CTP synthase filament/foci formation and structure are intimately connected with the major mechanisms used to regulate enzyme activity, but not catalytic function itself.

Results

CTP synthase filaments exhibit a bimodal length distribution

Previous analyses reporting the discovery of CTP synthase filament formation in yeast, *Drosophila*, and bacteria have described filament length of the wild-type enzyme using a qualitative classification scheme or as a single parameter such as average length (Ingerson-Mahar et al., 2010; Liu, 2010; Noree et al., 2010). A detailed analysis of Ura7-GFP filaments under our standard growth conditions for inducing filament formation, i.e., growth to saturation (OD_{600} > 7) at 30°C in YPD (2% peptone, 1% yeast extract, 2% dextrose), revealed a bimodal distribution of lengths. The first peak was comprised of short, foci-like structures (<0.75 μm in length; ~31% of the population), while the second peak was comprised of clearly defined filaments (>0.75 μm in length; ~ 69% of the population) (Figure 3.3). Thus, in order to provide the most quantitative assessment of the effects of mutations on filament assembly, we carefully measured two aspects of filament formation: (1) the frequency, defined as the percentage of cells possessing Ura7p-GFP filaments/foci, and (2) the length distribution of Ura7p-GFP filaments/foci.

Blocking UTP-mediated tetramerization increases the frequency of CTP synthase filament formation without altering the length distribution

We first examined whether tetramerization of the enzyme plays a role in CTP synthase filament formation. In the absence of nucleotides, CTP synthase is a catalytically inactive, tightly associated dimer (Pappas et al., 1998). In the presence of ATP, UTP or CTP, two dimers associate to form a tetramer (Figure 3.1C). This oligomerization event is required for proper function of both the glutamine

amidotransferase and amidoligase active sites (Pappas et al., 1998). Structural studies indicate that the dimer and tetramer interfaces are stabilized almost exclusively by polar and hydrophobic contacts between the amidoligase domains of the component monomers (Endrizzi et al., 2004; Goto et al., 2004). In the *E. coli* enzyme, a mutation in the binding site of the substrate UTP, which lies in the amidoligase domain near the tetramer interface, has been shown to severely compromise UTP binding and catalytic activity (Simard et al., 2003). Strains expressing Ura7p-GFP with the equivalent mutation (G148A) expressed from the endogenous *URA7* locus (see Materials and Methods) displayed a ~2.8 fold increase in the percentage of cells that form filaments/foci as compared to wild type (Table 3.1; Figure 3.4A). However, neither the median length nor the length distribution of the filaments was significantly altered by the G148A mutation (Table 3.1; Figure 3.4B). To determine if the enhanced filament formation caused by disruption of UTP binding was the consequence of destabilization of the tetramer and/or blockade of catalytic activity, we exploited previous studies that indicated that mutation of the active site cysteine of the glutamine amidotransferase domain eliminated enzyme activity (Figure 3.4A) (Paluh et al., 1985). We found that a strain expressing C404G Ura7p-GFP showed no significant difference in the number of cells with observable filaments or in filament length distribution relative to those expressing wild-type (Table 3.1; Figure 3.4A and B). Therefore, since merely inactivating CTP synthase catalytic activity had no effect on filament formation, we conclude that the increased filament formation of the G148A mutant is due to decreased UTP-stimulated tetramerization. These results also argue that Ura7p filaments are comprised of inactive dimers.

Increased catalytic activity is not responsible for the block in filament formation observed in feedback-resistant mutants of Ura7p

Our findings with the UTP binding site mutant led us to re-examine the role of CTP binding site mutations in regulating filament assembly. We previously found that the amidoligase domain mutation, E161K, which blocks feedback inhibition of yeast CTP synthase by CTP, abrogates the formation of full-length filaments, while also causing an increase in the formation of foci-like structures (Noree et al., 2010). Given this effect, we decided to use our new quantitative definition of foci and filaments to examine how this mutation affects the different types of structures that can be formed by CTP synthase. Analysis of the length distribution of the structures formed by E161K Ura7p-GFP revealed that when feedback inhibition is blocked, CTP synthase filament formation is completely disrupted and the enzyme can only form foci (Figure 3.5A and B). This strongly argues that feedback inhibition regulates the distribution of CTP synthase between filaments and foci.

The E161K mutation decreases the affinity of the enzyme for CTP, which 1) negatively impacts tetramerization and 2) increases enzyme activity since CTP is a competitive inhibitor of the enzyme (Ostrander et al., 1998). This apparently paradoxical behavior is highly dependent upon CTP concentrations. CTP synthase activity is stimulated by low concentrations of CTP due to increased tetramerization, whereas it is inhibited at high concentrations due to the overlap of the CTP and UTP binding sites (Endrizzi et al., 2004; Long and Pardee, 1967). To separate these two effects, we once again leveraged the properties of the C404G active site mutation (Figure 3.5A and B). If the effects of blocking feedback inhibition on filament formation/length are primarily due

to an increase in CTP synthase activity, we would predict that a Ura7p that is defective for both feedback inhibition and enzymatic function would form primarily filaments at the wild-type frequency. Therefore, we constructed a strain that expresses Ura7p-GFP bearing the feedback resistance mutation, E161K and the inactivating C404G mutation. Analysis of the length distributions of E161K-C404G Ura7p-GFP filaments indicated that the double mutant can still only form foci (99% of structures <0.75 μm) (Table 3.1; Figure 3.5A and B). The only difference between E161K Ura7p and the double mutant was a decrease in the frequency of foci formation to a value that was still significantly greater than that of wild-type (99% for E161K vs. 64% for E161K-C404G). Thus, we conclude that product binding regulates the distribution of CTP synthase between foci and filaments and that this effect is not dependent on competitive inhibition of catalytic activity. Further, the increased propensity of the E161K Ura7p to form foci, like that of the G148A mutant to form filaments, suggests that these mutations increase structure formation frequency via their common ability to inhibit nucleotide-stimulated tetramerization of the amidoligase domain.

Mutations in the ATP binding site of CTP synthase increase filament formation

We next investigated the role of the final nucleotide known to modulate tetramer formation, the substrate ATP. In the crystal structure of the ADP/CTP bound form of the *E. coli* CTP synthase (Endrizzi et al., 2005), the carboxylates of D72 and E140 (located in the amidoligase domain) chelate a magnesium ion that binds the β-phosphate of ADP. Hence, we predict that mutation of the equivalent residues in Ura7p (D70 and E146) should compromise ATP binding and hydrolysis. Strains expressing D70A and E146A

Ura7p-GFP exhibited a ~2-fold increase in the numbers of cells containing filaments (Table 3.1; Figure 3.6). In addition, the D70A and E146A mutant filaments were 15% shorter and 16% longer than wild-type. Not only do these results further support the role of tetramerization in filament formation frequency, they also highlight another region of the amidoligase domain involved in filament structure.

The allosteric GTP binding site regulates both the frequency of formation and the length of CTP synthase filaments

GTP is unique amongst the four nucleotide regulators of CTP synthase activity in that it is neither a substrate nor a product of CTP synthase. Instead, GTP is a positive allosteric regulator that acts to increase the rate of catalysis (k_{cat}) of the glutamine hydrolysis reaction (Levitzki and Koshland, 1972b; Willemoes et al., 2005). Multiple mutations that alter allosteric regulation of the enzyme have been identified in the L11 loop of CTP synthase, a mobile segment of the protein adjacent to the allosteric GTP binding cleft. Based on structural homology to the small GTP binding proteins, EF-Tu and EF-G, as well as other related glutamine amidotransferases, this loop has been proposed to form a "lid" that closes over the active site to enhance catalysis (Endrizzi et al., 2004; Willemoes et al., 2005). To ask whether the L11 lid plays a role in Ura7p filament formation, we first focused on analyzing the effects of two L11 lid mutants, R381M and R381P, which inhibit GTP binding and activation of CTP synthase from *L. lactis* (Figure 3.7A) (Willemoes et al., 2005). Strikingly, yeast strains that express either R381M or R381P Ura7p-GFP exhibited a ~3 fold increase in the number of cells forming filaments, compared to strains expressing wild type Ura7p-GFP (Table 3.1; Figure 3.7B).

Furthermore, the filaments formed by both mutants were significantly longer than those formed by wild type Ura7p-GFP. Indeed, the R381M mutation caused a 33% increase in median filament length, while the R381P mutation caused a 15% increase (Table 3.1). Indeed, 86% and 82% of structures formed by the R381M and R381P mutant CTP synthases, respectively, were longer than 0.75 μm (both percentages were greater than the 69% of structures that are >0.75 μm in wild type) (Figure 3.7B).

To further explore the importance of the L11 lid in filament formation, we characterized a third mutant, G382A, which in *L. lactis* CTP synthase increases the capacity of GTP to stimulate glutamine amidotransferase activity (Willemoes et al., 2005). Interestingly, when this mutation was introduced into Ura7p, it, like the R381 mutations, caused a ~2.2 fold increase in the number of cells with filaments/foci (Figure 3.7B), however the median length of the filaments was shortened by 25% (Table 3.1; Figure 3.7C). This change in median length was also reflected in a shift in the distribution of structures from long filaments to short foci, with only 54% of the structures formed by G382A Ura7p-GFP having a length >0.75 μm as compared to 69% of structures formed by wild type Ura7p-GFP. We conclude that the L11 lid contributes to regulating of both the frequency of filament formation and filament length. Moreover, activating and inactivating mutations in the allosteric control region of CTP synthase have opposing effects on filament length.

Phosphorylation is not a major regulator of CTP synthase filament formation

Yeast CTP synthase filament formation is potently stimulated by the kinase inhibitor staurosporine (Noree et al., 2010). This suggested to us that phosphorylation of

CTP synthase might play a direct role in regulating filament formation. Previous studies identified four major phosphorylation sites in yeast Ura7p, S36, S330, S354, and S424, that affect its catalytic activity (Choi et al., 2003; Park et al., 2003). Specifically, phosphorylation at S36, S354, or S424 stimulates Ura7p catalytic activity, while phosphorylation at S330 inhibits enzyme activity (Choi et al., 2003; Park et al., 2003). To determine whether any of these phosphorylation sites play a role in regulating filament formation, we generated yeast strains expressing mutant forms of Ura7p-GFP where single phosphorylation sites were inactivated by changing the serine in the site to alanine.

The S36A mutation caused a ~2-fold decrease in the frequency of filament formation (13.9% vs. 26% for WT), but had little effect on the length of the filaments formed (Figure 3.8A and B). This result suggested that phosphorylation at S36, in particular, might be required for efficient filament assembly. To test this possibility, we changed S36 to either aspartate or glutamate, two amino acid changes that are often used to mimic phosphorylation at serine. If phosphorylation of S36 were required for efficient nucleation of filaments, we would expect that these mutations would increase the frequency of filament formation. However, both the S36D and S36E mutations caused a ~5-fold decrease in the frequency of filament formation (Table 3.1). This result suggests that either the S36D and S36E mutations do not properly mimic phosphorylation at S36 or, alternatively, that S36 is merely an important residue for initiating filament formation independent of its phosphorylation state. In the *E. coli* CTP synthase crystal structure (Endrizzi et al., 2004), the equivalent residue, I38, is completely buried behind the ATP binding site. Therefore, it is likely that the S36 mutations are perturbing the structure of

CTP synthase (and filament formation) via alterations in hydrophobic packing (S36A mutation) or the introduction of a buried charge (S36D and S36E mutations).

In contrast, changing serines S354, S424, or S330 to alanine had no effect on the frequency of cells showing filament formation (Figure 3.8A). However, the S354A mutation caused a significant shift in the length distribution toward shorter structures, suggesting S354 might play a role in length control (Table 3.1; Figure 3.8B).

Discussion

The discovery of large numbers of enzymes that assemble into distinct intracellular structures in response to specific metabolic conditions has suggested that the formation of these structures is connected to the regulation of their enzyme activity. In order to address this, we have used the highly conserved filament forming behavior of CTP synthase as a test case to determine how enzyme activity is connected to filament formation. Yeast CTP synthase is activated by GTP-induced allosteric changes, ATP/UTP/CTP-induced tetramerization, and it is inhibited by CTP via feedback repression (Pappas et al., 1998). Phosphorylation has also been found to both positively and negatively regulate enzyme activity (Choi et al., 2003; Park et al., 2003). Here, we have systematically mutated sites required for these forms of enzyme regulation to assess their role in controlling CTP synthase filament formation. These studies revealed that the regulation of CTP synthase activity is tightly coupled to the control of filament formation and/or filament length. Furthermore, our results argue that CTP synthase filaments are comprised of an inactive form of the enzyme. Since many enzymes that form foci/filaments are regulated by mechanisms similar to those that control CTP synthase, our work suggests that the close coupling of enzyme activity to filament assembly may be a general feature of this class of metabolic enzymes.

Strikingly, our studies found that a mutation in the UTP binding site that blocks tetramerization increases the frequency of filament formation without altering the length distribution of the filaments. Since only the tetrameric form of CTP synthase is active, this is strong evidence that CTP synthase filaments are comprised of the inactive form of the enzyme. The finding that an active site mutation that blocks catalytic activity has no

effect on filament length or frequency suggests that it is not the loss of catalytic activity that drives filament formation, but the shift towards dimers that is responsible for the observed effects. These data are consistent with the fact that two mutations engineered to cripple binding of ATP (D70A and E146A) and hence tetramerization also increase filament formation but do not affect filament length (not shown).

While the model of a CTP synthase filament comprised of dimers is an attractive one, our studies of the L11 lid suggest that there are additional conformational changes that are required for efficient filament formation. All of the mutations in the L11 lid that we analyzed increased the frequency of filament formation suggesting that the conformation of this domain clearly contributes to the regulation of filament formation. Both mutations that prevent allosteric regulation by GTP, as well as one that causes increased activation by GTP, increase filament formation. However, they have opposite effects on filament length. This suggests that there are specific conformational changes within the L11 lid and likely other parts of the glutamine amidotransferase domain that affect the ability of CTP synthase to form either long filaments or short foci.

Another major site for controlling the length distribution of CTP synthase filaments is the feedback inhibition site. An E161K mutation blocks CTP binding to CTP synthase causing a corresponding increase in enzyme activity due to the loss of feedback inhibition by CTP as well as a decreased tendency to tetramerize. Our quantitative analysis of this mutation revealed that it completely eliminates filament formation, producing only foci and further causing an increase in the frequency of foci formation. Furthermore, our analysis of an Ura7p double mutant that has lost both feedback inhibition (E161K) and is catalytically defective (C404G) found that catalytic activity is

not required for the loss of filament formation, arguing that the increase in enzyme activity is not responsible for the block in filament formation. Thus, like the UTP/ATP substrate binding sites, the product feedback inhibition site probably increases the frequency of structure formation via effects on tetramer formation. Further, like the allosteric L11 lid, this site also plays a critical role in controlling filament length/structure.

Interestingly, while disruption of tetramerization, allosteric regulation, and feedback inhibition all appear to have strong effects on filament formation, only one of the four phosphorylation site mutations, S354A, had effects on filament formation that could not be attributable to the likely disruption of the CTP synthase structure. S354 appears to contribute to the control of filament length since the S354A mutation caused an increase in foci relative to filaments, while leaving the frequency of filament formation unaltered. Intriguingly, this residue is located on a surface loop ~10-15 Åfrom the L11 lid on the same face of the glutamine amidotransferase domain, further suggesting that this domain plays a critical role in filament structure.

In sum, our results argue that the mechanisms that control CTP synthase activity, allosteric changes, tetramerization, feedback inhibition and phosphorylation, are also regulators of both the length of CTP synthase filaments and number of CTP synthase filaments that form. These data would be consistent with a model of a CTP synthase polymer in which inactive dimers of the enzyme interacted via the surface of the glutamine amidotransferase domain containing the L11 lid and the surface of the amidoligase domain near the CTP binding site. Further structural studies will be required to confirm this proposal. The regulation of supramolecular complex formation in other

enzymes may be similarly coupled to the known mechanisms for regulating the activity of those enzymes.

Materials and Methods

Media and Yeast Strains

All yeast strains were derived from a parent strain with the genotype *MATa his3Δ1 leu2Δ0 met15Δ0 ura3Δ0* (S288C). Strains with GFP tagged genes were from the yeast GFP collection (Howson et al., 2005). All yeast strains were grown at 30°C in YPD (2% peptone, 1% yeast extract, 2% dextrose) unless otherwise indicated**.**

URA7-GFP plasmids were constructed with standard molecular biology techniques. A DNA cassette containing *URA7::GFP* plus 501 base pairs of flanking sequence was amplified by PCR from genomic DNA isolated from yeasts containing *URA7::GFP* (from the yeast GFP collection, Invitrogen^{TM}) using JW1064 and JW925 (sequences available on request). This URA7-GFP cassette was then subcloned into a pRS403 plasmid (a gift from Dr. Randy Hampton). The resulting plasmid, named JW206 (created by Dr. Brian Sato), was then used as a base plasmid for generating mutations in the URA7 gene by PCR-based site-directed mutagenesis (Noree et al., 2010), which were then validated by sequencing.

To introduce *URA7::GFP* variants into the endogenous *URA7* locus in yeasts, the mutant plasmids were used as templates to PCR amplify a cassette containing coding region of *ura7::GFP*, a copy of *HIS3* sequence (selectable marker) and a sequence homologous to 50 bps downstream of the *URA7* stop codon (required for homologous recombination at the endogenous *URA7* locus). Yeasts were transformed with the purified PCR product of the *ura7::GFP* cassette via the heat shock method (Noree et al., 2010),

incubated overnight at 30°C, then replica plated onto histidine-dropout plates. All yeast mutants were verified by DNA sequencing (Eton Bioscience and Retrogen).

Quantitation of URA7-encoded CTP synthase foci/filaments

Wild type or mutated *URA7::GFP* strains were grown in 5 ml YPD at 30°C with shaking for 1 day. Cells were fixed by adding 100 µl of 37% w/v formaldehyde to 1 ml of yeast liquid culture, incubated on a rotating platform for at least 15 min at room temperature, collected by centrifugation at 6000 rpm for 1 min, and washed once with sterile water. The cells were then resuspended in 1M sorbitol. A slide was prepared by pipetting a few microliters of the cell suspension onto a slide, which was then covered by a cover slip, inverted and some pressure applied on the slide to allow excess liquid to be removed from the sample to improve imaging.

In order to determine the percent of cells containing Ura7p-GFP structures, 5 different areas were selected (~50 cells/area) for counting using a Zeiss Axiovert 200M microscope with a 100X Plan-Apochromat 100X/1.40 Oil objective lens. The total number of cells and the number of cells with Ura7p-GFP structures were counted and reported as a percentage of cells showing Ura7p-GFP foci/filaments. Experiments were repeated five times for graphing and statistical analysis (Mean ± SEM).

For analysis of the length distribution of Ura7p-GFP foci and filaments, imaging was performed using a DeltaVision® system with an Olympus IX70 microscope, Olympus PlanApo 60X/1.40 Oil objective, and SoftWoRx™ software version 2.5 (Applied Precision). At least 10 areas on the slide were randomly picked. For each, images in the Z-axis were taken every 0.2 microns over ~1-2 microns. Each was then

deconvolved and compressed into a single image. The processed images were then quantified using Fiji, a public domain image-processing tool (available online at http://fiji.sc/). Each image was transformed into 8-bit format, adjusted to the threshold with a setting at 30, 255. The foci and filaments in each image were computed via the function "Analyze Particles" excluding structures with size less than 0.01 μm^2. The value of the 'major axis' of each Ura7p-GFP structure was collected for preparing a graphic distribution of Ura7p-GFP foci and filaments (>100 structures were analyzed per mutant per repeat). Three independent experiments were done for each condition or mutation. Statistical analysis was performed using Prism 6 (GraphPad Software Inc.). One-way anova was used to test if there was a statistically significant difference between wild-type and each mutant in the length distribution of Ura7p-GFP structures.

Protein sample preparation and Western blot analysis

Whole cell extract was obtained by growing yeasts *URA7(WT)::GFP* or *ura7(mt)::GFP* in 5 ml YPD at 30°C with shaking for 1 day. Yeast liquid culture with 2.5 OD_{600} was harvested by centrifugation at 6000 rpm for 1 min and resuspended in 100 µl sterile water. Cell suspension was treated with 100 µl of 0.2 N NaOH. After 5-min incubation at room temperature, cells were collected by centrifugation at 6000 rpm for 1 min. SDS-PAGE loading buffer (with 1X Protease Inhibitor Cocktail, Sigma) was added to the cell pellet. After vortexing vigorously and boiling for 5 min, protein sample was spun down at 10,000 rpm for 1 min and resolved by 10% SDS-PAGE. Proteins were transferred from the acrylamide gel to a nitrocellulose membrane by electroblot (Owl HEP-1, Thermo Scientific). Then standard protocol for Western blot was performed. To

detect WT or mutant Ura7p-GFP, 1:5,000 rabbit anti-GFP (Torrey Pines Biolabs Inc.) was used as a primary antibody and 1:10,000 ECL™ donkey anti-rabbit IgG, horseradish peroxidase-linked whole antibody (GE Healthcare UK Limited) as a secondary antibody. For internal loading control detection, 1:10,000 mouse anti-3-phosphoglycerate kinase (yeast) IgG_1 monoclonal antibody (Invitrogen) was used as a primary antibody and 1:2,500 ECL™ sheep anti-mouse IgG, horseradish peroxidase-linked whole antibody (GE Healthcare UK Limited) as a secondary antibody. Results of Western blots, analysis of relationship between expression level and structure formation frequency, and analysis of expression level and length of mutant Ura7p-GFP structures, relative to those of wild type are shown in Figure 3.9.

Acknowledgements

We thank D. Forbes for critical reading of the manuscript, and R. Aroian for use of his deconvolution microscope. This work was supported by National Science Foundation Grant IOS-1144409 and San Diego Foundation Blasker Science and Technology Grant (C-2011-0218) (to J.E.W.).

Chapter 3 is the manuscript which has been submitted for publication. It may appear in Proceedings of the National Academy of Sciences of the United States of America 2013. Noree, Chalongrat; Monfort-Prieto, Elena; Shiau, Andrew K.; Wilhelm, James E. “Common regulatory control of CTP synthase enzyme activity and filament formation”. I was the primary investigator and author of this paper. E. Monfort-Prieto created the yeast strains expressing c-terminally GFP-tagged CTP synthase with the following mutations; G148A, C404G, R381M, R381P, G382A, E161K-C404G and performed Western blot analysis. J. Wilhelm and A. Shiau wrote the manuscript.

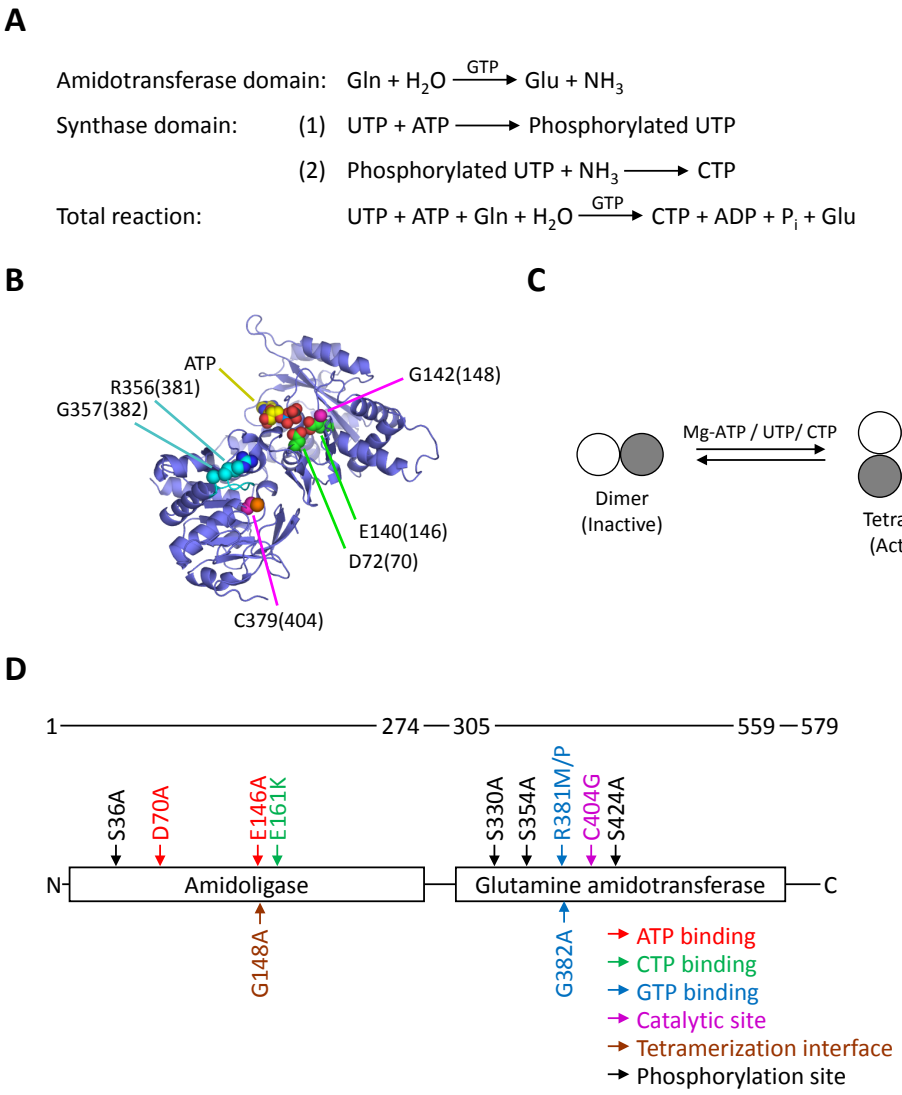

Figure 3.1 CTP biosynthetic reaction, monomeric structure, oligomerization, and structural domains of Ura7p with mutations included in this study

CTP biosynthesis requires ammonia which can be obtained by hydrolysis of glutamine, taking place in glutamine amidotransferase (or glutaminase) domain of CTP synthase. The amidoligase (or CTP synthase) domain is responsible for phosphorylation of UTP by ATP. Then the ammonia is transferred from glutamine amidotransferase domain to amidoligase domain, reacts with activated phosphorylated UTP, resulting in CTP production (A). 3D structure of monomeric bacterial CTP synthase with the labels on its critical residues (corresponding positions on the yeast sequence indicated in parentheses) (G148, tetramerization interface; C404, catalytic site in glutamine amidotransferase domain; R381 and G382, GTP binding sites) (B). Dimeric and tetrameric states of CTP synthase are depended on the availability of nucleotide-Mg complexes (C). Interfering mutations, included in this study, are highlighted with arrows: ATP binding site (red), CTP binding site (green), GTP binding site (blue), catalytic stie (purple), tetramerization interface (brown), phosphorylation sites (black) (D).

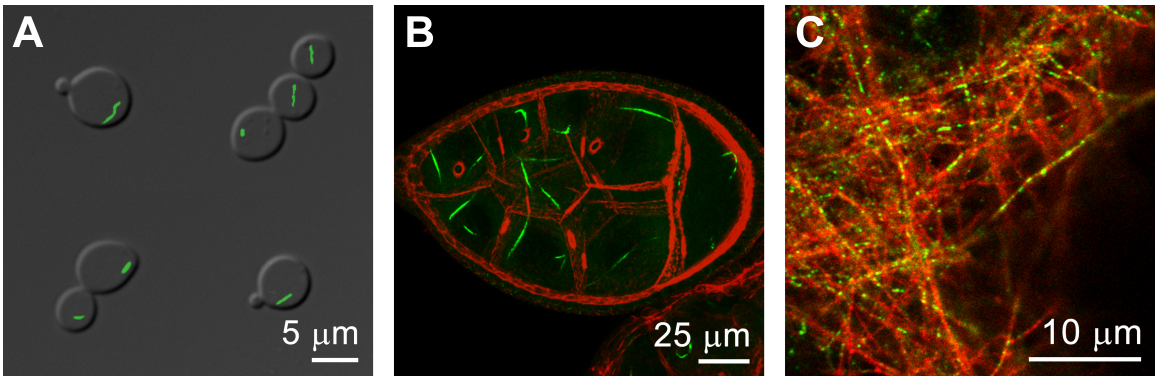

Figure 3.2 Conservation of CTP synthase filaments

CTP synthase filament is evolutionarily conserved in yeast (Ura7p-GFP; A), *Drosophila* (CTP synthase-GFP from The Carnegie Protein Trap library, actin stained in red; B), and rat hippocampal neurons (CTP synthase stained in green, axon in red; C).

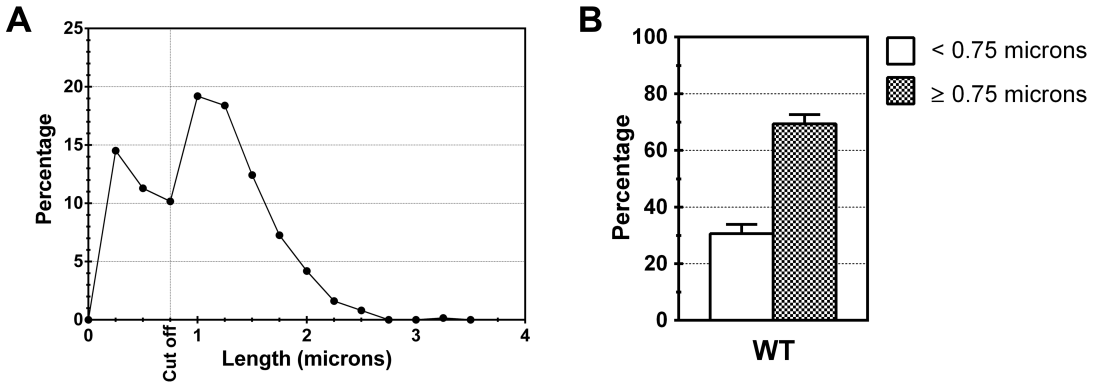

Figure 3.3 Two populations of CTP synthase structures in budding yeast

Histogram of length distrubution (n = 620) of wild-type Ura7p-GFP (A). Based on the histrogram, two populations of Ura7p-GFP structures have been existed; structures shorter than 0.75 microns and structures equal or longer than 0.75 microns (B).

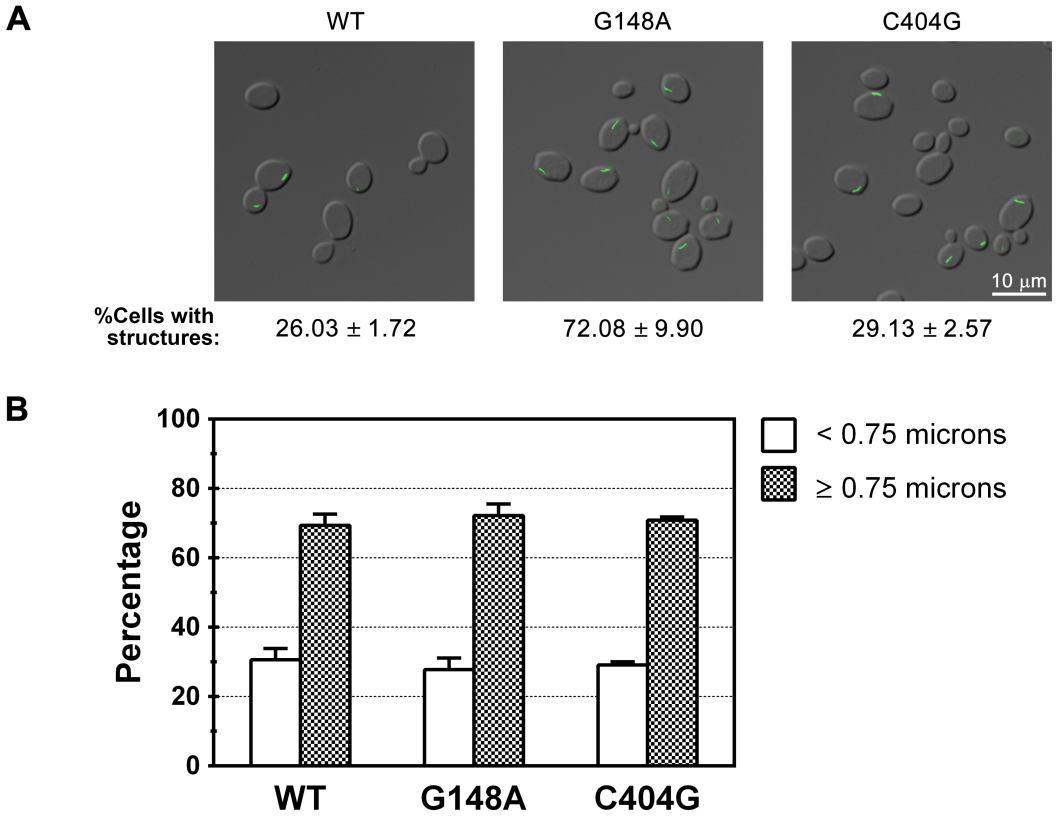

Figure 3.4 Analysis of yeast expressing WT, G148A, and C404G Ura7p-GFP

Representative images and percentage of cells with of WT/ G148A/ C404G Ura7p-GFP structures (A). Percentage of foci and filaments of WT, G148A, and C404G Ura7p-GFP on the basis of 0.75 μM cutoff (B).

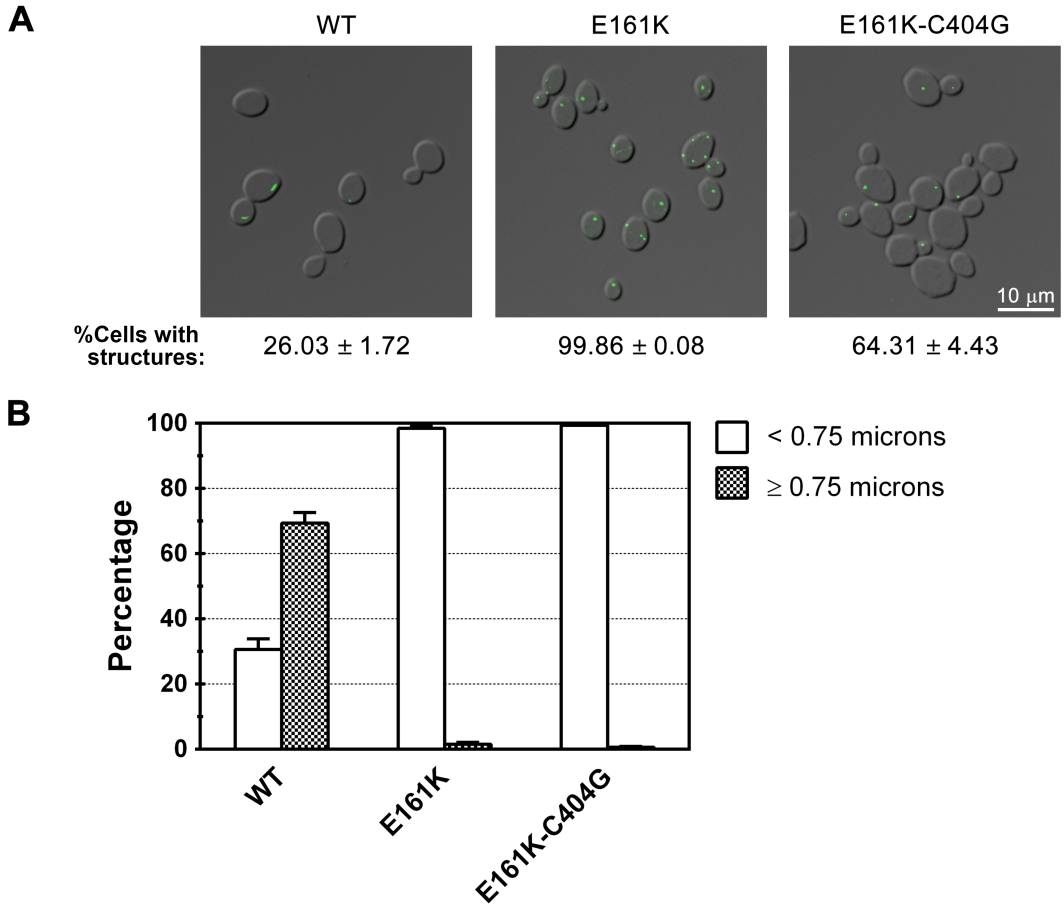

Figure 3.5 Analysis of yeast expressing E161K and E161K-C404G Ura7p-GFP

E161K mutation makes CTP synthase deficient in feedback inhibition by CTP. Whereas C404G mutation makes CTP synthase defected in glutamine hydrolysis (step 1 of CTP biosynthetic reaction). Representative images and percentage of cells with WT/ E161K/ E161K-C404G Ura7p-GFP structures (A). Percentage of foci and filaments of WT, E161K, and E161K-C404G Ura7p-GFP on the basis of 0.75 μM cutoff (B).

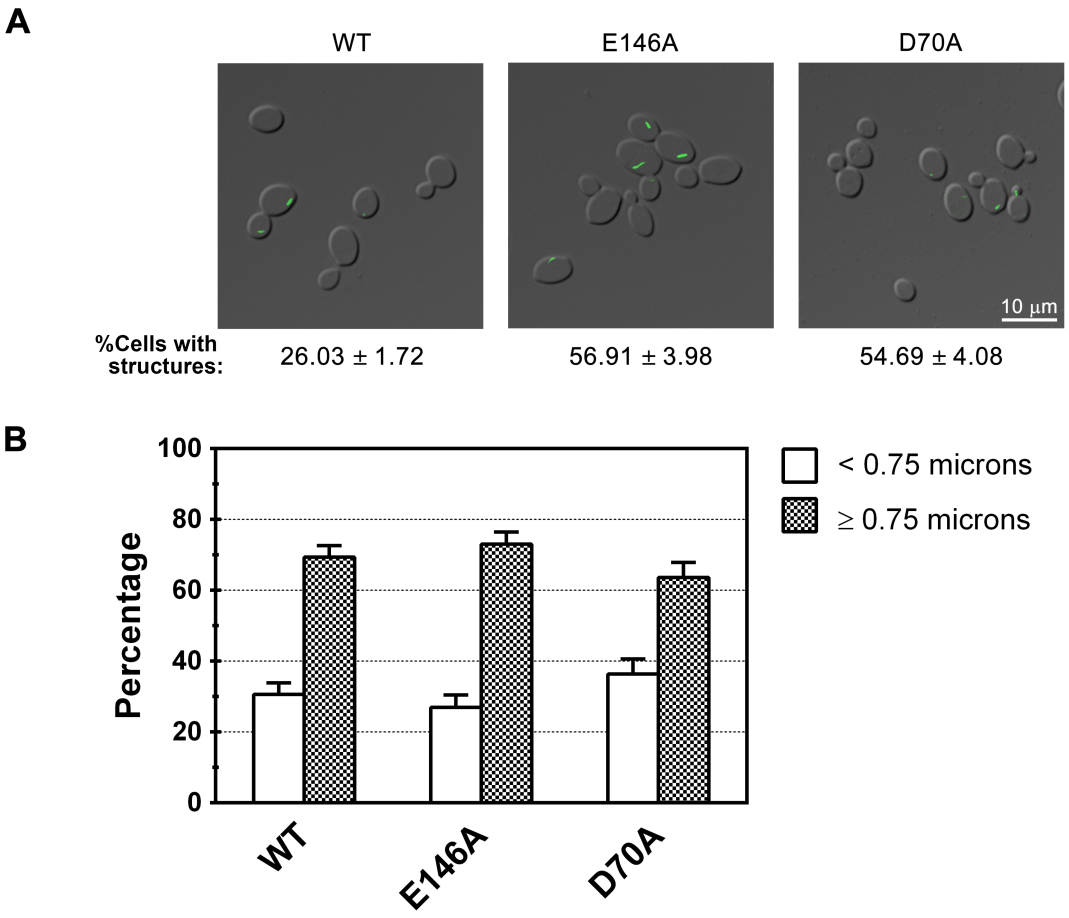

Figure 3.6 Analysis of yeast expressing E146A and D70A Ura7p-GFP

E146A and D70A mutations make CTP synthase defected in the binding of ATP to the enzyme. Representative images and percentage of cells with WT/ E146A/ D70A Ura7p-GFP structures (A). Percentage of foci and filaments of WT, E146A, and D70A Ura7p-GFP on the basis of 0.75 μM cutoff (B).

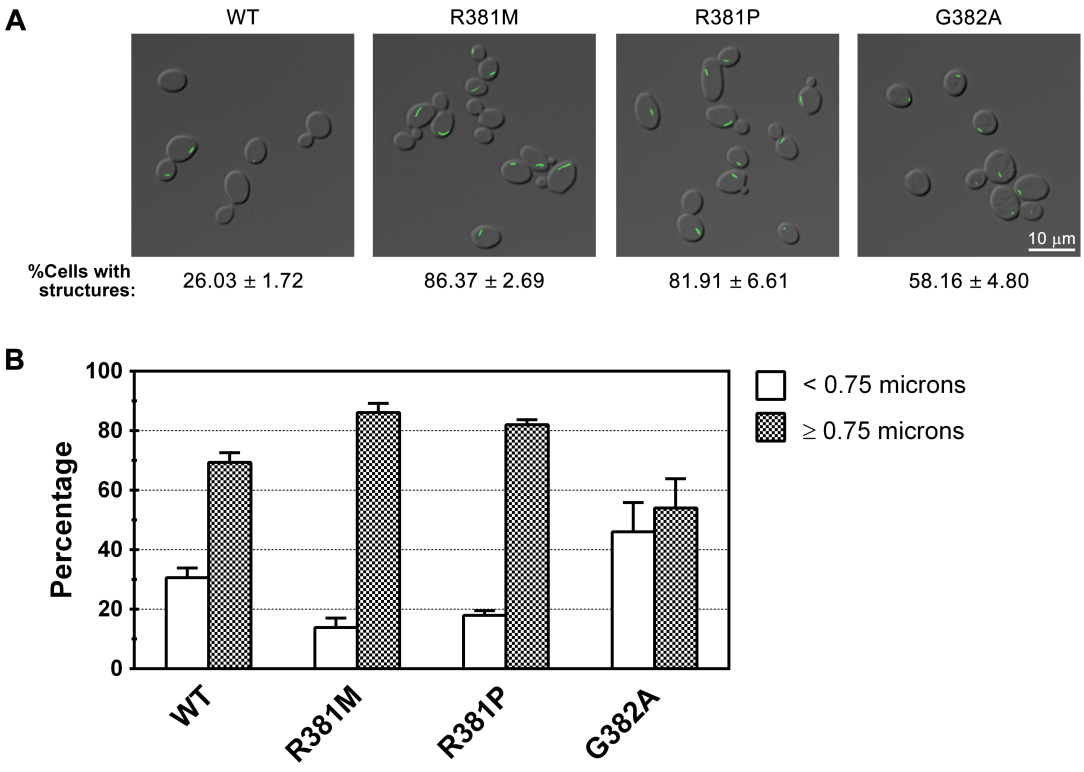

Figure 3.7 Analysis of yeast expressing R381M, R381P, and G382A Ura7p-GFP

R381 and G382 are GTP binding sites. Representative images and percentage of cells with WT/ R381M/ R381P/ G382A Ura7p-GFP structures (A). Percentage of foci and filaments of WT, R381M, R381P, and G382A Ura7p-GFP on the basis of 0.75 µM cutoff (B).

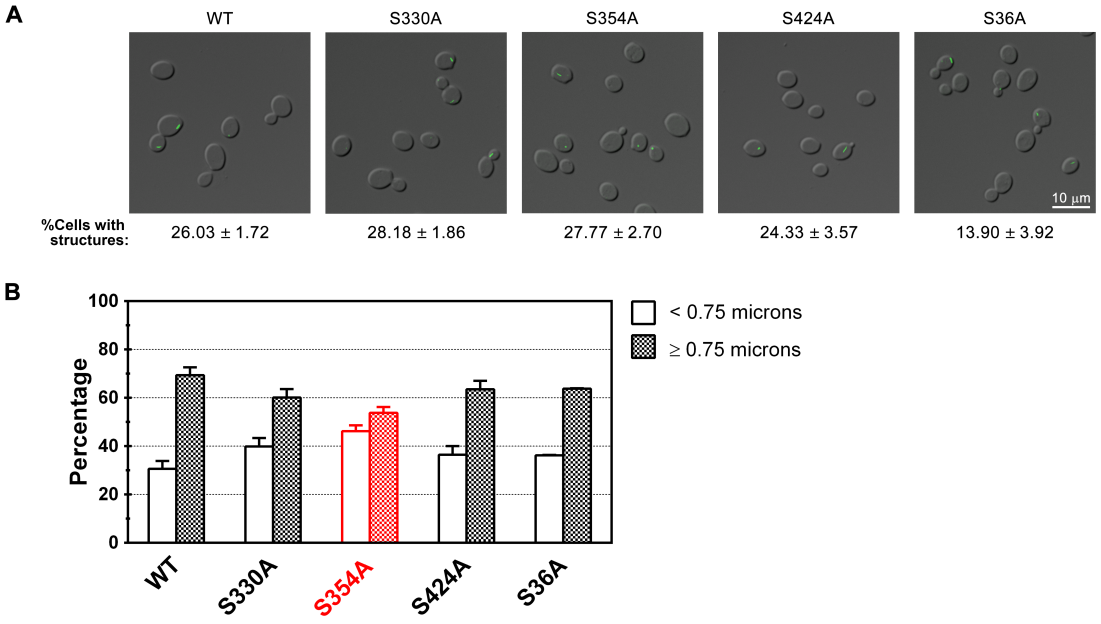

Figure 3.8 Analysis of yeast expressing S330A, S354A, S424A, and S36A Ura7p-GFP

S330, S354A, S424A, and S36 are phosphorylation sites. Representative images and percentage of cells with WT/ S330A/ S354A/ S424A/ S36A Ura7p-GFP structures (A). Percentage of foci and filaments of WT, S330A, S354A, S424A, and S36A Ura7p-GFP on the basis of 0.75 µM cutoff (B).

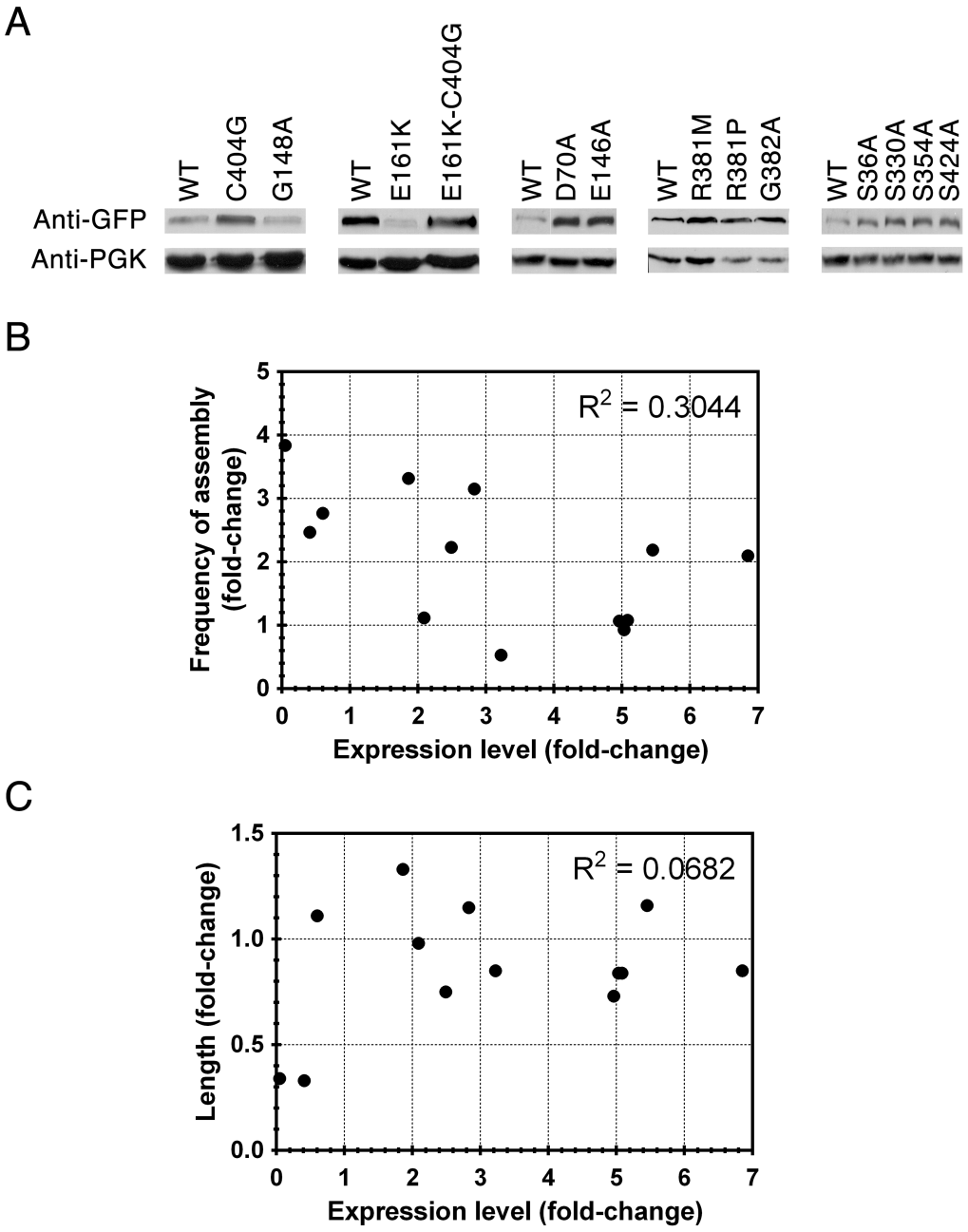

Figure 3.9 Frequency and length of Ura7p-GFP structures (WT and mutants) are not influenced by their expression levels

Western blots of WT and mutant Ura7p-GFP (A). Expression level versus frequency of structure formation of mutant Ura7p-GFP (B). Expression level versus median length of mutant Ura7p-GFP structures (B). Fold-change is calculated, relative to expression level, frequency, and length of WT Ura7p-GFP.

Table 3.1 Summary for frequency of Ura7p-GFP assembly, fractions of foci and filaments, average and median lengths of structures, and total number of structures used for analysis

Mutants	Description	% Cells with structures	% Foci	% Filaments	Average length of structures	Median length of structures	Total no. of structures analyzed
WT		26.03 ± 1.72	30.63 ± 3.24	69.37 ± 3.24	1.053 ± 0.039 μm	1.059 μm	620
G148A	Tetramerization	72.08 ± 9.90	27.80 ± 3.36	72.20 ± 3.36	1.150 ± 0.018 μm	1.179 μm	519
C404G	Catalytic site	29.13 ± 2.57	29.11 ± 0.93	70.89 ± 0.93	1.030 ± 0.016 μm	1.043 μm	385
E161K	CTP binding site	99.86 ± 0.09	98.47 ± 0.59	1.53 ± 0.59	0.363 ± 0.018 μm	0.359 μm	784
E161K-C404G	CTP binding site & catalytic site	64.31 ± 4.43	99.41 ± 0.30	0.59 ± 0.30	0.355 ± 0.007 μm	0.347 μm	322
E146A	ATP binding site	56.91 ± 3.98	26.99 ± 3.46	73.01 ± 3.46	1.171 ± 0.027 μm	1.233 μm	431
D70A	ATP binding site	54.69 ± 4.08	36.40 ± 4.24	63.60 ± 4.24	0.893 ± 0.048 μm	0.895 μm	402
R381M	GTP binding site	86.37 ± 2.69	13.90 ± 3.13	86.10 ± 3.13	1.370 ± 0.036 μm	1.407 μm	415
R381P	GTP binding site	81.91 ± 6.61	17.92 ± 1.59	82.08 ± 1.59	1.202 ± 0.022 μm	1.216 μm	388
G382A	GTP binding site	58.16 ± 4.80	46.00 ± 9.86	54.00 ± 9.86	0.828 ± 0.067 μm	0.789 μm	480
S330A	Phosphorylation site	28.18 ± 1.86	39.86 ± 3.50	60.14 ± 3.50	0.905 ± 0.042 μm	0.887 μm	315
S354A	Phosphorylation site	27.77 ± 2.70	46.20 ± 2.39	53.80 ± 2.39	0.806 ± 0.027 μm	0.778 μm	431
S424A	Phosphorylation site	24.33 ± 3.57	36.50 ± 3.54	63.50 ± 3.54	0.911 ± 0.040 μm	0.887 μm	404
S36A	Phosphorylation site	13.90 ± 3.92	36.20 ± 0.16	63.80 ± 0.16	0.913 ± 0.031 μm	0.905 μm	395
S36D	Phosphorylation site	6.084 ± 1.04	N/A	N/A	N/A	N/A	N/A
S36E	Phosphorylation site	5.346 ± 1.37	N/A	N/A	N/A	N/A	N/A

Note: % Cells with structures was collected by counting 250-300 cells grown for 1 day and fixed with 3.36% formaldehyde. The experiments were repeated for 5 times and the average ± SEM was calculated. % Foci and % Filaments were obtained by imaging cells grown for 1 day and fixed with 3.36% formaldehyde with DeltaVision system. Imaging was done for 3 independent repeats (Except WT = 6 repeats). Deconvolved and compressed images were analyzed by Fiji and the structures with length less than 0.75 μm were defined as foci, more or equal to 0.75 μm as filaments.

Chapter 4

Regulation of metabolic pathways via assembly into higher-order complexes

Abstract

In mammals, all six enzymes involved in *de novo* purine biosynthesis have been shown to assemble together into a single cytoplasmic structure, termed the purinosome. Here we demonstrate that in yeast, all of the *de novo* purine biosynthetic enzymes do not assemble into a single purinosome-like structure. Rather, we observe that only the enzymes at the nodes or branch points of the purine biosynthetic pathway and the enzymes catalyzing PRPP biosynthesis (PRPP is a starting precursor fed into *de novo* purine biosynthetic pathway) are capable of assembly. Colocalization experiments reveal that none of the enzymes possessing this assembly property are present in the same structures. The exceptions are Prs3p, co-assembled with Prs5p, and Ade16p with Ade17p, as they are structurally and functionally related. Media shift experiments showed that the kinetics of assembly and disassembly of each enzyme are different. Ade4p, catalyzing the first committed step of the *de novo* purine biosynthetic pathway, assembled when adenine was absent from the media, but failed to assemble when both adenine and glucose were absent. This suggests that Ade4p requires its substrate 'PRPP' for its assembly and, further, that assembly is how the Ade4p proteins re-organize to stimulate their productivity so that the purine nucleotides can be made. This is supported by a K333Q mutant form of *ADE4*, which makes the enzyme resistant to feedback inhibition, and caused an increase in Ade4p assembly. In contrast, the upstream enzymes, Prs3p and Prs5p, assembled under resting growth stage or in glucose-limiting conditions, which suggests that assembly of Prs3p and Prs5p is the means to sequester the enzymes so that they cannot perform their functions. It is not necessary to have all PRPP synthases subunits (Prs1-5p) for making the enzyme complexes to be functional. We conclude that

the assembly and disassembly of individual enzymes at the nodes in a biosynthetic pathway could be a novel cellular process to organize and regulate enzyme activity. Disorders in assembly/disassembly of metabolic enzymes may cause diseases in higher eukaryotes.

Introduction

The spatial organization and compartmentalization of biochemical reactions is a central theme of cell biology (LeDuc and Bellin, 2006; Luisi, 2002). However, while this concept has been developed and elaborated on for numerous membrane-bound organelles, such as mitochondria (Lenaz and Genova, 2009) and peroxisomes (Veenhuis et al., 2000), relatively little is known about how metabolic enzymes and pathways are organized within the cytoplasm.

Naturally occurring complexes of two or more enzymes catalyzing consecutive steps in a certain pathway have been identified and characterized, for example, enzymes involved in purine nucleotides, carbon, or fatty acid metabolism (An et al., 2008; Campanella et al., 2005; Ishikawa et al., 2004). As complexes, their activity and productivity has been shown to be significantly increased over the free enzyme. Together with the findings that the intermediate metabolites cannot be detected upon co-assembly of enzymes, it has been proposed that the juxtaposition of enzymes provides substrate channeling/tunneling so that the intermediate metabolites are not diffusing away and can directly be metabolized by the proximate enzymes in the following steps. This would be very advantageous in case the intermediates are highly toxic, unstable, labile, diffusible, secretory, or competitively hunted by other enzymes in different pathways (Conrado et al., 2008; Dunn, 2012; Lee et al., 2012; Zhang, 2011).

The evolution of multi-domain enzymes possessing multiple functions are the evidence of evolutionary gene/protein fusions that have occurred to better improve the metabolic productivity (Pasek et al., 2006). Also, the oligomerization of allosteric enzymes is utilized to regulate enzyme activity by providing a microenvironment suitable

for the binding of substrates, cofactors, and allosteric effectors or inhibitors to the enzymes (Fairman et al., 2011; Kim and Raushel, 2001). The posttranslational re-organization of metabolic enzymes is also known to be crucial for cells to respond to rapid changes in the extracellular environments (An et al., 2008; Buchan et al., 2008; Narayanaswamy et al., 2009; Noree et al., 2010).

However, less attention has been paid to the possibility of assembly of metabolic enzymes into large intracellular structures until visual screens of the yeast GFP collection were conducted under several conditions (Narayanaswamy et al., 2009; Noree et al., 2010). A number of proteins that assemble into cytoplasmic structures have been identified. The conditions for triggering their assembly are diverse for individual proteins. The observed assembly can be reversible in a quick response, suggesting that assembly is not the result of transcriptional/translational induction. It is thus possible that the assembly of metabolic enzymes is an important regulatory process that modulates enzyme activity, either in a positive or a negative manner.

Previous work on *de novo* purine biosynthesis found that the core enzymes in the pathway assemble together into a single structure, subsequently named the purinosome (An et al., 2008). To determine whether purinosome found in mammals is also conserved in yeast, we examined all the yeast enzymes that are orthologs of proteins that comprise the purinosome for the ability to form structures (Figure 4.1). We further extended this investigation to the enzymes located upstream and downstream of the core enzymes of *de novo* purine biosynthesis that form the purinosome in mammals (i.e., PRPP/AXP/GXP biosynthesis). We performed colocalization experiments to test the substrate channeling concept for purinosome-like structures in yeast. We further performed media shift

experiments and epistasis analyses to ask whether high-order structures are formed as a means of enzyme regulation. Overall, we have found that purinosome does not exist in yeast. However, enzymes at the nodes of the *de novo* purine biosynthetic pathway are capable of assembly into independent structures. Their assembly/disassembly is regulated individually by feedback inhibition of the enzymes and/or metabolic flux. Thus, the assembly of metabolic enzymes might be a common phenomenon to organize and regulate enzyme activity, depending on the cellular demand for the corresponding metabolites.

Results

Enzymes that act at nodes in the purine biosynthetic pathway assemble into distinct visible intracellular structures

Previous work on the *de novo* purine biosynthetic pathway in mammals found that a subset of enzymes assembled into a common structure in response to purine deprivation (An et al., 2008). This structure, the purinosome, is believed to accelerate purine biosynthesis by facilitating substrate channeling between consecutive steps in the pathway. Several visual screens for metabolic enzymes that self-assemble in response to nutrient deprivation in yeast also identified multiple purine biosynthetic enzymes that are present in large intracellular structures, suggesting that the purinosome might be a highly conserved metabolic regulatory structure. To test this possibility, we used the yeast GFP strain collection (Huh et al., 2003) to determine whether each of the enzymes in the *de novo* purine biosynthesis were capable of recruitment into intracellular structures and what growth conditions triggered the recruitment. The percentage of cells with GFP-labeled structures for each tagged enzyme was determined during log phase growth, as well as in cultures grown for 1, 3, or 5 days. As shown in Figure 4.2, the majority of purine biosynthetic enzymes displayed little if any assembly behavior (i.e. structures in <5% of cells). However, four biosynthetic enzymes, PRPP synthetase (Prs3p, Prs5p), phosphoribosylpyrophosphate amidotransferase (Ade4p), bifunctional 5-aminoimidazole-4-carboxamide ribonucleotide transformylase/IMP cyclohydrolase (Ade16/17p), and adenylosuccinate synthase (Ade12p) assembled into visible structures in 30-50% of cells under at least one growth condition. The fact that these four enzymes do not act on

consecutive steps, coupled with the observation that most of the yeast orthologs of enzymes that comprise the mammalian purinosome do not form structures, argues that the purinosome is not a broadly conserved structure.

One concern with our screen is that the GFP tag might alter the structure or function of the proteins causing them to form structures. We tested this possibility in two ways. First, we generated yeast strains in which each of the proteins identified in our screen was tagged at the C terminus with an HA epitope, instead of GFP. All of the HA-tagged proteins (Prs3p, Prs5p, Ade4p, Ade16p, Ade17p, and Ade12p) formed structures (Figure 4.3), similar to those we observed with the GFP tagged protein (Figure 4.2), arguing that GFP was not responsible for causing these proteins to assemble into filaments or foci.

As a second assay for the effects of the tag on the function of the proteins, we tested whether the GFP-tagged version of each protein caused phenotypes associated with impaired protein function. Ade4p and Ade12p are both required for growth in the absence of adenine. GFP-tagging either of these proteins at the endogenous locus did not affect growth on adenine drop-out plates arguing that the addition of GFP did not alter the function of these proteins. Ade16p, while non-essential, is one of two genes that encode the bifunctional 5-aminoimidazole-4-carboxamide ribonucleotide transformylase/IMP cyclohydrolase in *S. cerevisiae*, and the *ade16Δ ade17Δ* double mutant is a purine auxotroph. We took advantage of this synthetic auxotrophy to examine the effects of the GFP tag on Ade17p function. To do this, we created an *ade16*Δ deletion in an *ADE17::GFP* background. The *ADE17::GFP; ade16Δ* yeast strain was able to grow on adenine drop-out plates (not shown), arguing that the GFP tag did not alter the function of

the Ade17p. From these experiments, we conclude that the ability to form structures is not dependent on GFP and that the GFP tag does not affect protein function for the six proteins in the *de novo* purine biosynthetic pathway identified in our screen.

Higher order assembly is not used for substrate channeling or to coordinate activity at distinct nodes

While the four enzymes that are capable of recruitment into structures do not act on consecutive steps in purine biosynthesis, we found that they were also not randomly distributed throughout the pathway. PRPP synthetase produces PRPP for utilization by Ade4p, which is the first committed step in purine biosynthesis. Similarly, Ade16/17p produces IMP for use by Ade12p, the first committed step in AMP biosynthesis. Indeed, the four enzymes that assemble into structures act at key decision points in the *de novo* purine biosynthetic pathway. This observation suggested two possibilities. Yeast could possess a minimal purinosome where pairs of enzymes that act at key regulatory steps in the pathway co-assemble. Alternatively, self-assembly of single enzymes into a higher order structure could be a mechanism for regulating enzyme activity.

In order to distinguish between these two models, we performed pair-wise co-localization experiments between Prs3p, Prs5p, Ade4p, Ade16p, Ade17p, and Ade12p in which one protein was tagged with GFP while the second was tagged with mCherry (Figure 4.4). We did not observe co-localization for most enzyme pairs. In only for only two pairs did we see colocalization: Prs3p and Prs5p, which are both subunits of PRPP synthetase, and Ade6p and Ade17p, which are isozymes of the bifunctional 5-aminoimidazole-4-carboxamide ribonucleotide transformylase/IMP cyclohydrolase.

These results argue that the assembly of these enzymes into large structures is not a strategy for substrate channeling, since enzymes that act on different steps are not found in the same structure. Thus, there is no evidence for even a minimal purinosome. The results also argue that the structures formed are not for coordinating enzyme activity at different decision points within the same pathway, because only one enzyme activity is found in each structure observed.

The higher order assembly of enzymes is not part of a generalized response to metabolic stress

The failure of enzymes in the yeast *de novo* purine biosynthetic pathway to assemble into a purinosome-like structure suggested that self-assembly into higher order structures had functions apart from substrate channeling. Nutrient deprivation is known to induce the assembly of a number of cytoplasmic structures in yeast, such as the processing body (Buchan et al., 2008; Teixeira et al., 2005). If self-assembly of these enzymes were part of a general response to metabolic stress, we would expect self-assembly of all of the enzymes in the purine biosynthesis pathway to be coordinately regulated by the same set of nutrient conditions. To test this possibility, we examined whether Prs3p, Prs5p, Ade4p, Ade16p, Ade17p, and Ade12p assemble with the same kinetics in cultures undergoing log phase growth, as well as cultures grown for 1 day, 3 days, and 5 days. The results will be discussed in the next section.

First, we addressed a related possibility: one concern was that the intracellular structures formed by these PRPP and purine biosynthetic enzymes might be the aggregates of mis-folded proteins. To rule out this argument, we made double-

fluorescently labeled yeast strains. One of the chaperone components (Ssa1p or Hsp104p) was tagged with GFP, whereas the purine or PRPP biosynthetic enzyme to be tested was tagged with mCherry. We found, however, that the cellular localization of the chaperone machinery did not superimpose or overlap with that of any purine and PRPP biosynthetic enzymes, with the exception of the Ade16/17p structure. However, single deletion of *HSP104* or *SSA1* genes had no effect on Ade16/17p structure formation. These results argue that the assembly of purine and PRPP biosynthetic enzymes into structures is not due to the stress/unfolded protein response (Figure 4.5).

PRPP and purine biosynthetic enzymes possess different kinetics of assembly

Typically, at log phase growth, the assembly of *de novo* purine biosynthetic or PRPP biosynthetic enzymes into structures was never observed (Figure 4.2). Moreover, the each enzyme has a distinct temporal pattern of assembly in yeast cultures. Ade4p, which catalyzes the first committed step of the *de novo* purine biosynthesis, was the only enzyme that exhibited a high frequency of assembly (32%) upon transition from log phase to saturation (1-day) (Figure 4.2, middle panel). In contrast, Ade16p and Ade17p, two redundant isozymes that catalyze the last two steps of IMP production, showed the most abundant structures at stationary phase (5-day), with 39% and 19% of cells having structures, respectively (Figure 4.2, middle panel). Ade12p, the enzyme located at the branch point prior to AMP biosynthesis, also showed assembly into the most structures at stationary phase (82%) (Figure 4.2, bottom right panel). Prs3p and Prs5p, located one-step upstream of *de novo* purine biosynthetic pathway, producing PRPP as a precursor for Ade4p, were found to assemble into structures in a continuously increasing manner as

cells were grown for a longer period of time (Figure 4.2, top panel). Thus, the kinetics of assembly of these purine and PRPP biosynthetic enzymes differ from enzyme to enzyme. These observations also argue that the assembly of *de novo* purine biosynthetic enzymes acting at nodes in the pathway is regulated by distinct metabolic conditions.

Intracellular structures of Prs3p, Prs5p, Ade4p, Ade16p, Ade17p, and Ade12p disassemble in a glucose-dependent manner

Since most of the enzymes above assembled into structures at stationary phase, nutrient-limited conditions could well be critical regulators of their assembly. First, we tested whether a change in carbon source could affect the assembly/disassembly of these enzymes (Figure 4.6). Cells grown for 5 days were shifted to several glucose-supplemented or no glucose conditions for 30 minutes. This is less than doubling time of actively dividing yeasts, thus the observed effects should not be due to the transcriptional/translational issue, as evident in Figure 4.7. The presence of glucose gave rise to rapid disassembly, as seen by shifting cells to fresh YPD, adding glucose to the culture directly, or shifting to water with glucose only (Figure 4.6). In contrast, any conditions without glucose, i.e. YP media or water alone, did not cause disassembly of the intracellular structures of these enzymes (Figure 4.6). These results suggest that the disassembly of PRPP and purine enzymes is glucose-induced.

Prs5p and Ade4p can be rapidly triggered to assemble, but do so in response to different conditions

To test if glucose-induced disassembly can be reversible, media shift experiments designed for triggering assembly were conducted. Cells grown to log-phase, the growth

stage at which assembly had never been observed, were shifted to media lacking glucose for 30 minutes. Surprisingly, Prs5p was the only enzyme capable of assembly (Figure 4.8). Prs3p, although previously demonstrated to co-localize with Prs5p, was not able to assemble under the above condition (Figure 4.8). This implies that the assembly of Prs3p and Prs5p may be independently regulated. Potentially, Prs5p may serve as a sensor subunit of PRPP synthase complexes and then recruit its partner subunits to assemble upon abrupt carbon starvation. Because Prs3p and Prs5p structures assemble while glucose is limited or when cells are maintained at stationary phase and disassemble when glucose is present, this suggests that the assembly of PRPP synthase enzymes leads to down-regulation of enzyme activity.

Several enzymes, especially those acting at nodes of the *de novo* purine biosynthetic pathway, have been shown to be regulated by feedback inhibition from the pathway end products, i.e. guanine and adenosine nucleotides. We asked whether the PRPP and purine biosynthetic enzymes present in log phase cells could be triggered to assemble when adenine was not present in the media (Figure 4.8). Interestingly, Ade4p was the only enzyme that showed significant response to adenine dropout condition (48% cells showing structure assembly), suggesting that Ade4p assembly is required for stimulating purine biosynthesis upon purine starvation. Likewise, Ade4p not only functions as a catalytic enzyme, but also may act as a sensor responding rapidly to the situation where cells encounter low levels of extracellular purine. More interesting is when log phase cells were shifted to media lacking both glucose and adenine: Ade4p was unable to assemble, unlike the cells suspending in solely adenine-lacking media (Figure 4.8). This result argues that the regulatory hierarchy that controls enzyme assembly

mimics the pathway hierarchy; a downstream step is never activated if an upstream enzyme has been inactivated.

Here we propose that Prs5p assembles when the enzymes are in the 'non-active' state as evident by the glucose dependency experiments showing Prs5p assembly when glucose is absent and disassembly when glucose is added back. Ade4p, conversely, assembles when the enzymes are being 'active' state since the shortage of the end products can trigger the Ade4p assembly and this assembly also relies on the availability of its substrate 'PRPP'.

Assembly/disassembly can be directed by allosteric feedback inhibition and/or metabolic flux

To further investigate the proposal made above, we employed a genetics approach to disrupt any single gene product located upstream or downstream of the PRPP and purine biosynthetic enzymes of interest. We found that Prs3p-GFP and Prs5p-GFP showed a significant increase in assembly when the *de novo* purine biosynthetic pathway was disrupted (Figure 4.9). The largest effect was seen in an *ade4* deleted background, which caused a 4.9-fold increase in Prs3p assembly and a 3.8-fold increase in Prs5p assembly (Figure 4.9). This suggests that when PRPP cannot flow through one of the downstream pathways and becomes accumulated, PRPP synthases tends to assemble more in order to shut off PRPP synthase activity so that a regular PRPP level can be maintained inside the cells. An increase in Prs5p assembly was also observed (~3.4 fold) when there was no *ADE12* gene (Figure 4.9). *ADE12* encodes the enzyme at the branching point for AMP/ADP/ATP biosynthesis. We assume that IMP, the precursor for

making purine nucleotides, would flux into the GMP/GDP/GTP biosynthetic branch more than usual, resulting in inhibition of PRPP synthase activity by the excessive guanine nucleotides made. It is consistent with the fact that several end products from the *de novo* purine biosynthetic pathway have been previously found to have an allosterically inhibitory effect on PRPP synthase activity (Becker et al., 1975; Sperling et al., 1977; Zoref et al., 1975). This confirms that the assembly of PRPP synthases is due to the down-regulation of the enzyme complexes. We also quantitated the amount of expression levels (normalized by the internal loading control, Pgk1p) of Prs3p-GFP and Prs5p-GFP under different deletion backgrounds (Figure 4.9). It is unlikely that the increase of assembly is due to a larger amount of protein expressed, as several deletants with an increase of Prs3p/Prs5p assembly had expression levels of Prs3p/Prs5p lower than the control (Figure 4.10).

Ade4p-GFP assembly showed a slight increase (Figure 4.10) when the downstream steps of IMP biosynthesis were disrupted (1.5, 1.5, and 1.3-fold increase in *ade2Δ*, *ade1Δ*, *ade17Δ*, respectively), indicating that the accumulation of intermediate metabolites have some feedback effects on the activity and assembly of Ade4p. The marked increase (3-fold) of Ade4p-GFP assembly was seen when *ade12* was nulled. This could be explained as a result of the absence of ADP, the key allosteric feedback inhibitor of PRPP synthases (Becker et al., 1975; Sperling et al., 1977; Zoref et al., 1975). Without feedback inhibition, PRPP is continuously produced and non-stop fed into purine biosynthetic pathway, thus stimulating Ade4p assembly. Again, the increase of assembly was not due to the expression issue; *ade12Δ* had much lower expression of Ade4p-GFP than WT (0.07x) (Figure 4.10).

Biochemical study of *E. coli* amidophosphoribosyltransferase, the homologue of yeast Ade4p, revealed that K326Q mutation conferred resistance to feedback inhibition of the enzyme (Zhou et al., 1993). In addition to epistasis study, we introduced the same mutation (K333Q) into the chromosomal *ADE4* gene in yeast. The mutant displayed 2.6-fold increase of Ade4p assembly compared to WT when cells were grown to log-phase (Figure 4.11), indicating that the Ade4p assembly takes place with the enzymes being active. Again, the assembly was not caused by the overexpression of the mutant enzyme as Western blot analysis, indeed, revealed that it had expression level much lower (0.12 fold) than the WT enzyme (Figure 4.11).

Discussion

In this study, we demonstrated that the purinosome does not exist in *S. cerevisiae*. In contrast to mammalian *de novo* purine biosynthetic enzymes, only a subset of yeast enzymes involved in *de novo* purine biosynthesis were found capable of assembly. However, it is intriguing that we definitely observed the assembly of the enzymes that are located at the nodes of the PRPP and purine biosynthetic pathways. They are Prs3p, Prs5p, Ade4p, Ade16p, Ade17p, and Ade12p. None of these enzymes are present in the same structures as one another with the exception of Prs3p and Prs5p (Hernando et al., 1999; Hernando et al., 1998), and Ade16p and Ade17p (Tibbetts and Appling, 1997), since they are structurally and functionally similar to each other. These 6 enzymes possess different kinetics of assembly and disassembly. Ade4p, in particular, assembles earlier than other purine enzymes. The difference in kinetics suggests that their assembly might feature different activity states of the enzymes. All the assembled structures could be wiped out in the presence of glucose, indicating that all of them are glucose-responsive enzymes. However, the experiments for rapid assembly by glucose removal worked for Prs5p only. This suggests that Prs5p may act as a sensor to initiate assembly when the enzymes are sequestered from playing a role in PRPP biosynthesis. Likewise, but triggered under different conditions, Ade4p assembles rapidly in the absence of adenine. This was not observed with the other purine enzymes, suggesting that Ade4p may also be a sensor protein responding to cellular levels of the precursor 'PRPP' and the end products of purine biosynthetic pathway 'AXP and GXP' and stimulates the purine biosynthesis via its assembly. The mutant conferring resistance to feedback inhibition provides another piece of evidence that Ade4p structures are composed of active Ade4p

enzymes. The deletion of *ADE12* also stimulates Ade4p assembly which suggests that when PRPP synthase activity is not inhibited by the purine biosynthetic end products (i.e. ADP), the first committed step of purine biosynthesis, catalyzed by Ade4p is kept feeding with PRPP, therefore Ade4p assembly is observed more frequent.

Prs3p and Prs5p assemble in response to glucose level. However, Prs5p is the only subunit showing rapid assembly when glucose is removed from the media, indicating that Prs3p and Prs5p differ in their kinetics. In previous studies, it has been proposed that the formation of functional complexes of PRPP synthases does not necessary to have all 5 subunits together (Hernando et al., 1999; Hove-Jensen, 2004). The minimal complexes being active and stable *in vitro* could be a combination either of (1) Prs1p, Prs2p, Prs5p (2) Prs1p, Prs4p, Prs5p, (3) Prs2, Prs4p, Prs5p, or (4) Prs1p and Prs3p. Different combinations give rise to different degrees of PRPP synthase activity. Interestingly, one of the components in these combinations is always either Prs3p or Prs5p. Together with the finding that Prs3p and Prs5p possess different kinetics of assembly, we postulate that the assembly of each is the strategy of sequestration of that enzyme subunit. Cells may utilize this strategy to shuffle the components of active complexes in and out and the one when not in use is sequestered via assembly, therefore the activity of PRPP biosynthesis can be up- or down-regulated in several magnitudes depending on the cellular demand for PRPP.

The intracellular assembly of metabolic enzymes could be a novel strategy for the organization of enzyme activity. Metabolic flux and feedback inhibition, the keys to dictate the metabolic fate, might require assembly for enhancing their effects. It is possible that when cells are being active the assembly of metabolic enzymes might

promote the metabolic productivity whereas the assembly found in those at very late stage of growth might be the means of enzyme sequestration until cells exit the resting stage. Misregulation of metabolic enzymes related to several diseases might be due to the disorder in assembly/disassembly property of those enzymes. Based on our findings, it is interesting to explore whether enzymes at nodes in other metabolic pathways possess the reversible assembly property.

Materials and Methods

Media and Yeast Strains

All yeast strains were derived from a parent strain with the genotype *MATa his3Δ1 leu2Δ0 met15Δ0 ura3Δ0* (S288C). Strains with GFP tagged genes were from the yeast GFP collection (Howson et al., 2005). Yeast knockout strains (*MATα his3Δ1 leu2Δ0 lys2Δ0 ura3Δ0*) were gifts from M. Niwa (UCSD). All yeast strains were grown at 30°C in YPD (2% peptone, 1% yeast extract, 2% dextrose) unless otherwise indicated.

Pairwise colocalization experiments

GFP yeast strains from the GFP collection were used as a background. pBS34 plasmid was used for making a cassette of mCherry-KanR for C-terminal tagging a second protein. Primers were designed as described in the protocol provided by the University of Washington Yeast Resource Center (available at http://depts.washington.edu/yeastrc/pages/pBS34.html), except that 10 more nucleotides were added to the homology sequence to the gene of interest in order to improve the homologous recombination during yeast transformation. PCR was performed using KOD hot start DNA polymerase (Novagen®), following the manufacturer's instructions. Yeast GFP strains were transformed with the purified DNA cassette using the lithium acetate/PEG method as described in Noree, et al., 2010. The positive clones were validated by PCR and fluorescence microscopy.

Constructions of Yeast HA-tagged strains

pFA6a-3HA-kanMX6 was used as a DNA template. Forward primers were designed to have 50 bps upstream of the stop codon of the gene of interest, followed by 5'-GGTCGACGGATCCCCGGG-3'. Reverse primers were designed to have 50 bps downstream of the stop codon of gene of interest (reverse complemented), followed by 5'-ATCGATGAATTCGAGCTCG-3'. After PCR and purification, the yeast WT strain (S288C) was transformed with the DNA cassette harboring HA-kanMX6 (flanking with 50 bps homology to the sequence upstream of the start codon of gene of interest at 5' and 50 bps homology to the sequence downstream of the stop codon of gene of interest at 3') using the lithium acetate/PEG method. Positive clones were verified by PCR and indirect immunofluorescence.

Indirect Immunofluorescence

Yeast cultures (1 ml) were fixed with 37% formaldehyde (0.1 ml) for one hour on a rotator. Cells were collected by centrifugation at 6000 rpm for 1 min, washed 2-3 times with sterile water, and then resuspended in 0.5 ml SK buffer (1 M sorbitol; 43.4 mM K_2HPO_4; 6.7 mM KH_2PO_4). Another 0.5 ml SK buffer containing 5 µl BME was added to cell suspension and incubated for 2 min at RT. Spheroplasts were made by adding 1000 U/ml zymolyase (Zymo Research) and incubating on the rotator for 30 min. Spheroplasts were harvested at 2000 rpm for 3 min, and resuspended in 0.5 ml SK buffer (on ice until needed). This suspension was added to polylysine coated slides for 10 min. Supernatant was aspirated off and slides were incubated in -20°C MeOH for 6 min, followed by incubating in -20°C acetone for 30 sec. After air-drying for 2 min, they were incubated with 1% BSA in PBS for 20 min. Mouse anti-HA (1:1,000; Abcam) was used

as primary antibody and Alexa Fluor 568 goat anti-mouse (1:200; Invitrogen) as secondary antibody. The slides were mounted using Vectashield (Vector Laboratories).

Constructions of Yeast Strains for Epitasis Assays

GFP (*MATa*) x knockout (*MAT*α) haploid yeasts were mated on YPD plates and re-streaked onto Met^-/Lys^- double-dropout plates to select for diploid cells. Single colonies were then inoculated into 2 ml YPD, incubating for 8 hours at 30ºC. Cells were washed and resuspended in 1 ml Spo-UL media (0.1% yeast extract; 1% potassium acetate; 0.05% dextrose; 0.002% leucine, 0.004% uracil), and grown for 5-6 days on a rotator at room temperature. Tetrads' cell walls were digested with 200 U/ml zymolase (Zymo Research) and micro-dissected into single cells on YPD plates, incubating 30ºC for 48 hours. Colonies were gridded out onto YPD plates and grown overnight, then replica plated on $G418^+$ YPD or HIS^- plates and grown overnight. Haploid hybrid cells were genotyped and selected based on appropriate independent assortment patterns. Deletions were confirmed by PCR.

Construction of Ade4p feedback inhibition resistant yeasts

K333Q mutation was endogenously introduced into yeast *ADE4* allele by first amplifying the full-length *ADE4* coding sequence from the genomic DNA of yeast strain S288C using forward primer; 5'-GTTGTCGACATGTGTGGTATTTTAGGTATTG-3' (*Sal*I recognition site underlined) and reverse primer; 5'-CTTCCCGGGATAATCTGCACAATTATATAATCC-3' (*Sma*I recognition site underlined), followed by cloning into the *Sal*I and *Sma*I sites of pFA6a-GFP-kanMX6. The resulting plasmid, pFA6a-*ADE4*-GFP-kanMX6 was site-directed mutagenized to

introduce K333Q mutation into the *ADE4* coding sequence using 5'-phosphorylated forward primer; 5'-AGAGAGGGCTTTGTTCAGAACAGATACGTGGGC-3' (mutation site underlined) and 5'-phosphorylated reverse primer; 5'-ATAAGGCTTCCCTAACACATTAGCAC-3'. After ligation, bacterial transformation, and plasmid sequencing, the mutant plasmid was then used as a DNA template to PCR the 4054-bp cassette harboring *ade4*(K333Q)-GFP-kanMX6 (flanked with 50 bp upstream of the *ADE4* start codon at the 5' end and 50 bp downstream of the *ADE4* stop codon at the 3' end) using forward primer; 5'-CTAATAAGTTTAGCAAAGAAAGAGGTACAGCAAACAGCAGAATAGAAAAAATGTGTGGTATTTTAGGTATTG-3' (50 nucleotides upstream of the *ADE4* start codon underlined) and reverse primer; 5'-CGCATTTGGAAACTATTTTACATACAACTGAACAAGTTCGGAACAATCTAATCGATGAATTCGAGCTCG-3' (50 nucleotides downstream of the *ADE4* stop codon underlined). Yeast strain S288C was then transformed with the mutant DNA cassette. Transformants were selected on YPD agar plate containing G418 (400 μg/mL), and verified by sequencing (Retrogen). All PCR reactions were performed using KOD hot start DNA polymerase (Novagen®).

Imaging

Images were acquired using a DeltaVision® system with an Olympus IX70 microscope, Olympus PlanApo 60X/1.40 Oil objective, and SoftWoRx™ software version 2.5 (Applied Precision). The Z-axis were taken every 0.2 microns over ~1-2 microns, then deconvolved and compressed into a single image.

Quantitation

Cells were grown in YPD for indicated times at 30°C with shaking, then collected, washed, resuspended in indicated media, and put on a slide for quantitation by fluorescence microscopy (Zeiss Axiovert 200M microscope with a 100X Plan-Apochromat 100X/1.40 Oil objective lens). The total number of cells and the number of cells with structures were counted in 5 different fields (~50 cells/field) and reported as a percentage of cells with structures. Independent experiments were repeated at least 3 times for graphing (Mean ± SEM). For media shift experiments, cells were incubated in testing media for 30 minutes, long enough to see the treatment effect but short enough to not affect protein levels as demonstrated by Western blot.

Protein sample preparation and Western blot analysis

Whole cell extracts were obtained by growing yeasts cells in the indicated conditions. The cells with 2.5 OD_{600} were harvested by centrifugation at 6000 rpm for 1 min and resuspended in 100 µl sterile water. Next, this suspension was treated by adding an additional 100 µl of 0.2 N NaOH. After a 5-min incubation at room temperature, cells were collected by centrifugation at 6000 rpm for 1 min. SDS-PAGE loading buffer (with 1X Protease Inhibitor Cocktail, Sigma) was added to the cell pellet. After vortexing vigorously and boiling for 5 min, the sample was spun down at 10,000 rpm for 1 min and resolved by 10% SDS-PAGE. Proteins were transferred to a nitrocellulose membrane by electro-blotting (Owl HEP-1, Thermo Scientific). Then standard protocol for Western blot was performed. To detect GFP-tagged proteins, 1:5,000 rabbit anti-GFP (Torrey Pines Biolabs Inc.) was used as a primary antibody and 1:10,000 ECL™ donkey anti-

rabbit IgG, horseradish peroxidase-linked whole antibody (GE Healthcare UK Limited) as a secondary antibody. For internal loading control detection, 1:10,000 mouse anti-3-phosphoglycerate kinase (yeast) IgG_1 monoclonal antibody (Invitrogen) was used as a primary antibody and 1:2,500 ECL™ sheep anti-mouse IgG, horseradish peroxidase-linked whole antibody (GE Healthcare UK Limited) as a secondary antibody.

Acknowledgements

We would like to thank M. Niwa for all yeast knockout strains, R. Aroian for the use of his deconvolution microscope, and R. Hampton for use of his micromanipulation microscope.

Chapter 4 is a manuscript in preparation and will be submitted for publication. D. Samilo and K. Begovich helped collect the data, create yeast strains expressing double fluorescently-tagged proteins, and perform epistasis and Western blot analysis. Imaging, data analysis, and writing the manuscript was my responsibility. J. Wilhelm helped edit/revise the manuscript for publication.

Figure 4.1 *De novo* purine biosynthetic pathway in budding yeast

Abbreviations for intermediate metabolites and catalytic enzymes: R5P = Ribose-5-phosphate; PRPP = 5-Phosphoribosylpyrophosphate; PRA = 5-phosphoribosylamine; GAR = 5-phosphoribosylglycineamide; FGAR = 5'-phosphoribosyl-*N*-formylglycinamide; FGAM = 5'-phosphoribosyl-*N*-formylglycinamidine; AIR = 5'-phosphoribosyl-5-aminoimidazole; CAIR = 5'-phosphoribosyl-4-carboxy-5-aminoimidazole; SAICAR = 5'-phosphoribosyl-4-(N-succinocarboxamide)-5-aminoimidazole; AICAR = 5-amino-4-imidazolecarboxamide ribotide; FAICAR = 5-formamido-1-(5-phosphoribosyl)-imidazole-4-carboxamide; IMP = inosine-5'-monophosphate; XMP = xanthosine-5'-phosphate; GMP = guanosine-5'-phosphate; GDP = guanosine-5'-diphosphate; SAMP = adenylosuccinate; AMP = adenosine-5'-phosphate; ADP = adenosine-5'-diphosphate; Prs1-5p = phosphoribosylpyrophosphate synthetase; Ade4p = amidophosphoribosyltransferase; Ade5,7p = GAR synthetase/AIR synthetase; Ade8p = GAR transformylase; Ade6p = FGAM synthetase; Ade2p = AIR carboxylase; Ade1p = SAICAR synthase; Ade16/17p = IMP cyclohydrolase; Imd2-4p = IMP dehydrogenase; Gua1p = GMP synthetase; Guk1p = guanylate kinase; Ade12p = Adenylosuccinate synthetase; Ade13p = adenylosuccinate lyase; Adk2p = mitochondrial GTP:AMP phosphotransferase; Adk1p = adenylate kinase.

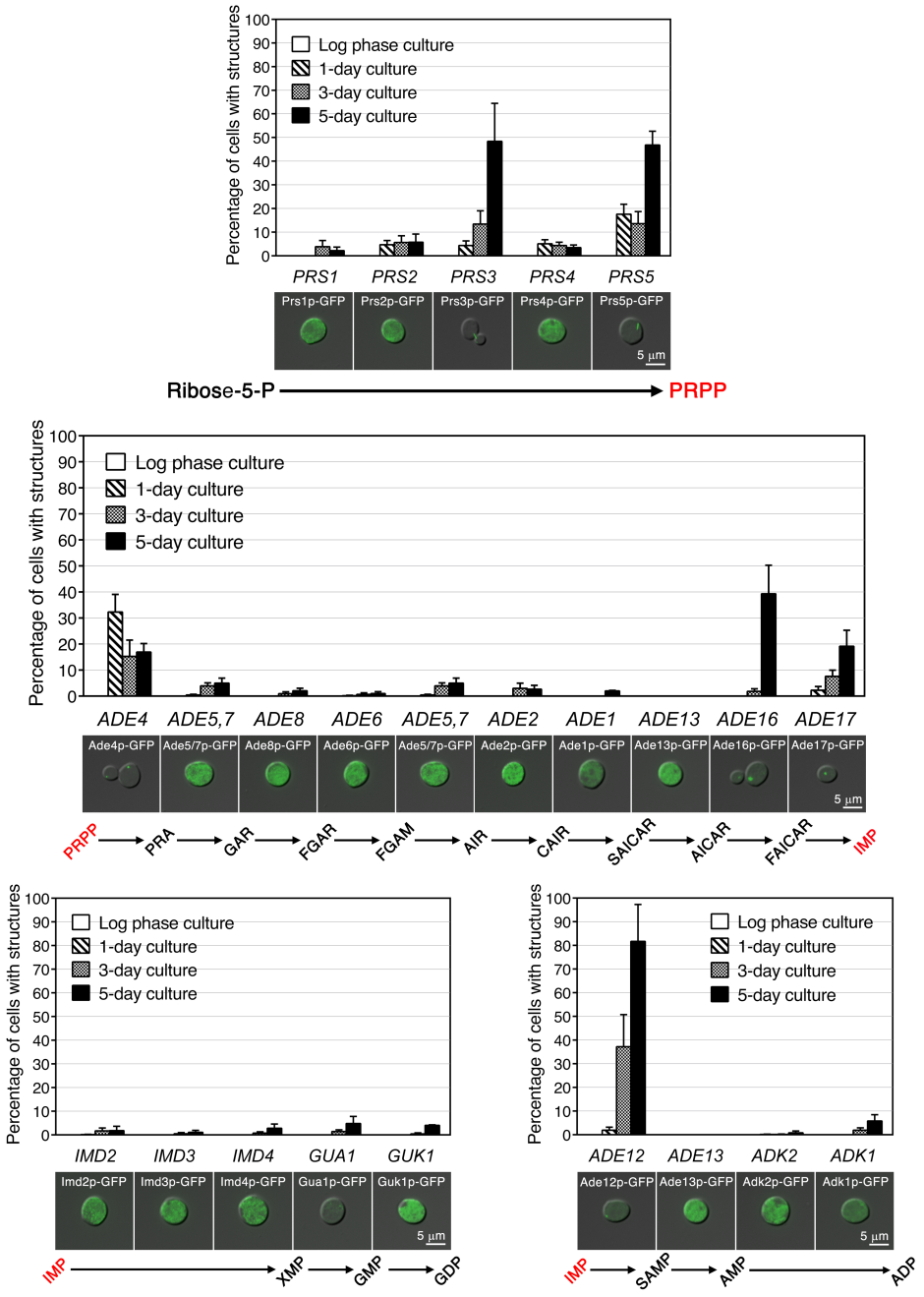

Figure 4.2 Kinetics of assembly of purine biosynthetic enzymes

Yeast cells expressing GFP-tagged purine biosynthetic enzymes were grown in YPD with indicated time points (log phase, 1-day, 3-day, and 5-day), and then fixed with formaldehyde. Cells with structures were counted from 5 different fields on a wet slide (~50 cells/field). Experiments were independently repeated 3 times. The data is illustrated as the percentage of cells with visible structures (average ± SEM). Representative images of each were shown below the graphs (taken from the culture condition with the largest degree of assembly).

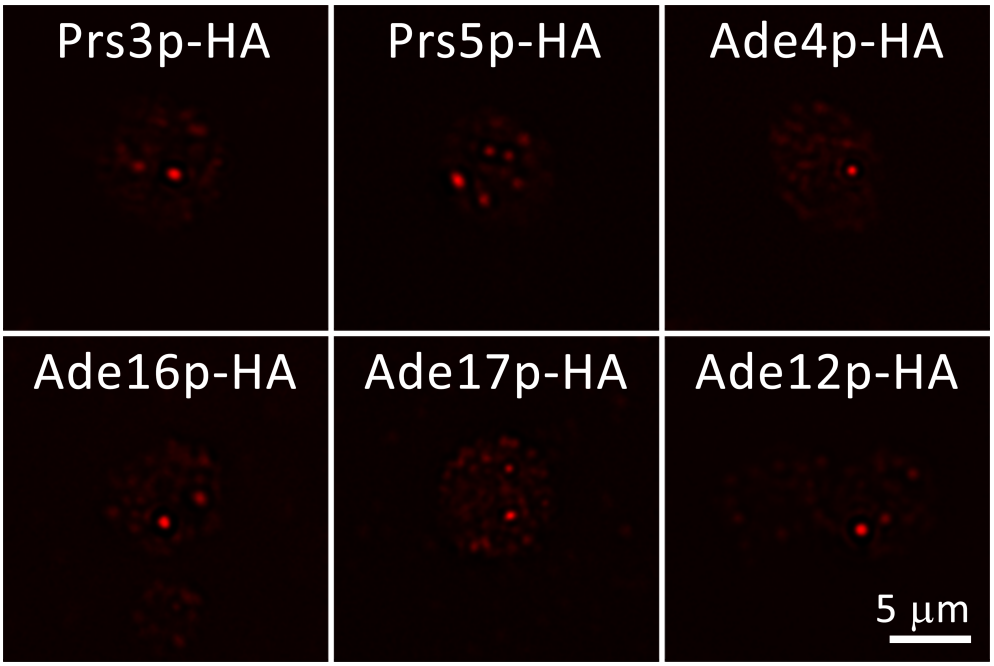

Figure 4.3 Representative images of HA-tagged purine biosynthetic enzymes

Yeast cells expressing HA-tagged purine biosynthetic enzymes were grown in YPD for 5 days. Indirect immunofluorescence was performed using mouse anti-HA (1:1,000) as primary antibody and Alexa Fluor 568 goat anti-mouse (1:200) as secondary antibody.

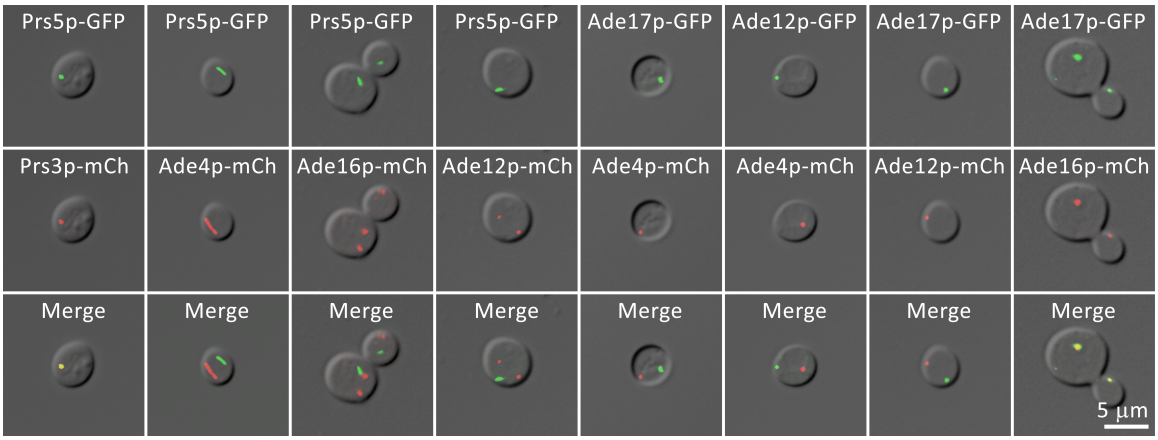

Figure 4.4 Pairwise colocalization assays of purine biosynthetic enzymes

Yeast cells expressing fluorescently-tagged purine biosynthetic enzymes were grown in YPD for 5 days and then fixed with formaldehyde. Representative images are shown. Images were acquired every 0.2 microns over 1-2 microns using a DeltaVision® system with an Olympus IX70 microscope, Olympus PlanApo 60X/1.40 Oil objective, and SoftWoRx™ software version 2.5 (Applied Precision). The images were deconvolved and then used to generate a maximum projection image of the data set.

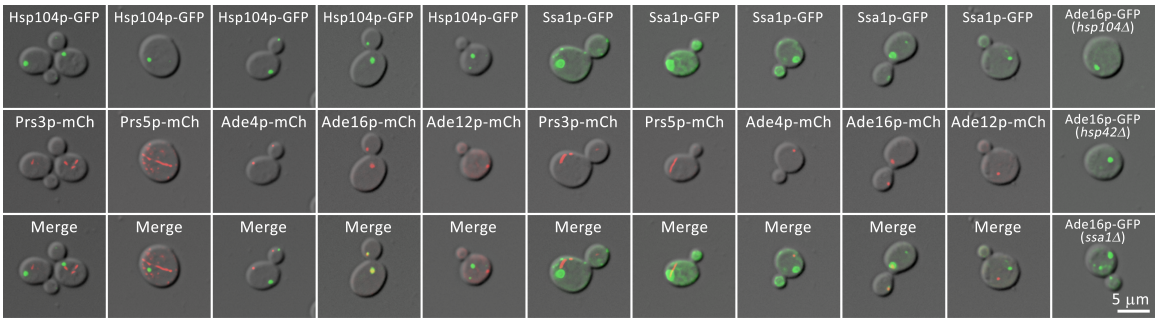

Figure 4.5 Assembly of purine biosynthetic enzymes is chaperone-independent

Yeast cells expressing GFP-tagged chaperone machinery (Ssa1p or Hsp104) and mCherry-tagged purine biosynthetic enzyme were grown in YPD for 5 days and then fixed with formaldehyde. Representative images are shown. Images were acquired every 0.2 microns over 1-2 microns using a DeltaVision® system with an Olympus IX70 microscope, Olympus PlanApo 60X/1.40 Oil objective, and SoftWoRx™ software version 2.5 (Applied Precision). The images were deconvolved and then used to generate a maximum projection image of the data set. As Ade16/17p colocalized to the same structures with chaperone machinery, disruption of *HSP104, HSP42, or SSA1* was introduced into the *ADE16::GFP* background strain. However, deletion of one of these chaperone components had no effect on Ade16p assembly.

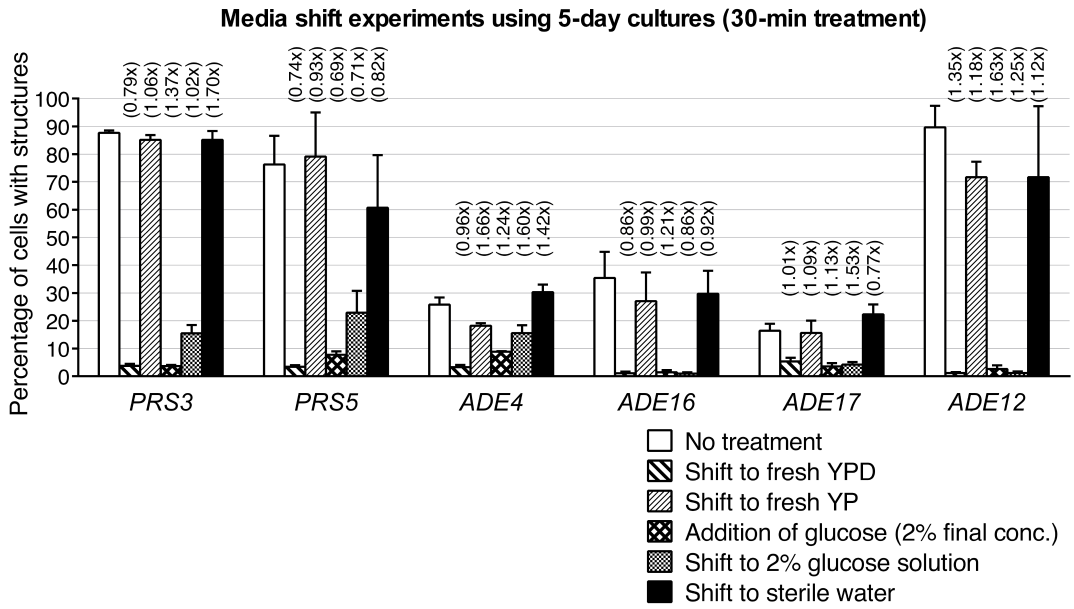

Figure 4.6 Disassembly of purine biosynthetic enzymes is carbon-dependent

Yeast cells expressing GFP-tagged purine biosynthetic enzymes were grown in YPD for 5 days, except for *ADE4::GFP* strain, where 1-day cultures were used as the largest frequency observed at this time point). Cells were washed once, resuspended in the indicated media and incubated for 30 min with rocking at RT. Cells with structures were counted from 5 different fields on a wet slide (~50 cells/field). Experiments were independently repeated 3 times and illustrated as percentage of cells with visible structures (average ± SEM). The protein expression level (detected by Western blot and quantitated by ImageJ) relative to no treatment was indicated above each bar.

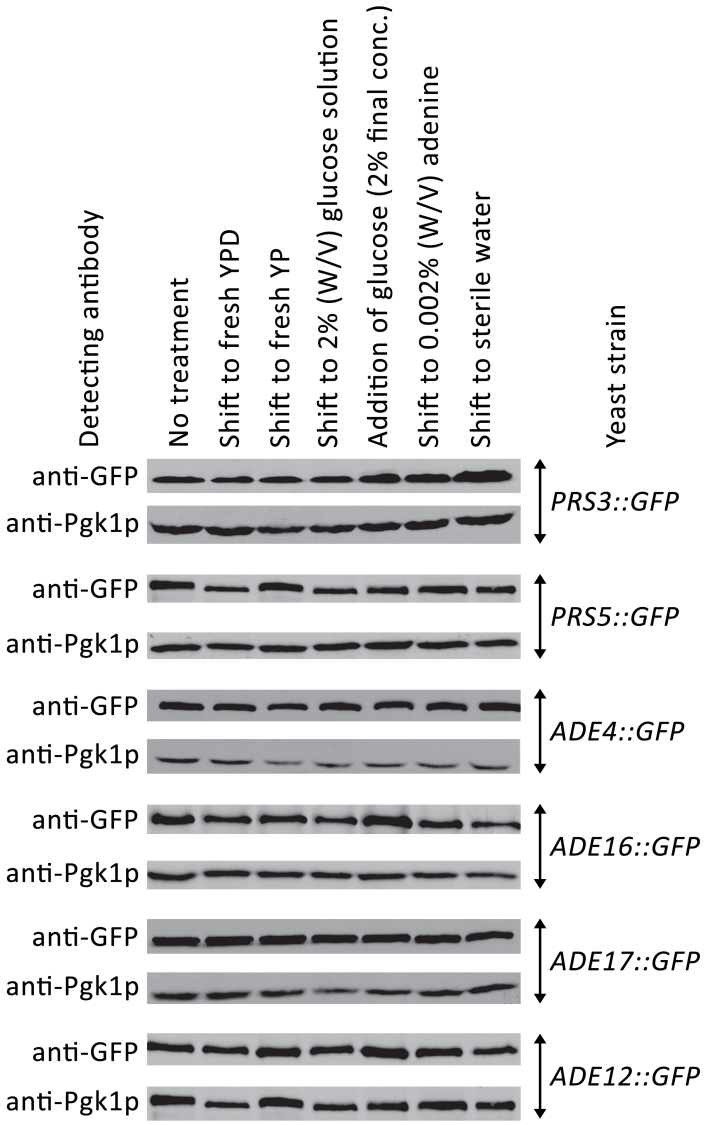

Figure 4.7 Expression levels of purine biosynthetic enzymes were not significantly affected by shifting cells to any media for 30 minutes

Yeast cells expressing GFP-tagged purine biosynthetic enzymes were grown in YPD for 5 days, except for *ADE4::GFP* strain, where 1-day cultures were used as the largest frequency observed at this time point). Cells were washed once, resuspended in the indicated media, incubated for 30 min with rocking at RT, and then the whole cell extracts were prepared for Western blots. Rabbit anti-GFP (1:5000) was used as a primary antibody and donkey anti-rabbit IgG (1:10,000) as a secondary antibody. For the internal loading control, mouse anti-yeast PGK (1:10,000) was used as primary antibody, and sheep anti-mouse IgG (1:2,500) as secondary antibody.

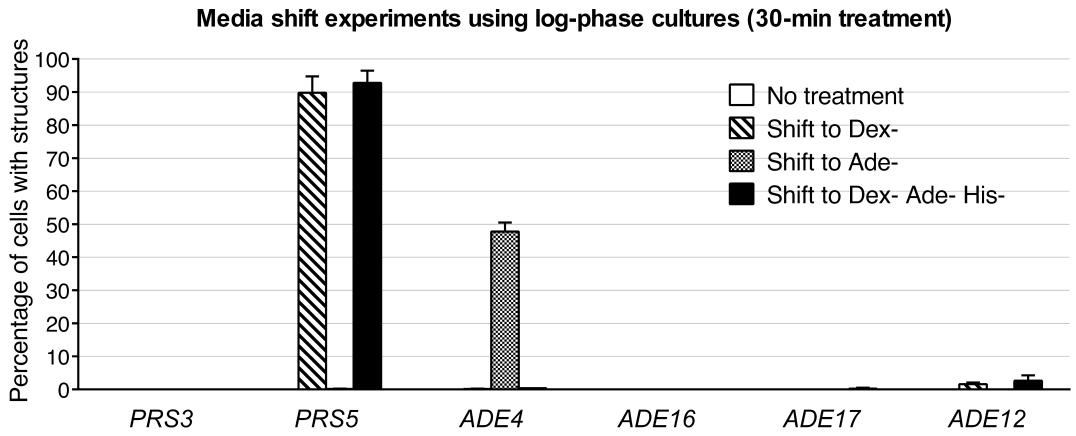

Figure 4.8 Assembly of Prs5p is carbon-dependent, whereas assembly of Ade4p is purine- and carbon-dependent

Yeast cells expressing GFP-tagged purine biosynthetic enzymes were grown to log phase in YPD. Cells were washed once, resuspended in the indicated media and incubated for 30 min with rocking at RT. Cells with structures were counted from 5 different fields on a wet slide (~50 cells/field). Experiments were independently repeated 3 times and illustrated as percentage of cells with visible structures (average ± SEM).

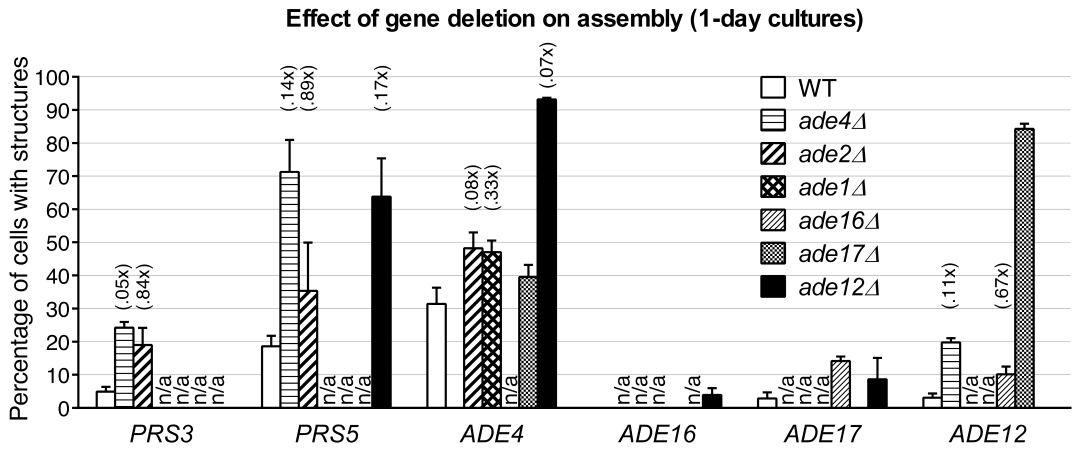

Figure 4.9 Effect of removal of upstream/downstream gene on assembly of PRPP and *de novo* purine biosynthetic enzymes

Yeast cells expressing GFP-tagged PRPP or *de novo* purine biosynthetic enzymes while simultaneously being deficient in one of the upstream/downstream genes in the pathway were grown in YPD for 1 day. Cells with structures were counted from 5 different fields on a wet slide (~50 cells/field). Experiments were independently repeated 3 times and illustrated as percentage of cells with visible structures (average ± SEM). The protein expression level (detected by Western blot) relative to WT was indicated above each bar.

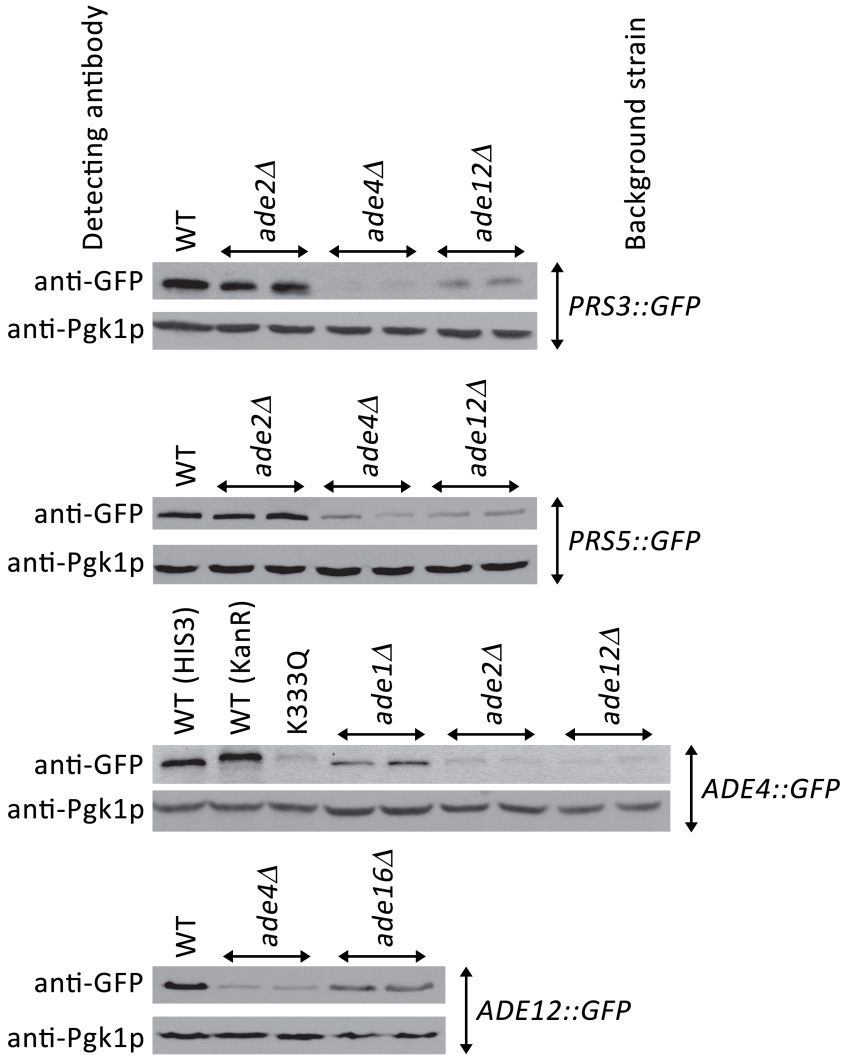

Figure 4.10 Increase in assembly of purine biosynthetic enzymes is inversely proportional to their expression levels when one of the enzymes being upstream/downstream in the pathway is disrupted

Yeast cells expressing GFP-tagged purine biosynthetic enzyme and simultaneously being deficient in one of the genes located upstream/downstream in the pathway were grown in YPD for 1 day (2 different clones were used). The whole cell extracts were prepared for Western blots. Rabbit anti-GFP (1:5000) was used as a primary antibody and donkey anti-rabbit IgG (1:10,000) as a secondary antibody. For detecting internal loading control, mouse anti-yeast PGK (1:10,000) was used as primary antibody, and sheep anti-mouse IgG (1:2,500) as secondary antibody. For *ADE4::GFP*, we showed that two different selectable markers (*HIS3* and KanR) did not have a significant effect on the expression of *ADE4*. In addition, K333Q mutation introduced endogenously to *ADE4* allele did show 2.6-fold assembly at log phase in spite of much lower of its expression level compared to WT.

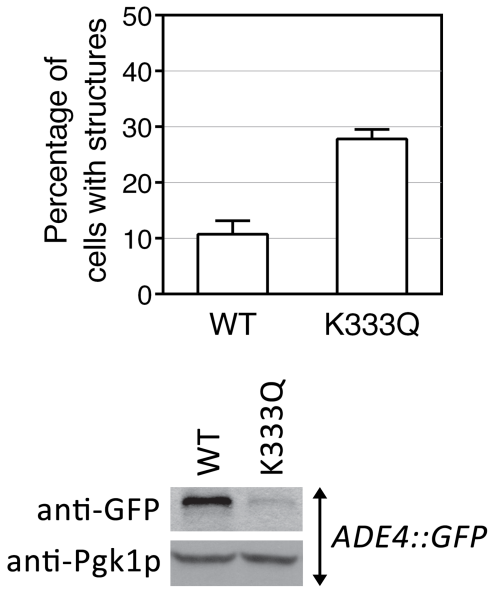

Figure 4.11 K333Q mutation causes 2.6-fold increase of Ade4p assembly, despite being 10-fold less expressed than WT enzyme

Yeast cells expressing Ade4p-GFP with K333Q mutation were grown to log phase (OD_{600} ~0.4-0.6) in YPD. Cells with structures were counted from 5 different fields on a wet slide (~50 cells/field). Experiments were independently repeated for 3 times and illustrated as percentage of cells with visible structures (average ± SEM). Western blot was performed using rabbit anti-GFP (1:5000) as primary antibody and donkey anti-rabbit IgG (1:10,000) as secondary antibody. For detecting internal loading control, mouse anti-yeast PGK (1:10,000) was used as a primary antibody, and sheep anti-mouse IgG (1:2,500) as a secondary antibody.

Chapter 5

Summary and future directions

Summary

In Chapter 2, we have identified 9 novel filament-forming proteins which assemble into 4 distinct filaments. CTP synthase filaments were shown to be conserved in yeast, *Drosophila*, and mammals. Basic characterization by shifting cells into a variety of nutrient-rich or nutrient-lacking conditions demonstrated that such assembly of each protein was affected by different triggers, suggesting that they might have distinct biological roles, depending on the enzyme. Based on the experimental data from both exogenous sodium azide and nucleotide treatments, CTP synthase filaments were concluded to be storage places for inactive enzymes (Noree et al., 2010).

In Chapter 3, mutational studies of CTP synthase *in vivo* showed that the regulation of CTP synthase polymerization is mediated by nucleotide binding. Moreover, filament formation is coupled to the regulation of CTP synthase activity. Multiple pieces of data argue for these conclusions: (1) Disruption of ATP or UTP binding affected the polymerization of CTP synthase, promoted an increased filament formation frequency and increased filament length. (2) A mutant defective in CTP binding, which confers insensitivity to feedback inhibition, conferred CTP synthase assembly on 100% of mutant cells. Interestingly, however, the structures were all present as foci, rather than filaments. This suggested that CTP binding is critical for negative regulation of filament formation. (3) A mutation which prevented tetramerization resulted in an increase of CTP synthase polymerization frequency and a slight increase in their length. Consistent with the data in Chapter 2, this argued that the CTP synthase filaments are composed of inactive dimers. (4) Phosphorylation has been shown previously to regulate CTP synthase enzyme activity. However, phosphorylation seems not to play a fundamental role in the

polymerization of CTP synthase, except for the phosphorylation sites which are located close to the other key regulatory sites or the dimer/tetramer interface. In sum, the binding of substrate (ATP and UTP) to the enzyme promotes the tetramerization of CTP synthase, and therefore stimulates CTP synthase enzyme activity. Conversely, either the absence of substrate or the presence of high CTP levels prevents substrate binding to the enzyme, therefore preventing tetramerization of CTP synthase. Eventually, inactive dimers of CTP synthase tend to polymerize into filaments, acting as storage place of inactive enzymes.

In Chapter 4, it was demonstrated that the purinosome is not conserved in budding yeast. Unlike mammalian purine biosynthetic enzymes, not all of yeast purine enzymes are capable of self-assembly. Intriguingly, however, the yeast enzymes at the nodes or branch points of the *de novo* purine biosynthetic pathway each display independent assembly when cells are grown to saturation. Furthermore, this assembly is regulated by the purine biosynthetic pathway intermediate metabolites. This implies that metabolic flux is probably related to the assembly of the enzymes located at nodes of biochemical pathways.

Future directions

To investigate whether the assembly of metabolic enzymes into intracellular structures is a common biological event, we have conducted a second screen of the yeast GFP collection again, but only of the yeast metabolic enzymes. Based on the information gathered by YeastCyc Biochemical Pathways (SGD database; available at www.yeastgenome.org), 537 proteins have been listed as proteins involved in biochemical pathways in *S. cerevisiae*. However, 440 proteins on that list were made as GFP-tagged proteins and available in the yeast GFP collection (Huh et al., 2003). We have initially investigated all of these 440 yeast strains at several growth conditions, covering log phase, saturation (1-day culture), and stationary phase (5-day culture). The lists of proteins found here that showed intracellular structures (on the basis that they did show more than 10% of cells with structures in one of the growth conditions observed) are indicated in Tables 5.1 and 5.2 for proteins known to be expressed in the cytoplasm, and in mitochondrion, respectively.

Using data obtained from our first publication (Noree et al., 2010) and the latest re-screen of yeast strains expressing GFP-tagged metabolic enzymes, the proteins which have been identified to be able to form filaments are being examined to determine if any are present in the same filaments. Pairwise colocalization experiments have been employed to address this question. To date, we have identified at least 9 novel intracellular filaments in yeast, as delineated in Figure 5.1. These filaments are composed of: (1) Acetyl-CoA carboxylase (Acc1p), (2) asparagine synthase (Asn1p and Asn2p), (3) kynureninase (Bna5p), (4) the translation initiation eIF2/2B complex (Gcd2p, Gcd6p, Gcd7p, Gcn3p, and Sui2p), (5) glycogen debranching enzyme (Gdb1p), (6) glutamate

synthase (Glt1p), (7) PRPP synthase (Prs2p, Prs3p, Prs4p, and Prs5p), (8) GDP-mannose pyrophosphorylase (Psa1p), and (9) CTP synthase (Ura7p and Ura8p).

The questions to be further studied include: (1) Are these filaments conserved in other living organisms? (2) What is the underlying mechanism of their assembly? (3) What is the biological importance of their existence as filaments? We will continue our work in the same fashion that we have done for the case of CTP synthase filaments by performing basic characterization (media shift experiments), and mutational analyses *in vivo* in respect to the previous studies of their molecular structures and functions.

Additionally, *in vitro* polymerization studies should prove valuable in revealing the details of how the metabolic enzymes self-organize into polymers. Both *in vitro* and *in vivo* studies of such enzyme should ultimately inform us as to whether their polymerization state is associated with metabolic disorders and diseases in humans. Table 5.3 shows the connection between abnormal activity/level of certain metabolic enzymes and human diseases in which they are involved. If the abnormality in the enzymatic activity displays a correlation with the loss of regulated structure formation by the studied enzymes, this could shed light on finding treatments for the impaired regulation of these enzymes.

Material and Methods

Media and Yeast Strains

Strains with GFP tagged genes were from the yeast GFP collection (Huh et al., 2003). All yeast strains were grown at 30°C in YPD (2% peptone, 1% yeast extract, and 2% dextrose) for indicated time points with shaking.

Pairwise colocalization experiments

GFP yeast strains (from the yeast GFP collection) were used as a background. pBS34 is a plasmid for making a cassette of mCherry-KanR for tagging a second protein. The primers were designed as described in the protocol provided by the University of Washington Yeast Resource Center (available at http://depts.washington.edu/yeastrc/pages/pBS34.html), except that we extended 10 more nucleotides for the homology sequence to the gene of interest in order to improve the homologous recombination during transforming yeasts with the purified PCR cassette. PCR was performed using KOD hot start DNA polymerase (Novagen®), following to the protocol instructed by the manufacturer. Yeast GFP strains were transformed with the purified DNA cassette using standard protocol of lithium acetate/PEG method as described in Noree, et al., 2010. The positive clones were validated by PCR and fluorescence microscopy.

Microscopy

Cells were fixed by adding 100 µl of 37% w/v formaldehyde to 1 ml of yeast liquid culture, incubated on a rotating platform for at least 15 min at room temperature, collected by centrifugation at 6000 rpm for 1 min, and washed once with sterile water.

The cells were then resuspended in 1M sorbitol. Imaging was performed using a DeltaVision® system with an Olympus IX70 microscope, Olympus PlanApo 60X/1.40 Oil objective, and SoftWoRx™ software version 2.5 (Applied Precision).

Acknowledgements

I would like to thank K. Begovich for helping screen the yeast GFP collection at the 5-day time point, E. Monfort-Prieto for making yeast strains expressing double-fluorescently tagged proteins for the pairwise colocalization experiments, and R. Aroian for use of his deconvolution microscope.

Figure 5.1 Pairwise colocalization experiments of novel filament-forming proteins

Nine distinct filaments were formed by the following proteins; (1) Acc1p, (2) Asn1p and Asn2p, (3) Bna5p, (4) Gcd2p, Gcd6p, Gcd7p, Gcn3, and Sui2, (5) Gdb1p, (6) Glt1p, (7) Prs2p, Prs3p, Prs4p, and Prs5p, (8) Psa1p, and (9) Ura7p and Ura8p.

Table 5.1 Cytoplasmic proteins identified to be able to form intracellular structures

Proteins	Molecular Function (SGD)	Pathways (SGD)	Cellular components (SGD)	Abundance (% cells with structures)		
				Log	1-day	5-day
Acs1p	Acetate-CoA ligase	Acetate utilization Ethanol degradation	Cytosol Integral to membrane Mitochondrion	0%	4%	92%
Ade4p	Amidophosphoribosyltransferase	*de novo* biosynthesis of purine nucleotides	Cytoplasm	0%	18%	10%
Ade12p	Adenylosuccinate synthase	*de novo* biosynthesis of purine nucleotides	Cytoplasm	0%	0%	44%
Ade16p	IMP cyclohydrolase Phosphoribosylaminoimidazolecarboxamide formyltransferase	*de novo* biosynthesis of purine nucleotides	Cytosol	0%	0%	42%
Ade17p	IMP cyclohydrolase Phosphoribosylaminoimidazolecarboxamide formyltransferase	*de novo* biosynthesis of purine nucleotides	Cytosol Plasma membrane enriched fraction	0%	4%	33%
Adh2p	Alcohol dehydrogenase (NAD)	Ethanol degradation Glucose fermentation Isoleucine degradation Leucine degradation Phenylalanine degradation Tryptophan degradation Valine degradation	Cytoplasm	0%	0%	10%
Ald6p	Aldehyde dehydrogenase (NADP+)	Glucose fermentation	Cytosol Mitochondrion	0%	13%	66%
Aro1p	3-dehydroquinate dehydratase 3-dehydroquinate synthase 3-phosphoshikimate 1-Carboxyvinyltransferase Shikimate 3-dehydrogenase (NADP+) Shikimate kinase	Chorismate biosynthesis Phenylalanine biosynthesis Tyrosine biosynthesis Tryptophan biosynthesis	Cytoplasm	0%	2%	16%
Asn1p	Asparagine synthase (glutamine-hydrolyzing)	Asparagine biosynthesis	Cytoplasm	0%	10%	90%
Asn2p	Asparagine synthase (glutamine-hydrolyzing)	Asparagine biosynthesis	Cytoplasm	0%	12%	92%
Bna5p	Kynureninase	*de novo* NAD biosynthesis Tryptophan degradation via kynurenine	Cytoplasm Nucleus	0%	10%	80%
Cdc19p	Pyruvate kinase	Glucose fermentation Glycolysis	Cytosol Plasma membrane enriched fraction	5%	34%	85%
Cys4p	Cystathionine beta-synthase	Cysteine biosynthesis from homocysteine Homocysteine and cysteine interconversion Homocysteine degradation	Cytoplasm Mitochondrion	3%	11%	3%
Dph2p	Unknown	Diphthamide biosynthesis	Cytoplasm	0%	0%	28%
Faa4p	Long-chain fatty acid-CoA ligase	Fatty acid oxidation	Lipid particle Cytoplasm	28%	61%	5%
Fas1p	3-hydroxyacyl-[acyl-carrier-protein] dehydratase [acyl-carrier-protein] S-acetyltransferase [acyl-carrier-protein] S-malonyltransferase enoyl-[acyl-carrier-protein] reductase (NADPH, B-specific) Contributes to fatty acid synthase Palmitoyltransferase	Fatty acid biosynthesis Myristate biosynthesis Palmitate biosynthesis Stearate biosynthesis	Cytosol Fatty acid synthase complex Lipid particle Cytoplasm Mitochondrion	0%	3%	26%
Fba1p	Fructose-bisphosphate aldolase	Gluconeogenesis Glucose fermentation Glycolysis	Cytosol Mitochondrion Cytoplasm	0%	0%	15%
Fum1p	Fumarate hydratase	TCA cycle, aerobic respiration	Cytosol Mitochondrial matrix Mitochondrion	0%	13%	67%
Gdb1p	4-alpha-glucanotransferase Amylo-alpha-1,6-glucosidase	Glycogen catabolism	Cytoplasm Mitochondrion	0%	12%	39%
Gdh1p	Glutamate dehydrogenase (NADP+)	Glutamate biosynthesis from ammonia	Nucleus Soluble fraction Cytoplasm	0%	17%	12%
Glk1p	Glucokinase	Glucose fermentation Glucose-6-phosphate biosynthesis Mannose degradation	Cytosol Plasma membrane enriched fraction	22%	2%	25%

Table 5.1 Cytoplasmic proteins identified to be able to form intracellular structures (continued)

Proteins	Molecular Function (SGD)	Pathways (SGD)	Cellular components (SGD)	Abundance (% cells with structures)		
				Log	1-day	5-day
Gln1p	Glutamate-ammonia ligase	Glutamine biosynthesis	Cytoplasm	5%	63%	86%
Gly1p	L-allo-threonine aldolase Threonine aldolase	Glycine biosynthesis from threonine	Cytosol	0%	11%	9%
Gpd1p	Glycerol-3-phosphate dehydrogenase (NAD+)	Glycerol biosynthesis Phosphatidate biosynthesis II (the glycerol-3-phosphate pathway)	Cytosol Nucleus Peroxisome	89%	86%	1%
Gre3p	Alditol:NADP+ 1-oxidoreductase D-xylose:NADP reductase Glucose 1-dehydrogenase (NADP+) mRNA binding	Xylose metabolism	Cytoplasm Nucleus	0%	10%	0%
Hem2p	Porphobilinogen synthase	Tetrapyrrole biosynthesis Heme and siroheme biosynthesis	Cytoplasm Nucleus	0%	12%	73%
Hem13p	Coproporphyrinogen oxidase	Heme biosynthesis	Cytosol	0%	15%	0%
Mdh2p	L-Malate dehydrogenase	Gluconeogenesis Glyoxylate cycle	Cytosol Cytoplasm	100%	100%	0%
Pdc1p	Pyruvate decarboxylase	Acetoin biosynthesis II Glucose fermentation Isoleucine degradation Phenylalanine degradation Tryptophan degradation Valine degradation	Cytosol Nucleus Cytoplasm	0%	0%	72%
Pnc1p	Nicotinamidase	NAD salvage pathway	Cytoplasm Nucleus Peroxisome	100%	96%	87%
Pro3p	Pyrroline-5-carboxylate reductase	Arginine degradation Proline biosynthesis	Cytoplasm	0%	12%	2%
Prs2p	Contributes to ribose phosphate diphosphokinase	Histidine, purine, and pyrimidine biosynthesis	Cytoplasm	0%	10%	1%
Prs3p	Contributes to ribose phosphate diphosphokinase	Histidine, purine, and pyrimidine biosynthesis	Cytoplasm	0%	6%	63%
Prs5p	Ribose phosphate diphosphokinase	Histidine, purine, and pyrimidine biosynthesis	Cytoplasm	0%	40%	55%
Psa1p	Mannose-1-phosphate guanylyltransferase	Dolichyl phosphate D-mannose biosynthesis	Cytoplasm	0%	23%	6%
Rnr4p	Ribonucleoside-diphosphate reductase	*de novo* biosynthesis of purine nucleotides *de novo* biosynthesis of pyrimidine deoxyribonucleotides	Cytoplasm Nucleus Ribonucleoside-diphosphate reductase complex	2%	27%	80%
Sam1p	Methionine adenosyltransferase	S-adenosylmethionine biosynthesis	Cytoplasm	0%	19%	95%
Sam2p	Methionine adenosyltransferase	S-adenosylmethionine biosynthesis	Unknown	0%	11%	60%
Sec53p	Phosphomannomutase	Dolichyl phosphate D-mannose biosynthesis	Cytosol	0%	9%	41%
Shm2p	Glycine hydroxymethyltransferase	Folate biosynthesis Folate polyglutamylation Glycine biosynthesis from serine Serine biosynthesis from glyoxylate	Cytoplasm Mating projection tip Plasma membrane enriched fraction	19%	45%	27%
Tal1p	sedoheptulose-7-phosphate:D-glyceraldehyde-3-phosphate glyceronetransferase	Non-oxidative branch of the pentose phosphate pathway	Cytoplasm Nucleus	15%	58%	71%
Tdh3p	glyceraldehyde-3-phosphate dehydrogenase (NAD+) (phosphorylating)	Gluconeogenesis Glucose fermentation Glycolysis	Cytoplasm Fungal-type cell wall Lipid particle Mitochondrion Plasma membrane enriched fraction	0%	N/A	41%
Thr1p	Homoserine kinase	Threonine biosynthesis	Unknown	81%	78%	56%
Tpi1p	Triosephosphate isomerase	Glucose fermentation Glycolysis	Mitochondrion Cytoplasm Plasma membrane enriched fraction	0%	3%	20%

Table 5.1 Cytoplasmic proteins identified to be able to form intracellular structures (continued)

Proteins	Molecular Function (SGD)	Pathways (SGD)	Cellular components (SGD)	Abundance (% cells with structures)		
				Log	1-day	5-day
Trr1p	Ferrous iron binding Thioredoxin-disulfide reductase	Thioredoxin system	Cytosol	0%	13%	29%
Ura7p	CTP synthase	*de novo* biosynthesis of pyrimidine ribonucleotides	Cytosol	0%	9%	90%
Ura8p	CTP synthase	*de novo* biosynthesis of pyrimidine ribonucleotides	Cytosol	0%	6%	89%

Table 5.2 Mitochondrial proteins identified to be able to form intracellular structures

Proteins	Molecular Function (SGD)	Pathways (SGD)	Cellular component (SGD)	Abundance (% cells with structures)		
				Log	1-day	5-day
Acc1p	Acetyl-CoA carboxylase Biotin carboxylase	Fatty acid biosynthesis	Endoplasmic reticulum membrane Mitochondrion	19%	8%	37%
Acs1p	Acetate-CoA ligase	Acetate utilization Ethanol degradation	Cytosol Integral to membrane Mitochondrion	0%	4%	92%
Adh3p	Alcohol dehydrogenase (NAD)	Glucose fermentation Ethanol degradation Isoleucine degradation Leucine degradation Phenylalanine degradation Tryptophan degradation Valine degradation	Mitochondrial matrix Soluble fraction Mitochondrion	N/A	41%	4%
Ald4p	Aldehyde dehydrogenase (NAD) Aldehyde dehydrogenase [NAD(P)+]	Glucose fermentation	Mitochondrial nucleoid Mitochondrion	59%	97%	94%
Ald5p	Aldehyde dehydrogenase [NAD(P)+]	Glucose fermentation	Mitochondrion	N/A	18%	11%
Ald6p	Aldehyde dehydrogenase (NADP+)	Glucose fermentation	Cytosol Mitochondrion	0%	13%	66%
Cha1p	L-serine ammonia-lyase L-threonine ammonia-lyase	L-serine degradation Threonine catabolism	Mitochondrial nucleoid Mitochondrion	0%	29%	5%
Coq5p	2-hexaprenyl-6-methoxy-1,4-benzoquinone methyltransferase	Ubiquinone biosynthesis from 4-hydroxybenzoate	Mitochondrial matrix Mitochondrion	N/A	N/A	41%
Cys4p	Cystathionine beta-synthase	Cysteine biosynthesis from homocysteine Homocysteine and cysteine interconversion Homocysteine degradation	Cytoplasm Mitochondrion	3%	11%	3%
Fas1p	3-hydroxyacyl-[acyl-carrier-protein] dehydratase [acyl-carrier-protein] S-acetyltransferase [acyl-carrier-protein] S-malonyltransferase enoyl-[acyl-carrier-protein] reductase (NADPH, B-specific) Contributes to fatty acid synthase Palmitoyltransferase	Fatty acid biosynthesis Myristate biosynthesis Palmitate biosynthesis Stearate biosynthesis	Cytosol Fatty acid synthase complex Lipid particle Cytoplasm Mitochondrion	0%	3%	26%
Fba1p	Fructose-bisphosphate aldolase	Gluconeogenesis Glucose fermentation Glycolysis	Cytosol Mitochondrion Cytoplasm	0%	0%	15%
Fum1p	Fumarate hydratase	TCA cycle, aerobic respiration	Cytosol Mitochondrial matrix Mitochondrion	0%	13%	67%
Gdb1p	4-alpha-glucanotransferase Amylo-alpha-1,6-glucosidase	Glycogen catabolism	Cytoplasm Mitochondrion	0%	12%	39%
Gdh2p	Glutamate dehydrogenase (NAD+)	Glutamate degradation IX	Mitochondrion	19%	89%	95%
Glt1p	Glutamate synthase (NADH)	Glutamate biosynthesis from glutamine	Mitochondrion	24%	64%	98%
Idh2p	Contributes to isocitrate dehydrogenase (NAD+)	TCA cycle, aerobic respiration	Mitochondrial isocitrate dehydrogenase complex (NAD+) Mitochondrial matrix Mitochondrion	18%	58%	31%
Ilv1p	L-threonine ammonia-lyase	Isoleucine biosynthesis	Mitochondrion	43%	4%	1%
Ilv2p	Acetolactate synthase Flavin adenine dinucleotide binding	Acetoin biosynthesis Isoleucine biosynthesis Valine biosynthesis	Acetolactate synthase complex Mitochondrion	N/A	N/A	20%
Kgd1p	Oxoglutarate dehydrogenase (succinyl-transferring)	2-ketoglutarate dehydrogenase complex TCA cycle, aerobic respiration	Mitochondrial matrix Mitochondrial nucleoid Mitochondrial oxoglutarate dehydrogenase complex Mitochondrion	47%	95%	100%

Table 5.2 Mitochondrial proteins identified to be able to form intracellular structures (continued)

Proteins	Molecular Function (SGD)	Pathways (SGD)	Cellular component (SGD)	Abundance (% cells with structures)		
				Log	1-day	5-day
Kgd2p	Dihydrolipoyllysine-residue succinyltransferase	2-ketoglutarate dehydrogenase complex TCA cycle, aerobic respiration	Mitochondrial nucleoid Mitochondrial oxoglutarate dehydrogenase complex Mitochondrion	0%	0%	19%
Lpd1p	Dihydrolipoyl dehydrogenase Glycine dehydrogenase (decarboxylating) Oxoglutarate dehydrogenase (succinyl-transferring) Pyruvate dehydrogenase	2-ketoglutarate dehydrogenase complex Folate biosynthesis Glycine cleavage complex Pyruvate dehydrogenase complex TCA cycle, aerobic respiration	Glycine cleavage complex Mitochondrial nucleoid Mitochondrial oxoglutarate dehydrogenase complex Mitochondrion	N/A	N/A	85%
Mdh1p	L-malate dehydrogenase mRNA binding	TCA cycle, aerobic respiration	Mitochondrial matrix Mitochondrion	N/A	N/A	12%
Pda1p	Pyruvate dehydrogenase (acetyl-transferring)	Pyruvate dehydrogenase complex	Mitochondrial nucleoid Mitochondrial pyruvate dehydrogenase complex Mitochondrion	97%	96%	20%
Rip1p	Contributes to ubiquinol-cytochrome-c reductase	Aerobic respiration, electron transport chain	Mitochondrial respiratory chain complex III Mitochondrion	N/A	N/A	29%
Sdh4p	Contributes to: succinate dehydrogenase (ubiquinone)	Aerobic respiration, electron transport chain TCA cycle, aerobic respiration	Mitochondrial respiratory chain complex III Mitochondrion	0%	12%	22%
Tdh3p	glyceraldehyde-3-phosphate dehydrogenase (NAD+) (phosphorylating)	Gluconeogenesis Glucose fermentation Glycolysis	Cytoplasm Fungal-type cell wall Lipid particle Mitochondrion Plasma membrane enriched fraction	0%	N/A	41%
Tpi1p	Triosephosphate isomerase	Glucose fermentation Glycolysis	Mitochondrion Cytoplasm Plasma membrane enriched fraction	0%	3%	20%

Table 5.3 Human diseases associated with abnormality in metabolic enzyme activity

Enzymes	Yeast gene(s)	Human diseases/disorders	References
Acetyl-CoA carboxylase	ACC1	Metabolic syndrome, heart disease, type 2 diabetes	(Harwood, 2004; Harwood, 2005)
Purine enzymes	ADE genes	Lesch-Nyhan syndrome, rheumatoid arthritis, gout, cancer	(Ho et al., 1986; Kerstens et al., 1995; Kerstens et al., 1994; Minana et al., 1984; Zborovskii et al., 2000)
Aldehyde dehydrogenase	ALD genes	Liver disease, type 2 diabetes, Parkinson's, Alzheimer's,	(Fitzmaurice et al., 2012; Jerntorp et al., 1986; Mazzanti et al., 1989; Michel et al., 2010)
Asparagine synthase	ASN1, ASN2	Cancer	(Haskell and Canellos, 1969; Sircar et al., 2012)
Pyruvate kinase	CDC19	Neuromuscular disease, anaemia	(Alli et al., 2008; Cohen-Solal et al., 1998; Manco et al., 2010; Weinstock et al., 1977)
PRPP synthase	PRS genes	Deafness, gout, mental retardation ataxia, Arts syndrome	(Becker et al., 1986; Becker et al., 1989; de Brouwer et al., 2010; de Brouwer et al., 2007; Duley et al., 2011; Fujimori, 1996; Iizasa, 2008; Kawasugi and Takeuchi, 2003; Lopez Jimenez et al., 1990; Micheli and Taddeo, 1981; Nishida et al., 1981; Zoref-Shani and Sperling, 1979; Zoref et al., 1978)
Fumarate hydratase	FUM1	Fumaric aciduria, encephalopathy	(Feldmann, 2012)
Glucokinase	GLK1	Obesity, type 2 diabetes, hypoglycemia, hyperglycemia	(Froguel et al., 1993; Mahalingam et al., 1999; Otaegui et al., 2003; Shiota et al., 2001)
Aminolevolunate dehydratase	HEM2	Hepatic porphyria	(Feldmann, 2012)
Pyruvate dehydrogenase	PDA1	Leigh's disease, Alzheimer's	(Sheu et al., 1985; Sheu et al., 1989)
Pyruvate decarboxylase	PDC1	Leigh's disease	(Toshima et al., 1982; Van Biervliet et al., 1980)
Methionine adenosyltransferase	SAM1, SAM2	Parkinson's, liver disease, hypermethioninanemia, mental retardation	(Cheng et al., 1997; Feldmann, 2012; Lu et al., 2006)
Glyceraldehyde-3-phosphate dehydrogenase	TDH3	Alzheimer's, Huntington's, Parkinson's	(Huang et al., 2011; Mazzola and Sirover, 2001; Mazzola and Sirover, 2003)
CTP synthase	URA7, URA8	Cancer	(Whelan et al., 1994; Williams et al., 1978)

References

Alli, N., M. Coetzee, V. Louw, B. van Rensburg, G. Rossouw, L. Thompson, S. Pissard, and S.L. Thein. 2008. Sickle cell disease in a carrier with pyruvate kinase deficiency. *Hematology*. 13:369-372.

An, S., Y. Deng, J.W. Tomsho, M. Kyoung, and S.J. Benkovic. 2010a. Microtubule-assisted mechanism for functional metabolic macromolecular complex formation. *Proceedings of the National Academy of Sciences of the United States of America*. 107:12872-12876.

An, S., R. Kumar, E.D. Sheets, and S.J. Benkovic. 2008. Reversible compartmentalization of *de novo* purine biosynthetic complexes in living cells. *Science*. 320:103-106.

An, S., M. Kyoung, J.J. Allen, K.M. Shokat, and S.J. Benkovic. 2010b. Dynamic regulation of a metabolic multi-enzyme complex by protein kinase CK2. *The Journal of biological chemistry*. 285:11093-11099.

Aronow, B., and B. Ullman. 1986. Mammalian mutants genetically altered in CTP synthetase activity. *Advances in experimental medicine and biology*. 195 Pt B:263-269.

Aronow, B., and B. Ullman. 1987. In situ regulation of mammalian CTP synthetase by allosteric inhibition. *The Journal of biological chemistry*. 262:5106-5112.

Ausmees, N., J.R. Kuhn, and C. Jacobs-Wagner. 2003. The bacterial cytoskeleton: an intermediate filament-like function in cell shape. *Cell*. 115:705-713.

Barany, M., J.T. Barron, L. Gu, and K. Barany. 2001. Exchange of the actin-bound nucleotide in intact arterial smooth muscle. *The Journal of biological chemistry*. 276:48398-48403.

Bashkirov, V.I., H. Scherthan, J.A. Solinger, J.M. Buerstedde, and W.D. Heyer. 1997. A mouse cytoplasmic exoribonuclease (mXRN1p) with preference for G4 tetraplex substrates. *The Journal of cell biology*. 136:761-773.

Baudin, A., O. Ozier-Kalogeropoulos, A. Denouel, F. Lacroute, and C. Cullin. 1993. A simple and efficient method for direct gene deletion in Saccharomyces cerevisiae. *Nucleic acids research*. 21:3329-3330.

Baudoin, C., G. Meneguzzi, M.M. Portier, M. Demarchez, F. Bernerd, A. Pisani, and J.P. Ortonne. 1993. Peripherin, a neuronal intermediate protein, is stably expressed by neuroendocrine carcinomas of the skin, their xenograft on nude mice, and the corresponding primary cultures. *Cancer research*. 53:1175-1181.

Becker, M.A., P.J. Kostel, and L.J. Meyer. 1975. Human phosphoribosylpyrophosphate synthetase. Comparison of purified normal and mutant enzymes. *The Journal of biological chemistry*. 250:6822-6830.

Becker, M.A., M.J. Losman, A.L. Rosenberg, I. Mehlman, D.J. Levinson, and E.W. Holmes. 1986. Phosphoribosylpyrophosphate synthetase superactivity. A study of five patients with catalytic defects in the enzyme. *Arthritis and rheumatism*. 29:880-888.

Becker, M.A., J.G. Puig, F.A. Mateos, M.L. Jimenez, M. Kim, and H.A. Simmonds. 1989. Neurodevelopmental impairment and deranged PRPP and purine nucleotide synthesis in inherited superactivity of PRPP synthetase. *Advances in experimental medicine and biology*. 253A:15-22.

Benavente, R., and G. Krohne. 1986. Involvement of nuclear lamins in postmitotic reorganization of chromatin as demonstrated by microinjection of lamin antibodies. *The Journal of cell biology*. 103:1847-1854.

Bi, E.F., and J. Lutkenhaus. 1991. FtsZ ring structure associated with division in Escherichia coli. *Nature*. 354:161-164.

Bignami, A., T. Raju, and D. Dahl. 1982. Localization of vimentin, the nonspecific intermediate filament protein, in embryonal glia and in early differentiating neurons. *In vivo* and *in vitro* immunofluorescence study of the rat embryo with vimentin and neurofilament antisera. *Developmental biology*. 91:286-295.

Bork, P., C. Sander, and A. Valencia. 1992. An ATPase domain common to prokaryotic cell cycle proteins, sugar kinases, actin, and hsp70 heat shock proteins. *Proceedings of the National Academy of Sciences of the United States of America*. 89:7290-7294.

Brown, H.P. 1945. On the structure and mechanics of the protozoan flagellum. *The Ohio journal of science*. 45:247-301.

Buchan, J.R., D. Muhlrad, and R. Parker. 2008. P bodies promote stress granule assembly in Saccharomyces cerevisiae. *The Journal of cell biology*. 183:441-455.

Burke, B., J. Tooze, and G. Warren. 1983. A monoclonal antibody which recognises each of the nuclear lamin polypeptides in mammalian cells. *The EMBO journal*. 2:361-367.

Buszczak, M., S. Paterno, D. Lighthouse, J. Bachman, J. Planck, S. Owen, A.D. Skora, T.G. Nystul, B. Ohlstein, A. Allen, J.E. Wilhelm, T.D. Murphy, R.W. Levis, E. Matunis, N. Srivali, R.A. Hoskins, and A.C. Spradling. 2007. The carnegie

protein trap library: a versatile tool for Drosophila developmental studies. *Genetics*. 175:1505-1531.

Campanella, M.E., H. Chu, and P.S. Low. 2005. Assembly and regulation of a glycolytic enzyme complex on the human erythrocyte membrane. *Proceedings of the National Academy of Sciences of the United States of America*. 102:2402-2407.

Campbell, S.G., N.P. Hoyle, and M.P. Ashe. 2005. Dynamic cycling of eIF2 through a large eIF2B-containing cytoplasmic body: implications for translation control. *The Journal of cell biology*. 170:925-934.

Carlier, M.F., D. Didry, and D. Pantaloni. 1987. Microtubule elongation and guanosine 5'-triphosphate hydrolysis. Role of guanine nucleotides in microtubule dynamics. *Biochemistry*. 26:4428-4437.

Carman, G.M., and G.M. Zeimetz. 1996. Regulation of phospholipid biosynthesis in the yeast Saccharomyces cerevisiae. *The Journal of biological chemistry*. 271:13293-13296.

Chang, Y.F., S.S. Martin, E.P. Baldwin, and G.M. Carman. 2007. Phosphorylation of human CTP synthetase 1 by protein kinase C: identification of Ser(462) and Thr(455) as major sites of phosphorylation. *The Journal of biological chemistry*. 282:17613-17622.

Chant, J. 1996. Septin scaffolds and cleavage planes in Saccharomyces. *Cell*. 84:187-190.

Cheng, H., C. Gomes-Trolin, S.M. Aquilonius, A. Steinberg, C. Lofberg, J. Ekblom, and L. Oreland. 1997. Levels of L-methionine S-adenosyltransferase activity in erythrocytes and concentrations of S-adenosylmethionine and S-adenosylhomocysteine in whole blood of patients with Parkinson's disease. *Experimental neurology*. 145:580-585.

Chernoff, Y.O., S.L. Lindquist, B. Ono, S.G. Inge-Vechtomov, and S.W. Liebman. 1995. Role of the chaperone protein Hsp104 in propagation of the yeast prion-like factor [psi+]. *Science*. 268:880-884.

Chien, C.L., and R.K. Liem. 1994. Characterization of the mouse gene encoding the neuronal intermediate filament protein alpha-internexin. *Gene*. 149:289-292.

Choi, M.G., and G.M. Carman. 2007. Phosphorylation of human CTP synthetase 1 by protein kinase A: identification of Thr455 as a major site of phosphorylation. *The Journal of biological chemistry*. 282:5367-5377.

Choi, M.G., T.S. Park, and G.M. Carman. 2003. Phosphorylation of Saccharomyces cerevisiae CTP synthetase at Ser424 by protein kinases A and C regulates

phosphatidylcholine synthesis by the CDP-choline pathway. *The Journal of biological chemistry*. 278:23610-23616.

Cid, V.J., L. Adamikova, R. Cenamor, M. Molina, M. Sanchez, and C. Nombela. 1998. Cell integrity and morphogenesis in a budding yeast septin mutant. *Microbiology*. 144 (Pt 12):3463-3474.

Cohen-Solal, M., C. Prehu, H. Wajcman, C. Poyart, J. Bardakdjian-Michau, J. Kister, D. Prome, C. Valentin, D. Bachir, and F. Galacteros. 1998. A new sickle cell disease phenotype associating Hb S trait, severe pyruvate kinase deficiency (PK Conakry), and an alpha2 globin gene variant (Hb Conakry). *British journal of haematology*. 103:950-956.

Conrado, R.J., J.D. Varner, and M.P. DeLisa. 2008. Engineering the spatial organization of metabolic enzymes: mimicking nature's synergy. *Current opinion in biotechnology*. 19:492-499.

Costa, M.L., R. Escaleira, A. Cataldo, F. Oliveira, and C.S. Mermelstein. 2004. Desmin: molecular interactions and putative functions of the muscle intermediate filament protein. *Brazilian journal of medical and biological research = Revista brasileira de pesquisas medicas e biologicas / Sociedade Brasileira de Biofisica ... [et al.]*. 37:1819-1830.

Cowan, N.J. 1984. Tubulin genes and the diversity of microtubule function. *Oxford surveys on eukaryotic genes*. 1:36-60.

Dagenais, A., V. Bibor-Hardy, and R. Simard. 1984. Characterization of lamin proteins in BHK cells. *Experimental cell research*. 155:435-447.

Dahlstrand, J., L.B. Zimmerman, R.D. McKay, and U. Lendahl. 1992. Characterization of the human nestin gene reveals a close evolutionary relationship to neurofilaments. *Journal of cell science*. 103 (Pt 2):589-597.

de Boer, P., R. Crossley, and L. Rothfield. 1992a. The essential bacterial cell-division protein FtsZ is a GTPase. *Nature*. 359:254-256.

de Boer, P.A., R.E. Crossley, and L.I. Rothfield. 1992b. Roles of MinC and MinD in the site-specific septation block mediated by the MinCDE system of Escherichia coli. *Journal of bacteriology*. 174:63-70.

de Brouwer, A.P., H. van Bokhoven, S.B. Nabuurs, W.F. Arts, J. Christodoulou, and J. Duley. 2010. PRPS1 mutations: four distinct syndromes and potential treatment. *American journal of human genetics*. 86:506-518.

de Brouwer, A.P., K.L. Williams, J.A. Duley, A.B. van Kuilenburg, S.B. Nabuurs, M. Egmont-Petersen, D. Lugtenberg, L. Zoetekouw, M.J. Banning, M. Roeffen, B.C. Hamel, L. Weaving, R.A. Ouvrier, J.A. Donald, R.A. Wevers, J. Christodoulou, and H. van Bokhoven. 2007. Arts syndrome is caused by loss-of-function mutations in PRPS1. *American journal of human genetics*. 81:507-518.

Desai, A., and T.J. Mitchison. 1998. Tubulin and FtsZ structures: functional and therapeutic implications. *BioEssays : news and reviews in molecular, cellular and developmental biology*. 20:523-527.

Doi, M., M. Wachi, F. Ishino, S. Tomioka, M. Ito, Y. Sakagami, A. Suzuki, and M. Matsuhashi. 1988. Determinations of the DNA sequence of the mreB gene and of the gene products of the mre region that function in formation of the rod shape of Escherichia coli cells. *Journal of bacteriology*. 170:4619-4624.

Duley, J.A., J. Christodoulou, and A.P. de Brouwer. 2011. The PRPP synthetase spectrum: what does it demonstrate about nucleotide syndromes? *Nucleosides, nucleotides & nucleic acids*. 30:1129-1139.

Dunn, M.F. 2012. Allosteric regulation of substrate channeling and catalysis in the tryptophan synthase bienzyme complex. *Archives of biochemistry and biophysics*. 519:154-166.

Endrizzi, J.A., H. Kim, P.M. Anderson, and E.P. Baldwin. 2004. Crystal structure of Escherichia coli cytidine triphosphate synthetase, a nucleotide-regulated glutamine amidotransferase/ATP-dependent amidoligase fusion protein and homologue of anticancer and antiparasitic drug targets. *Biochemistry*. 43:6447-6463.

Endrizzi, J.A., H. Kim, P.M. Anderson, and E.P. Baldwin. 2005. Mechanisms of product feedback regulation and drug resistance in cytidine triphosphate synthetases from the structure of a CTP-inhibited complex. *Biochemistry*. 44:13491-13499.

Erickson, H.P. 2007. Evolution of the cytoskeleton. *BioEssays : news and reviews in molecular, cellular and developmental biology*. 29:668-677.

Ettema, T.J., A.C. Lindas, and R. Bernander. 2011. An actin-based cytoskeleton in archaea. *Molecular microbiology*. 80:1052-1061.

Eystathioy, T., E.K. Chan, S.A. Tenenbaum, J.D. Keene, K. Griffith, and M.J. Fritzler. 2002. A phosphorylated cytoplasmic autoantigen, GW182, associates with a unique population of human mRNAs within novel cytoplasmic speckles. *Molecular biology of the cell*. 13:1338-1351.

Fairman, J.W., S.R. Wijerathna, M.F. Ahmad, H. Xu, R. Nakano, S. Jha, J. Prendergast, R.M. Welin, S. Flodin, A. Roos, P. Nordlund, Z. Li, T. Walz, and C.G. Dealwis. 2011. Structural basis for allosteric regulation of human ribonucleotide reductase by nucleotide-induced oligomerization. *Nature structural & molecular biology*. 18:316-322.

Fares, H., L. Goetsch, and J.R. Pringle. 1996. Identification of a developmentally regulated septin and involvement of the septins in spore formation in Saccharomyces cerevisiae. *The Journal of cell biology*. 132:399-411.

Feldmann, H. 2012. Yeast molecular and cell biology. John Wiley,, Hoboken. 1 online resource (444 p.).

Figge, R.M., A.V. Divakaruni, and J.W. Gober. 2004. MreB, the cell shape-determining bacterial actin homologue, co-ordinates cell wall morphogenesis in Caulobacter crescentus. *Molecular microbiology*. 51:1321-1332.

Fitzmaurice, A.G., S.L. Rhodes, A. Lulla, N.P. Murphy, H.A. Lam, K.C. O'Donnell, L. Barnhill, J.E. Casida, M. Cockburn, A. Sagasti, M.C. Stahl, N.T. Maidment, B. Ritz, and J.M. Bronstein. 2012. Aldehyde dehydrogenase inhibition as a pathogenic mechanism in Parkinson disease. *Proceedings of the National Academy of Sciences of the United States of America*.

Franke, W.W., E. Schmid, M. Osborn, and K. Weber. 1979. Intermediate-sized filaments of human endothelial cells. *The Journal of cell biology*. 81:570-580.

Frazier, J.A., M.L. Wong, M.S. Longtine, J.R. Pringle, M. Mann, T.J. Mitchison, and C. Field. 1998. Polymerization of purified yeast septins: evidence that organized filament arrays may not be required for septin function. *The Journal of cell biology*. 143:737-749.

Froguel, P., H. Zouali, N. Vionnet, G. Velho, M. Vaxillaire, F. Sun, S. Lesage, M. Stoffel, J. Takeda, P. Passa, and et al. 1993. Familial hyperglycemia due to mutations in glucokinase. Definition of a subtype of diabetes mellitus. *The New England journal of medicine*. 328:697-702.

Fuchs, E., and K. Weber. 1994. Intermediate filaments: structure, dynamics, function, and disease. *Annual review of biochemistry*. 63:345-382.

Fujimori, S. 1996. [PRPP synthetase superactivity]. *Nihon rinsho. Japanese journal of clinical medicine*. 54:3309-3314.

Gardner, M.K., A.J. Hunt, H.V. Goodson, and D.J. Odde. 2008. Microtubule assembly dynamics: new insights at the nanoscale. *Current opinion in cell biology*. 20:64-70.

Gatenby, J.B. 1961. The electron microscopy of centriole, flagellum and cilium. *Journal. Royal Microscopical Society*. 79:299-317.

Gitai, Z., N.A. Dye, A. Reisenauer, M. Wachi, and L. Shapiro. 2005. MreB actin-mediated segregation of a specific region of a bacterial chromosome. *Cell*. 120:329-341.

Goto, M., R. Omi, N. Nakagawa, I. Miyahara, and K. Hirotsu. 2004. Crystal structures of CTP synthetase reveal ATP, UTP, and glutamine binding sites. *Structure*. 12:1413-1423.

Granger, B.L., and E. Lazarides. 1980. Synemin: a new high molecular weight protein associated with desmin and vimentin filaments in muscle. *Cell*. 22:727-738.

Halliburton, W.D. 1887. On Muscle-Plasma. *The Journal of physiology*. 8:133-202.

Harwood, H.J., Jr. 2004. Acetyl-CoA carboxylase inhibition for the treatment of metabolic syndrome. *Current opinion in investigational drugs*. 5:283-289.

Harwood, H.J., Jr. 2005. Treating the metabolic syndrome: acetyl-CoA carboxylase inhibition. *Expert opinion on therapeutic targets*. 9:267-281.

Haskell, C.M., and G.P. Canellos. 1969. l-asparaginase resistance in human leukemia--asparagine synthetase. *Biochemical pharmacology*. 18:2578-2580.

Hernando, Y., A.T. Carter, A. Parr, B. Hove-Jensen, and M. Schweizer. 1999. Genetic analysis and enzyme activity suggest the existence of more than one minimal functional unit capable of synthesizing phosphoribosyl pyrophosphate in Saccharomyces cerevisiae. *The Journal of biological chemistry*. 274:12480-12487.

Hernando, Y., A. Parr, and M. Schweizer. 1998. PRS5, the fifth member of the phosphoribosyl pyrophosphate synthetase gene family in Saccharomyces cerevisiae, is essential for cell viability in the absence of either PRS1 or PRS3. *Journal of bacteriology*. 180:6404-6407.

Higgins, M.J., D. Loiselle, T.A. Haystead, and L.M. Graves. 2008. Human cytidine triphosphate synthetase 1 interacting proteins. *Nucleosides, nucleotides & nucleic acids*. 27:850-857.

Ho, A.D., G. Dietz, I. Trede, R. Schwartz, A.V. Hoffbrand, and W. Hunstein. 1986. Enzymes of purine metabolism in hairy cell leukemia. *Cancer*. 58:96-99.

Holmes, K.C., D. Popp, W. Gebhard, and W. Kabsch. 1990. Atomic model of the actin filament. *Nature*. 347:44-49.

Horton, R.M., H.D. Hunt, S.N. Ho, J.K. Pullen, and L.R. Pease. 1989. Engineering hybrid genes without the use of restriction enzymes: gene splicing by overlap extension. *Gene*. 77:61-68.

Hove-Jensen, B. 2004. Heterooligomeric phosphoribosyl diphosphate synthase of Saccharomyces cerevisiae: combinatorial expression of the five PRS genes in Escherichia coli. *The Journal of biological chemistry*. 279:40345-40350.

Howard, J., and A.A. Hyman. 2009. Growth, fluctuation and switching at microtubule plus ends. *Nature reviews. Molecular cell biology*. 10:569-574.

Howson, R., W.K. Huh, S. Ghaemmaghami, J.V. Falvo, K. Bower, A. Belle, N. Dephoure, D.D. Wykoff, J.S. Weissman, and E.K. O'Shea. 2005. Construction, verification and experimental use of two epitope-tagged collections of budding yeast strains. *Comparative and functional genomics*. 6:2-16.

Huang, J., N. Xiong, C. Chen, J. Xiong, M. Jia, Z. Zhang, X. Cao, Z. Liang, S. Sun, Z. Lin, and T. Wang. 2011. Glyceraldehyde-3-phosphate dehydrogenase: activity inhibition and protein overexpression in rotenone models for Parkinson's disease. *Neuroscience*. 192:598-608.

Huh, W.K., J.V. Falvo, L.C. Gerke, A.S. Carroll, R.W. Howson, J.S. Weissman, and E.K. O'Shea. 2003. Global analysis of protein localization in budding yeast. *Nature*. 425:686-691.

Hung, G.C., and D.C. Masison. 2006. N-terminal domain of yeast Hsp104 chaperone is dispensable for thermotolerance and prion propagation but necessary for curing prions by Hsp104 overexpression. *Genetics*. 173:611-620.

Iizasa, T. 2008. [Increased activity of PRPP synthetase]. *Nihon rinsho. Japanese journal of clinical medicine*. 66:694-698.

Ingelfinger, D., D.J. Arndt-Jovin, R. Luhrmann, and T. Achsel. 2002. The human LSm1-7 proteins colocalize with the mRNA-degrading enzymes Dcp1/2 and Xrnl in distinct cytoplasmic foci. *Rna*. 8:1489-1501.

Ingerson-Mahar, M., A. Briegel, J.N. Werner, G.J. Jensen, and Z. Gitai. 2010. The metabolic enzyme CTP synthase forms cytoskeletal filaments. *Nature cell biology*. 12:739-746.

Ishikawa, M., D. Tsuchiya, T. Oyama, Y. Tsunaka, and K. Morikawa. 2004. Structural basis for channelling mechanism of a fatty acid beta-oxidation multienzyme complex. *The EMBO journal*. 23:2745-2754.

Ito, H., Y. Fukuda, K. Murata, and A. Kimura. 1983. Transformation of intact yeast cells treated with alkali cations. *Journal of bacteriology*. 153:163-168.

Izant, J.G., and E. Lazarides. 1977. Invariance and heterogeneity in the major structural and regulatory proteins of chick muscle cells revealed by two-dimensional gel electrophoresis. *Proceedings of the National Academy of Sciences of the United States of America*. 74:1450-1454.

Jacque, C.M., C. Vinner, M. Kujas, M. Raoul, J. Racadot, and N.A. Baumann. 1978. Determination of glial fibrillary acidic protein (GFAP) in human brain tumors. *Journal of the neurological sciences*. 35:147-155.

Jerntorp, P., H. Ohlin, and L.O. Almer. 1986. Aldehyde dehydrogenase activity and large vessel disease in diabetes mellitus. A preliminary study. *Diabetes*. 35:291-294.

Jones, L.J., R. Carballido-Lopez, and J. Errington. 2001. Control of cell shape in bacteria: helical, actin-like filaments in Bacillus subtilis. *Cell*. 104:913-922.

Kabsch, W., H.G. Mannherz, D. Suck, E.F. Pai, and K.C. Holmes. 1990. Atomic structure of the actin:DNase I complex. *Nature*. 347:37-44.

Kaplan, M.P., S.S. Chin, K.H. Fliegner, and R.K. Liem. 1990. Alpha-internexin, a novel neuronal intermediate filament protein, precedes the low molecular weight neurofilament protein (NF-L) in the developing rat brain. *The Journal of neuroscience : the official journal of the Society for Neuroscience*. 10:2735-2748.

Katsumoto, T., A. Mitsushima, and T. Kurimura. 1990. The role of the vimentin intermediate filaments in rat 3Y1 cells elucidated by immunoelectron microscopy and computer-graphic reconstruction. *Biology of the cell / under the auspices of the European Cell Biology Organization*. 68:139-146.

Kawasugi, K., and F. Takeuchi. 2003. [PRPP synthetase superactivity]. *Nihon rinsho. Japanese journal of clinical medicine*. 61 Suppl 1:284-287.

Keizer, D.W., C.M. Slupsky, M. Kalisiak, A.P. Campbell, M.P. Crump, P.A. Sastry, B. Hazes, R.T. Irvin, and B.D. Sykes. 2001. Structure of a pilin monomer from Pseudomonas aeruginosa: implications for the assembly of pili. *The Journal of biological chemistry*. 276:24186-24193.

Kerstens, P.J., J.N. Stolk, A.M. Boerbooms, R.A. De Abreu, and L.B. Van de Putte. 1995. Purine enzymes in rheumatoid arthritis. A clue to the prediction of the response to azathioprine? Review and hypothesis. *Clinical and experimental rheumatology*. 13:107-111.

Kerstens, P.J., J.N. Stolk, A.M. Boerbooms, L.H. Lambooy, R. de Graaf, R.A. De Abreu, and L.B. van de Putte. 1994. Purine enzymes in rheumatoid arthritis: possible association with response to azathioprine. A pilot study. *Annals of the rheumatic diseases*. 53:608-611.

Kim, J., and F.M. Raushel. 2001. Allosteric control of the oligomerization of carbamoyl phosphate synthetase from Escherichia coli. *Biochemistry*. 40:11030-11036.

King, M.D., and D. Marsh. 1987. Head group and chain length dependence of phospholipid self-assembly studied by spin-label electron spin resonance. *Biochemistry*. 26:1224-1231.

Kizaki, H., F. Ohsaka, and T. Sakurada. 1982. Role of GTP in CTP synthetase from Ehrlich ascites tumor cells. *Biochemical and biophysical research communications*. 108:286-291.

Korn, E.D., M.F. Carlier, and D. Pantaloni. 1987. Actin polymerization and ATP hydrolysis. *Science*. 238:638-644.

Kruse, T., and K. Gerdes. 2005. Bacterial DNA segregation by the actin-like MreB protein. *Trends in cell biology*. 15:343-345.

Kruse, T., J. Moller-Jensen, A. Lobner-Olesen, and K. Gerdes. 2003. Dysfunctional MreB inhibits chromosome segregation in Escherichia coli. *The EMBO journal*. 22:5283-5292.

Kueh, H.Y., and T.J. Mitchison. 2009. Structural plasticity in actin and tubulin polymer dynamics. *Science*. 325:960-963.

Lara, B., A.I. Rico, S. Petruzzelli, A. Santona, J. Dumas, J. Biton, M. Vicente, J. Mingorance, and O. Massidda. 2005. Cell division in cocci: localization and properties of the Streptococcus pneumoniae FtsA protein. *Molecular microbiology*. 55:699-711.

Lazarides, E., and B.D. Hubbard. 1976. Immunological characterization of the subunit of the 100 A filaments from muscle cells. *Proceedings of the National Academy of Sciences of the United States of America*. 73:4344-4348.

LeDuc, P.P., and R.R. Bellin. 2006. Nanoscale intracellular organization and functional architecture mediating cellular behavior. *Annals of biomedical engineering*. 34:102-113.

Lee, H., W.C. DeLoache, and J.E. Dueber. 2012. Spatial organization of enzymes for metabolic engineering. *Metabolic engineering*. 14:242-251.

Lenaz, G., and M.L. Genova. 2009. Structural and functional organization of the mitochondrial respiratory chain: a dynamic super-assembly. *The international journal of biochemistry & cell biology*. 41:1750-1772.

Levitzki, A., and D.E. Koshland, Jr. 1972a. Ligand-induced dimer-to-tetramer transformation in cytosine triphosphate synthetase. *Biochemistry*. 11:247-253.

Levitzki, A., and D.E. Koshland, Jr. 1972b. Role of an allosteric effector. Guanosine triphosphate activation in cytosine triphosphate synthetase. *Biochemistry*. 11:241-246.

Liu, J.L. 2010. Intracellular compartmentation of CTP synthase in Drosophila. *Journal of genetics and genomics = Yi chuan xue bao*. 37:281-296.

Liu, J.L., and J.G. Gall. 2007. U bodies are cytoplasmic structures that contain uridine-rich small nuclear ribonucleoproteins and associate with P bodies. *Proceedings of the National Academy of Sciences of the United States of America*. 104:11655-11659.

Lockwood, A.H. 1978. Tubulin assembly protein: immunochemical and immunofluorescent studies on its function and distribution in microtubules and cultured cells. *Cell*. 13:613-627.

Long, C.W., and A.B. Pardee. 1967. Cytidine triphosphate synthetase of Escherichia coli B. I. Purification and kinetics. *The Journal of biological chemistry*. 242:4715-4721.

Longtine, M.S., D.J. DeMarini, M.L. Valencik, O.S. Al-Awar, H. Fares, C. De Virgilio, and J.R. Pringle. 1996. The septins: roles in cytokinesis and other processes. *Current opinion in cell biology*. 8:106-119.

Lopez Jimenez, M., J. Garcia Puig, F. Mateos Anton, T. Ramos Hernandez, J. Sebastian Melian, and V. Garcia Neito. 1990. [Metabolism of purine nucleotides in the central nervous system in patients with phosphoribosylpyrophosphate synthetase hyperactivity and neurosensory deafness]. *Neurologia*. 5:14-17.

Lu, S.C., M.L. Martinez-Chantar, and J.M. Mato. 2006. Methionine adenosyltransferase and S-adenosylmethionine in alcoholic liver disease. *Journal of gastroenterology and hepatology*. 21 Suppl 3:S61-64.

Luisi, P.L. 2002. Toward the engineering of minimal living cells. *The Anatomical record*. 268:208-214.

Lunn, F.A., T.J. Macleod, and S.L. Bearne. 2008. Mutational analysis of conserved glycine residues 142, 143 and 146 reveals Gly(142) is critical for tetramerization of CTP synthase from Escherichia coli. *The Biochemical journal*. 412:113-121.

Lutkenhaus, J. 2007. Assembly dynamics of the bacterial MinCDE system and spatial regulation of the Z ring. *Annual review of biochemistry*. 76:539-562.

Mahalingam, B., A. Cuesta-Munoz, E.A. Davis, F.M. Matschinsky, R.W. Harrison, and I.T. Weber. 1999. Structural model of human glucokinase in complex with glucose and ATP: implications for the mutants that cause hypo- and hyperglycemia. *Diabetes*. 48:1698-1705.

Manco, L., J.M. Vagace, L. Relvas, U. Rebelo, C. Bento, A. Villegas, and M. Leticia Ribeiro. 2010. Chronic haemolytic anaemia because of pyruvate kinase (PK) deficiency in a child heterozygous for haemoglobin S and no clinical features of sickle cell disease. *European journal of haematology*. 84:89-90.

Mazzanti, R., S. Moscarella, G. Bensi, E. Altavilla, and P. Gentilini. 1989. Hepatic lipid peroxidation and aldehyde dehydrogenase activity in alcoholic and non alcoholic liver disease. *Alcohol and alcoholism*. 24:121-128.

Mazzola, J.L., and M.A. Sirover. 2001. Reduction of glyceraldehyde-3-phosphate dehydrogenase activity in Alzheimer's disease and in Huntington's disease fibroblasts. *Journal of neurochemistry*. 76:442-449.

Mazzola, J.L., and M.A. Sirover. 2003. Subcellular alteration of glyceraldehyde-3-phosphate dehydrogenase in Alzheimer's disease fibroblasts. *Journal of neuroscience research*. 71:279-285.

McKeon, F.D. 1987. Nuclear lamin proteins and the structure of the nuclear envelope: where is the function? *BioEssays : news and reviews in molecular, cellular and developmental biology*. 7:169-173.

Michalczyk, K., and M. Ziman. 2005. Nestin structure and predicted function in cellular cytoskeletal organisation. *Histology and histopathology*. 20:665-671.

Michel, T.M., W. Gsell, L. Kasbauer, T. Tatschner, A.J. Sheldrick, I. Neuner, F. Schneider, E. Grunblatt, and P. Riederer. 2010. Increased activity of mitochondrial aldehyde dehydrogenase (ALDH) in the putamen of individuals with Alzheimer's disease: a human postmortem study. *Journal of Alzheimer's disease : JAD*. 19:1295-1301.

Micheli, V., and A. Taddeo. 1981. [Spectrophotometric assay of 5-phosphoribosyl-1-pyrophosphate synthetase (PRPP) in erythrocyte lysate (author's transl)]. *Quaderni Sclavo di diagnostica clinica e di laboratorio*. 17:209-215.

Minana, M.D., M. Portoles, A. Jorda, and S. Grisolia. 1984. Lesch-Nyhan syndrome, caffeine model: increase of purine and pyrimidine enzymes in rat brain. *Journal of neurochemistry*. 43:1556-1560.

Mizuno, Y., T.G. Thompson, J.R. Guyon, H.G. Lidov, M. Brosius, M. Imamura, E. Ozawa, S.C. Watkins, and L.M. Kunkel. 2001. Desmuslin, an intermediate filament protein that interacts with alpha -dystrobrevin and desmin. *Proceedings of the National Academy of Sciences of the United States of America*. 98:6156-6161.

Mohri, H. 1976. The function of tubulin in motile systems. *Biochimica et biophysica acta*. 456:85-127.

Moller-Jensen, J., J. Borch, M. Dam, R.B. Jensen, P. Roepstorff, and K. Gerdes. 2003. Bacterial mitosis: ParM of plasmid R1 moves plasmid DNA by an actin-like insertional polymerization mechanism. *Molecular cell*. 12:1477-1487.

Moller-Jensen, J., and J. Lowe. 2005. Increasing complexity of the bacterial cytoskeleton. *Current opinion in cell biology*. 17:75-81.

Nadkarni, A.K., V.M. McDonough, W.L. Yang, J.E. Stukey, O. Ozier-Kalogeropoulos, and G.M. Carman. 1995. Differential biochemical regulation of the URA7- and URA8-encoded CTP synthetases from Saccharomyces cerevisiae. *The Journal of biological chemistry*. 270:24982-24988.

Narayanaswamy, R., M. Levy, M. Tsechansky, G.M. Stovall, J.D. O'Connell, J. Mirrielees, A.D. Ellington, and E.M. Marcotte. 2009. Widespread reorganization of metabolic enzymes into reversible assemblies upon nutrient starvation. *Proceedings of the National Academy of Sciences of the United States of America*. 106:10147-10152.

Narita, A., S. Takeda, A. Yamashita, and Y. Maeda. 2006. Structural basis of actin filament capping at the barbed-end: a cryo-electron microscopy study. *The EMBO journal*. 25:5626-5633.

Newey, S.E., E.V. Howman, C.P. Ponting, M.A. Benson, R. Nawrotzki, N.Y. Loh, K.E. Davies, and D.J. Blake. 2001. Syncoilin, a novel member of the intermediate filament superfamily that interacts with alpha-dystrobrevin in skeletal muscle. *The Journal of biological chemistry*. 276:6645-6655.

Nishida, Y., I. Akaoka, and Y. Horiuchi. 1981. Altered isoelectric property of a superactive 5-phosphoribosyl-1-pyrophosphate (PRPP) synthetase in a patient with clinical gout. *Biochemical medicine*. 26:387-394.

Noree, C., B.K. Sato, R.M. Broyer, and J.E. Wilhelm. 2010. Identification of novel filament-forming proteins in Saccharomyces cerevisiae and Drosophila melanogaster. *The Journal of cell biology*. 190:541-551.

Osborn, M., W. Franke, and K. Weber. 1980. Direct demonstration of the presence of two immunologically distinct intermediate-sized filament systems in the same cell by double immunofluorescence microscopy. Vimentin and cytokeratin fibers in cultured epithelial cells. *Experimental cell research*. 125:37-46.

Ostrander, D.B., D.J. O'Brien, J.A. Gorman, and G.M. Carman. 1998. Effect of CTP synthetase regulation by CTP on phospholipid synthesis in Saccharomyces cerevisiae. *The Journal of biological chemistry*. 273:18992-19001.

Otaegui, P.J., T. Ferre, E. Riu, and F. Bosch. 2003. Prevention of obesity and insulin resistance by glucokinase expression in skeletal muscle of transgenic mice. *FASEB journal : official publication of the Federation of American Societies for Experimental Biology*. 17:2097-2099.

Owen, H.M. 1949. Flagellar structure; the flagellum as a taxonomic character. *Transactions of the American Microscopical Society*. 68:261-274.

Ozier-Kalogeropoulos, O., M.T. Adeline, W.L. Yang, G.M. Carman, and F. Lacroute. 1994. Use of synthetic lethal mutants to clone and characterize a novel CTP synthetase gene in Saccharomyces cerevisiae. *Molecular & general genetics : MGG*. 242:431-439.

Ozier-Kalogeropoulos, O., F. Fasiolo, M.T. Adeline, J. Collin, and F. Lacroute. 1991. Cloning, sequencing and characterization of the Saccharomyces cerevisiae URA7 gene encoding CTP synthetase. *Molecular & general genetics : MGG*. 231:7-16.

Pachter, J.S., and R.K. Liem. 1985. alpha-Internexin, a 66-kD intermediate filament-binding protein from mammalian central nervous tissues. *The Journal of cell biology*. 101:1316-1322.

Paluh, J.L., H. Zalkin, D. Betsch, and H.L. Weith. 1985. Study of anthranilate synthase function by replacement of cysteine 84 using site-directed mutagenesis. *J Biol Chem*. 260:1889-1894.

Pappas, A., W.L. Yang, T.S. Park, and G.M. Carman. 1998. Nucleotide-dependent tetramerization of CTP synthetase from Saccharomyces cerevisiae. *The Journal of biological chemistry*. 273:15954-15960.

Park, T.S., D.J. O'Brien, and G.M. Carman. 2003. Phosphorylation of CTP synthetase on Ser36, Ser330, Ser354, and Ser454 regulates the levels of CTP and

phosphatidylcholine synthesis in Saccharomyces cerevisiae. *The Journal of biological chemistry*. 278:20785-20794.

Park, T.S., D.B. Ostrander, A. Pappas, and G.M. Carman. 1999. Identification of Ser424 as the protein kinase A phosphorylation site in CTP synthetase from Saccharomyces cerevisiae. *Biochemistry*. 38:8839-8848.

Pasek, S., J.L. Risler, and P. Brezellec. 2006. Gene fusion/fission is a major contributor to evolution of multi-domain bacterial proteins. *Bioinformatics*. 22:1418-1423.

Patrick, G.N., B. Bingol, H.A. Weld, and E.M. Schuman. 2003. Ubiquitin-mediated proteasome activity is required for agonist-induced endocytosis of GluRs. *Current biology : CB*. 13:2073-2081.

Poon, E., E.V. Howman, S.E. Newey, and K.E. Davies. 2002. Association of syncoilin and desmin: linking intermediate filament proteins to the dystrophin-associated protein complex. *The Journal of biological chemistry*. 277:3433-3439.

Portier, M.M., B. de Nechaud, and F. Gros. 1983. Peripherin, a new member of the intermediate filament protein family. *Developmental neuroscience*. 6:335-344.

RayChaudhuri, D., and J.T. Park. 1992. Escherichia coli cell-division gene ftsZ encodes a novel GTP-binding protein. *Nature*. 359:251-254.

Sackett, D.L. 1995. Structure and function in the tubulin dimer and the role of the acidic carboxyl terminus. *Sub-cellular biochemistry*. 24:255-302.

Schweizer, J., P.E. Bowden, P.A. Coulombe, L. Langbein, E.B. Lane, T.M. Magin, L. Maltais, M.B. Omary, D.A. Parry, M.A. Rogers, and M.W. Wright. 2006. New consensus nomenclature for mammalian keratins. *The Journal of cell biology*. 174:169-174.

Shea, T.B., and M.L. Beermann. 1999. Neuronal intermediate filament protein alpha-internexin facilitates axonal neurite elongation in neuroblastoma cells. *Cell motility and the cytoskeleton*. 43:322-333.

Shelton, K.R., P.M. Egle, and D.L. Cochran. 1981. Nuclear envelope proteins: identification of lamin B subtypes. *Biochemical and biophysical research communications*. 103:975-981.

Sheth, U., and R. Parker. 2003. Decapping and decay of messenger RNA occur in cytoplasmic processing bodies. *Science*. 300:805-808.

Sheth, U., and R. Parker. 2006. Targeting of aberrant mRNAs to cytoplasmic processing bodies. *Cell*. 125:1095-1109.

Sheu, K.F., Y.T. Kim, J.P. Blass, and M.E. Weksler. 1985. An immunochemical study of the pyruvate dehydrogenase deficit in Alzheimer's disease brain. *Annals of neurology*. 17:444-449.

Sheu, K.F., P. Szabo, L.W. Ko, and L.M. Hinman. 1989. Abnormalities of pyruvate dehydrogenase complex in brain disease. *Annals of the New York Academy of Sciences*. 573:378-391.

Shiota, M., C. Postic, Y. Fujimoto, T.L. Jetton, K. Dixon, D. Pan, J. Grimsby, J.F. Grippo, M.A. Magnuson, and A.D. Cherrington. 2001. Glucokinase gene locus transgenic mice are resistant to the development of obesity-induced type 2 diabetes. *Diabetes*. 50:622-629.

Simard, D., K.A. Hewitt, F. Lunn, A. Iyengar, and S.L. Bearne. 2003. Limited proteolysis of Escherichia coli cytidine 5'-triphosphate synthase. Identification of residues required for CTP formation and GTP-dependent activation of glutamine hydrolysis. *European journal of biochemistry / FEBS*. 270:2195-2206.

Sircar, K., H. Huang, L. Hu, D. Cogdell, J. Dhillon, V. Tzelepi, E. Efstathiou, I.H. Koumakpayi, F. Saad, D. Luo, T.A. Bismar, A. Aparicio, P. Troncoso, N. Navone, and W. Zhang. 2012. Integrative molecular profiling reveals asparagine synthetase is a target in castration-resistant prostate cancer. *The American journal of pathology*. 180:895-903.

Sondheimer, N., and S. Lindquist. 2000. Rnq1: an epigenetic modifier of protein function in yeast. *Molecular cell*. 5:163-172.

Soufo, H.J., and P.L. Graumann. 2003. Actin-like proteins MreB and Mbl from Bacillus subtilis are required for bipolar positioning of replication origins. *Current biology : CB*. 13:1916-1920.

Sperling, O., P. Boer, S. Brosh, E. Zoref, and A. de Vries. 1977. Superactivity of phosphoribosylpyrophosphate synthetase, due to feedback resistance, causing purine overproduction and gout. *Ciba Foundation symposium*:143-164.

Stearns, T., and M. Kirschner. 1994. *In vitro* reconstitution of centrosome assembly and function: the central role of gamma-tubulin. *Cell*. 76:623-637.

Straub, F.B., and G. Feuer. 1989. Adenosinetriphosphate. The functional group of actin. 1950. *Biochimica et biophysica acta*. 1000:180-195.

Tardy, M., C. Fages, G. Le Prince, B. Rolland, and J. Nunez. 1990. Regulation of the glial fibrillary acidic protein (GFAP) and of its encoding mRNA in the developing brain and in cultured astrocytes. *Advances in experimental medicine and biology*. 265:41-52.

Teixeira, D., and R. Parker. 2007. Analysis of P-body assembly in Saccharomyces cerevisiae. *Molecular biology of the cell*. 18:2274-2287.

Teixeira, D., U. Sheth, M.A. Valencia-Sanchez, M. Brengues, and R. Parker. 2005. Processing bodies require RNA for assembly and contain nontranslating mRNAs. *Rna*. 11:371-382.

Telford, J.L., M.A. Barocchi, I. Margarit, R. Rappuoli, and G. Grandi. 2006. Pili in gram-positive pathogens. *Nature reviews. Microbiology*. 4:509-519.

Tibbetts, A.S., and D.R. Appling. 1997. Saccharomyces cerevisiae expresses two genes encoding isozymes of 5-aminoimidazole-4-carboxamide ribonucleotide transformylase. *Archives of biochemistry and biophysics*. 340:195-200.

Toshima, K., Y. Kuroda, T. Hashimoto, M. Ito, T. Watanabe, M. Miyao, and K. Ii. 1982. Enzymologic studies and therapy of Leigh's disease associated with pyruvate decarboxylase deficiency. *Pediatric research*. 16:430-435.

Van Biervliet, J.P., M. Duran, S.K. Wadman, J.F. Koster, and A. van Rossum. 1980. Leigh's disease with decreased activities of pyruvate carboxylase and pyruvate decarboxylase. *Journal of inherited metabolic disease*. 2:15-18.

van den Ent, F., L.A. Amos, and J. Lowe. 2001. Prokaryotic origin of the actin cytoskeleton. *Nature*. 413:39-44.

van den Ent, F., and J. Lowe. 2000. Crystal structure of the cell division protein FtsA from Thermotoga maritima. *The EMBO journal*. 19:5300-5307.

van den Ent, F., J. Moller-Jensen, L.A. Amos, K. Gerdes, and J. Lowe. 2002. F-actin-like filaments formed by plasmid segregation protein ParM. *The EMBO journal*. 21:6935-6943.

van Dijk, E., N. Cougot, S. Meyer, S. Babajko, E. Wahle, and B. Seraphin. 2002. Human Dcp2: a catalytically active mRNA decapping enzyme located in specific cytoplasmic structures. *The EMBO journal*. 21:6915-6924.

Veenhuis, M., F.A. Salomons, and I.J. Van Der Klei. 2000. Peroxisome biogenesis and degradation in yeast: a structure/function analysis. *Microscopy research and technique*. 51:584-600.

Walther, T.C., J.H. Brickner, P.S. Aguilar, S. Bernales, C. Pantoja, and P. Walter. 2006. Eisosomes mark static sites of endocytosis. *Nature*. 439:998-1003.

Weinstein, D.E., M.L. Shelanski, and R.K. Liem. 1991. Suppression by antisense mRNA demonstrates a requirement for the glial fibrillary acidic protein in the formation

of stable astrocytic processes in response to neurons. *The Journal of cell biology*. 112:1205-1213.

Weinstock, I.M., J. Behrendt, H.E. Wittshire, Jr., J. Keleman, and S. Louis. 1977. Pyruvate kinase: diagnostic value in neuromuscular disease. *Clinica chimica acta; international journal of clinical chemistry*. 80:415-422.

Wells, W.A. 2005. The discovery of tubulin. *The Journal of cell biology*. 169:552.

Whelan, J., G. Phear, M. Yamauchi, and M. Meuth. 1993. Clustered base substitutions in CTP synthetase conferring drug resistance in Chinese hamster ovary cells. *Nature genetics*. 3:317-322.

Whelan, J., T. Smith, G. Phear, A. Rohatiner, A. Lister, and M. Meuth. 1994. Resistance to cytosine arabinoside in acute leukemia: the significance of mutations in CTP synthetase. *Leukemia : official journal of the Leukemia Society of America, Leukemia Research Fund, U.K*. 8:264-265.

Wickstead, B., and K. Gull. 2011. The evolution of the cytoskeleton. *The Journal of cell biology*. 194:513-525.

Wilhelm, J.E., M. Hilton, Q. Amos, and W.J. Henzel. 2003. Cup is an eIF4E binding protein required for both the translational repression of oskar and the recruitment of Barentsz. *The Journal of cell biology*. 163:1197-1204.

Willemoes, M., A. Molgaard, E. Johansson, and J. Martinussen. 2005. Lid L11 of the glutamine amidotransferase domain of CTP synthase mediates allosteric GTP activation of glutaminase activity. *The FEBS journal*. 272:856-864.

Williams, J.C., H. Kizaki, G. Weber, and H.P. Morris. 1978. Increased CTP synthetase activity in cancer cells. *Nature*. 271:71-73.

Wright, S.D., R.A. Ramos, M. Patel, and D.S. Miller. 1992. Septin: a factor in plasma that opsonizes lipopolysaccharide-bearing particles for recognition by CD14 on phagocytes. *The Journal of experimental medicine*. 176:719-727.

Yang, W.L., M.E. Bruno, and G.M. Carman. 1996. Regulation of yeast CTP synthetase activity by protein kinase C. *The Journal of biological chemistry*. 271:11113-11119.

Yang, W.L., and G.M. Carman. 1996. Phosphorylation and regulation of CTP synthetase from Saccharomyces cerevisiae by protein kinase A. *The Journal of biological chemistry*. 271:28777-28783.

Yang, W.L., V.M. McDonough, O. Ozier-Kalogeropoulos, M.T. Adeline, M.T. Flocco, and G.M. Carman. 1994. Purification and characterization of CTP synthetase, the product of the URA7 gene in Saccharomyces cerevisiae. *Biochemistry*. 33:10785-10793.

Zborovskii, A.B., M. Stazharov, and V.F. Martem'ianov. 2000. [Purine metabolism enzymes in diagnosis and differential diagnosis of osteoarthritis and gout arthritis]. *Terapevticheskii arkhiv*. 72:21-24.

Zhang, Y.H. 2011. Substrate channeling and enzyme complexes for biotechnological applications. *Biotechnology advances*. 29:715-725.

Zhou, G., H. Charbonneau, R.F. Colman, and H. Zalkin. 1993. Identification of sites for feedback regulation of glutamine 5-phosphoribosylpyrophosphate amidotransferase by nucleotides and relationship to residues important for catalysis. *The Journal of biological chemistry*. 268:10471-10481.

Zhou, P., I.L. Derkatch, and S.W. Liebman. 2001. The relationship between visible intracellular aggregates that appear after overexpression of Sup35 and the yeast prion-like elements [PSI(+)] and [PIN(+)]. *Molecular microbiology*. 39:37-46.

Zoref-Shani, E., and O. Sperling. 1979. Alterations in purine metabolism in cultured fibroblasts with HGPRT deficiency and with PRPP synthetase superactivity. *Advances in experimental medicine and biology*. 122B:19-24.

Zoref, E., A. De Vries, and O. Sperling. 1975. Mutant feedback-resistant phosphoribosylpyrophosphate synthetase associated with purine overproduction and gout. Phosphoribosylpyrophosphate and purine metabolism in cultured fibroblasts. *The Journal of clinical investigation*. 56:1093-1099.

Zoref, E., A. de Vries, and O. Sperling. 1978. Kinetic aspects of purine metabolism in cultured fibroblasts. A comparative study of cells from patients overproducing purines due to HGPRT deficiency and PRPP synthetase superactivity. *Monographs in human genetics*. 10:96-99.